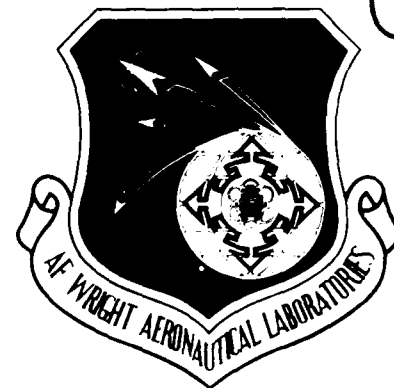


AD-A208 808

AFWAL-TR-88-3114



TIME SERIES MODELING FOR STRUCTURAL RESPONSE PREDICTION

**Stephen M. Batill
Joseph J. Hollkamp**

**Department of Aerospace and Mechanical Engineering
University of Notre Dame
Notre Dame, Indiana 46556**

Approved for Public Release; Distribution is Unlimited

November 1988

Final Report for Period : March 1985 to August 1988

SDTICD
ELECTE
JUN 09 1989

Handwritten initials: JH

**FLIGHT DYNAMICS LABORATORY
AIR FORCE WRIGHT AERONAUTICAL LABORATORIES
AIR FORCE SYSTEMS COMMAND
WRIGHT-PATTERSON AIR FORCE BASE, OHIO 45433-
6553**


80 6 09 029

NOTICE

When Government drawings, specifications, or other data are used for any purpose other than in connection with a definitely Government-related procurement, the United States Government incurs no responsibility or any obligation whatsoever. The fact that the Government may have formulated or in any way supplied the said drawings, specifications, or other data, is not to be regarded by implication, or otherwise as in any manner, as licensing the holder or any other person or corporation; or as conveying any rights or permission to manufacture, use, or sell any patented invention that may in any way be related thereto.

This report is releasable to the National Technical Information Service (NTIS). At NTIS, it will be available to the general public, including foreign nations.

This technical report has been reviewed and is approved for publication.



GREGORY E. MOSTER
Project Engineer
Aeroelasticity Group



TERRY M. HARRIS, Technical Manager
Aeroelasticity Group
Analysis & Optimization Branch

FOR THE COMMANDER



JOHN T. ACH, Chief
Analysis Optimization Branch
Structures Division

If your address has changed, if you wish to be removed from our mailing list, or if the addressee is no longer employed by your organization please notify WRDC/FIBRC, WPAFB, OH 45433-6523 to help us maintain a current mailing list .

Copies of this report should not be returned unless return is required by security considerations, contractual obligations, or notice on a specific document.

REPORT DOCUMENTATION PAGE				Form Approved OMB No. 0704-0188	
1a. REPORT SECURITY CLASSIFICATION UNCLASSIFIED			1b. RESTRICTIVE MARKINGS		
2a. SECURITY CLASSIFICATION AUTHORITY			3. DISTRIBUTION/AVAILABILITY OF REPORT Approved for public release; distribution is unlimited.		
2b. DECLASSIFICATION/DOWNGRADING SCHEDULE					
4. PERFORMING ORGANIZATION REPORT NUMBER(S)			5. MONITORING ORGANIZATION REPORT NUMBER(S) AFWAL-TR-88-3114		
6a. NAME OF PERFORMING ORGANIZATION Department of Aerospace and Mechanical Engineering		6b. OFFICE SYMBOL (if applicable)	7a. NAME OF MONITORING ORGANIZATION Flight Dynamics Laboratory (AFWAL/FDSRC) Air Force Wright Aeronautical Laboratories		
6c. ADDRESS (City, State, and ZIP Code) Department of Aerospace and Mechanical Engr. University of Notre Dame Notre Dame, IN 46556			7b. ADDRESS (City, State, and ZIP Code) Wright-Patterson AFB, OH 45433-6553		
8a. NAME OF FUNDING/SPONSORING ORGANIZATION		8b. OFFICE SYMBOL (if applicable)	9. PROCUREMENT INSTRUMENT IDENTIFICATION NUMBER F33615-85-C-3205		
8c. ADDRESS (City, State, and ZIP Code)			10. SOURCE OF FUNDING NUMBERS		
			PROGRAM ELEMENT NO. 62201F	PROJECT NO. 2401	TASK NO. 02
11. TITLE (Include Security Classification) Time Series Modeling for Structural Response Prediction					
12. PERSONAL AUTHOR(S) Batill, Stephen M., Hollkamp, Joseph J.					
13a. TYPE OF REPORT Final		13b. TIME COVERED FROM 850301 TO 880801		14. DATE OF REPORT (Year, Month, Day) 881114	
15. PAGE COUNT 164					
16. SUPPLEMENTARY NOTATION					
17. COSATI CODES			18. SUBJECT TERMS (Continue on reverse if necessary and identify by block number) Parameter Identification ARMA Model Time Series Modeling Structural Response Prediction		
FIELD	GROUP	SUB-GROUP			
01	04				
13	06				
19. ABSTRACT (Continue on reverse if necessary and identify by block number) A numerical and experimental study of time domain methods for modeling and parameter identification of structural systems is presented. Models are developed which can be used to predict the transient response of multiple-degree-of-freedom systems subjected to arbitrary input. The linear, discrete time transfer function is expressed in a form called the Autoregressive Moving Average (ARMA) model. The ARMA model is a minimum parameter model that may be parameterized with a minimum number of measured quantities. The ARMA model is contrasted to traditional models such as differential equation models and modal methods. The ARMA model identification algorithms are also compared to time domain modal methods. Though it has proven useful for a number of low-order systems, the identification of the ARMA model is often hampered by the sensitivity of parameter estimates to measurement noise bias. Modal methods and signal processing algorithms reduce the sensitivity to noise by using methods such as model overspecification or complex iterative procedures. Numerous algorithms and their effectiveness in reducing noise bias are presented. Finally, a two-stage identification technique is					
20. DISTRIBUTION/AVAILABILITY OF ABSTRACT <input checked="" type="checkbox"/> UNCLASSIFIED/UNLIMITED <input type="checkbox"/> SAME AS RPT <input type="checkbox"/> DTIC USERS				21. ABSTRACT SECURITY CLASSIFICATION UNCLASSIFIED	
22a. NAME OF RESPONSIBLE INDIVIDUAL Gregory E. Mosier				22b. TELEPHONE (Include Area Code) (513) 255-7384	
				22c. OFFICE SYMBOL AFWAL/FDSRC	

Block 19. Continued

presented which uses overspecified models to estimate the poles of the ARMA model from system-free vibration response data using a form of the Principal Eigenvectors Method. A least squares algorithm is then used to identify the transfer function zeroes from forced response records. Experimental response data for both single-degree-of-freedom and multiple-degree-of-freedom systems are used to evaluate the different methods of identification. An extension of the methods to nonlinear discrete time series models are also presented. These models are a logical extension of the linear models. The nonlinear model forms are discussed and both simulated and actual experimental data from an oleopneumatic landing gear strut are used to evaluate the model forms.

PREFACE

The work described in this report was conducted during the period from March 1985 to August 1988 under contract F33615-85-C-3205. The research program was entitled "Parameter Identification for Aerospace Structures," and was conducted by the Department of Aerospace and Mechanical Engineering at the University of Notre Dame, Notre Dame, Indiana for the Flight Dynamics Laboratory of the Wright Aeronautical Laboratories. The Principal Investigator for the contract was Dr. Stephen M. Batill. The Project Engineers for the contract were Dr. Charles L. Keller, from March 1985 to January 1988, and Mr. Gregory E. Moster, from January 1988 to the completion of the contract. The authors acknowledge the support of the Department of Aerospace and Mechanical Engineering which provided the graduate student support and research facilities necessary to successfully complete this project.



Accession For	
NTIS GRA&I	<input checked="checked" type="checkbox"/>
DTIC TAB	<input type="checkbox"/>
Unannounced	<input type="checkbox"/>
Justification	
By	
Distribution/	
Availability Codes	
Dist	Avail and/or Special
A-1	

TABLE OF CONTENTS

	Page
INTRODUCTION	1
Background	1
The Problem	2
Overview	3
 DYNAMIC SYSTEM MODELS	 5
Differential Equations	5
Modal Models	6
Difference Models	7
Overview	8
 DISCRETE TIME SERIES MODELS	 9
The Z-transform	9
Transformation to the Discrete Time Domain	11
Applications of the ARMA Models	13
Advantages and Disadvantages of the ARMA model	13
Examples	14
Overview	20
 PARAMETER IDENTIFICATION	 27
Data Acquisition and Filtering	27
System Order	29
Examples	31
Overview	33
 IDENTIFICATION OF THE ARMA MODEL	 40
The ARMA model	40
The Least Squares Algorithm	40
Generalized Least Squares	42
Instrumental Variables	43
Maximum Likelihood Method	44

The Overspecified LS model	44
Examples	45
Overview	46
FREE RESPONSE METHODS	52
The AR model	52
Pisarenko Harmonic Decomposition	61
The Correlation Fit	61
Overspecification of the AR Model	62
The Principal Eigenvectors Method	62
The Modified Principal Eigenvectors Method	63
Examples	65
Overview	80
APPLICATIONS	84
MA Parameter Identification	84
Examples	85
Overview	111
NONLINEAR SYSTEMS	120
The Nonlinear AR model	120
Examples	121
Overview	133
CONCLUSIONS AND RECOMMENDATIONS	134
REFERENCES	136
BIBLIOGRAPHY	138
APPENDICES	
Appendix A - Alternative Formulation	145
Appendix B - The AR model	147
Appendix C - Singular Value Decomposition	149
Appendix D - Singular Value Decomposition Solution of the Normal Equations	151
Appendix E - The Frequency Error Envelopes	153

LIST OF FIGURES

1. Schematic of the SDOF base motion system.	15
2. Tustin's Rule used to approximate a SDOF system transfer function.	17
3. Tustin's Rule used to approximate a MDOF system transfer function.	18
4. Periodic input to the MDOF system.	19
5. Simulated response of the MDOF system to the periodic input.	21
6. Pseudo-random input to the MDOF system.	22
7. Frequency response of digital filter.	23
8. Filtered pseudo-random input to the MDOF system.	24
9. Simulated response of the MDOF system to the filtered pseudo-random input.	25
10. Singular Value Spectra of the autocorrelation matrix of unity variance gaussian noise.	32
11. Singular Value Spectra of the autocorrelation matrix of a signal containing three damped sinusoids.	34
12. Singular Value Spectra of the autocorrelation matrices.	35
13. Power Spectrum of a noisy signal.	36
14. Singular Value Spectra of the autocorrelation matrices.	37
15. Power Spectrum of a noisy signal.	38
16. Input Case 1.	47
17. Input Case 2.	48
18. Input Case 3.	49
19. Contour map of discrete time transformation.	54
20. Envelope of percent damped frequency error (radius of uncertainty =0.01).	55
21. Envelope of percent damping error (radius of uncertainty =0.01).	56
22. Envelope of percent damped frequency error (radius of uncertainty =0.001).	57
23. Envelope of percent damping error (radius of uncertainty =0.001).	58
24. Envelope of percent damped frequency error (radius of uncertainty =0.0001).	59
25. Envelope of percent damping error (radius of uncertainty =0.0001).	60
26. Estimated pole location from the LS algorithm (n=6).	74
27. Estimated pole location from the overspecified LS algorithm (n=12).	76
28. Estimated pole location from the overspecified LS algorithm (n=30).	77
29. Estimated pole location from the PEM algorithm (n=30).	78
30. Estimated pole location from the MPEM algorithm (n=30).	79
31. Singular Value Spectra of the backward autocorrelation matrix for two closely spaced modes.	81

32. Pseudo-random binary input.	87
33. Noisy response to the pseudo-random binary input.	88
34. Frequency Response Function magnitude for SLS models (unfiltered data used).	89
35. Frequency Response of digital filter.	90
36. Filtered pseudo-random binary input.	91
37. Filtered noisy response to the pseudo-random binary input.	92
38. Frequency Response Function magnitude for SLS models (filtered data used).	93
39. Frequency Response Function magnitude for 2LS models.	94
40. Typical free response of the SDOF system.	96
41. Base acceleration, Case A.	97
42. Base acceleration, Case B.	98
43. Base acceleration, Case C.	99
44. Second order SLS model prediction of SDOF response to input Case B.	101
45. Second order 2LS model prediction of SDOF response to input Case A.	102
46. Second order 2LS model prediction of SDOF response to input Case B.	103
47. Second order 2LS model prediction of SDOF response to input Case C.	104
48. Magnitude frequency response plots of second order 2LS models.	105
49. Magnitude frequency response plots of second order SLS models.	106
50. Magnitude frequency response plots of overspecified SLS models (input Case A).	107
51. Tenth order 2LS model prediction of SDOF response to input Case B.	109
52. Acceleration input to the MDOF system, input Case D.	112
53. Acceleration input to the MDOF system, input Case E.	113
54. Magnitude frequency response plots of SLS models (input Case D).	114
55. Magnitude frequency response plots of 2LS models (input Case D).	115
56. Sixth order SLS model used to predict response of the MDOF system to input Case E.	116
57. Tenth order SLS model used to predict response of the MDOF system to input Case E.	117
58. Fourth order 2LS model used to predict response of the MDOF system to Case E.	118
59. Oleo-pneumatic shock strut experimental apparatus.	122
60. Duffing oscillator response and predictions from NLAR and AR models.	126
61. Frequency of the Duffing oscillator and the models as a function of displacement.	127

62. Duffing oscillator response and response predictions from NLAR models (larger initial amplitude).	128
63. Viscous-coulomb damped oscillator response and predictions from NLAR and AR models.	131
64. Experimental data and NLAR and AR model response predictions.	132

LIST OF TABLES

1. Parameter estimates.	50
2. One DOF simulated data.	67
3. 2DOF simulated data results for 1st mode.	68
4. 2DOF simulated data results for 2nd mode.	69
5. 3DOF simulated data.	71
6. Experimental data.	72
7. Simulated data.	75
8. MPEM estimates for MDOF data with closely spaced modes.	82
9. Frequency and damping estimates from single-stage LS estimates of Case A.	108
10. MPEM estimates for MDOF experimental data.	110
11. Models used for Duffing Oscillator.	124
12. Models used for Viscous-Coulomb Damped Oscillator.	130

NOMENCLATURE

A_i, a_i	Autoregressive parameters
A_m	steering matrix of overdetermined set of equations
AR	Autoregressive
ARMA	Autoregressive Moving Average
$A(z)$	Autoregressive polynomial
b	vector of responses
B	input function matrix
B_i, b_i	Moving Average parameters
b_m	vector of MA model response
$B(z)$	Moving Average polynomial
c	vector of Residual AR model
C	damping matrix
CEM	Complex Exponential Method
CF	Correlation Fit Method
$C(z)$	overspecified AR polynomial
DFT	Discrete Fourier Transform
$D(z)$	any polynomial in z
e, ε	residual vectors
$e(k), \varepsilon(k)$	residual time series
ERA	Eigensystem Realization Algorithm
f	vector used in the MPEM
FEM	Finite Element Method
FFT	Fast Fourier Transform
$f^*(t)$	sampled data function
$f(k)$	sampled data time series
FRF	Frequency Response Function
$F(s)$	Laplace Transform of the sampled data time series
$F(z)$	Z-transform of the sampled data time series
$F_y(z)$	digital transfer function of input filter
$F_u(z)$	digital transfer function of output filter
$F(\omega)$	transfer function of anti-aliasing filter
GLS	Generalized Least Squares Method
g_m	vector used in the LS algorithm
$G(s)$	transfer function in the Laplace domain

$G(z)$	discrete time transfer function
$h, \Delta t$	sampling time increment
I	Identity matrix
ITD	Ibrahim's Time Domain Method
IV	Instrumental Variables Method
j	square of negative one
K	stiffness matrix
L	overspecification order
LS	Least Squares Method
M	mass matrix
MA	Moving Average
MDOF	Multiple-degree-of-freedom
MIMO	Multiple input multiple output
MISO	Multiple input single output
MLE	Maximum Likelihood Estimation
MPEM	Modified Principal Eigenvectors Method
NLAR	Nonlinear Autoregressive
$n(k)$	discrete time series of noise
p	order of the system
PEM	Principal Eigenvectors Method
PHD	Pisarenko Harmonic Decomposition
Q_m	steering matrix of MPEM overdetermined equations
$R_{yy}(k)$	discrete time autocorrelation function
R_{yy}	autocorrelation matrix
s	Laplace variable
SDOF	Single-degree-of-freedom
SLS	Single-stage Least Squares Method
SISO	Single input single output
SNR	signal to noise ratio
U	right hand eigenvector matrix of SVD algorithm
$u(k)$	input time series
U_m	steering matrix of MA LS overdetermined set of equations
$u_m(k)$	measured input time series
$U(s)$	Laplace transform of the input time function
$U(z)$	Z-transform of the input time function
V	left hand eigenvector matrix of SVD algorithm

$x(k)$	noisy process discrete time series
$X_{in}(\omega)$	Discrete Fourier Transform of input to the filter
$X_{out}(\omega)$	Discrete Fourier Transform of output of the filter
$X_{in}(z)$	Z-transform of the filter input
$X_{out}(z)$	Z-transform of the filter output
$y(k)$	output time series
$y_m(k)$	measured output time series
$Y(s)$	Laplace Transform of the response
$Y(z)$	Z-transform of the response
z	forward shift operator
Z	Instrumental Variable matrix
$z_m(k)$	transformed response (GLS algorithm)
$\kappa(A)$	condition number of matrix A
α	Duffing equation stiffness term
β	Duffing equation nonlinear stiffness term
ω	natural frequency (rad/sec)
ω_d	damped natural frequency (rad/sec)
ζ	damping factor
Σ	singular value matrix
σ	standard deviation of added noise
σ_k	kth singular value
θ	parameter vector
θ_{LS}	Least Squares estimated parameter vector
θ_{iv}	Instrumental Variable estimated parameter vector
Ω	steering matrix of residual time series
2DOF	Two-degree-of-freedom
2LS	Two-stage Least Squares Method
3DOF	Three-degree-of-freedom

SUMMARY

A numerical and experimental study of time domain methods for modeling and parameter identification of structural systems is presented. Models are developed which can be used to predict the transient response of multiple degree of freedom systems subjected to arbitrary input. The linear, discrete time transfer function is expressed in a form called the Autoregressive Moving Average (ARMA) model. The ARMA model is a minimum parameter model that may be parameterized with a minimum number of measured quantities. The ARMA model is contrasted to traditional models such as differential equation models and modal methods. The ARMA model identification algorithms are also compared to time domain modal methods. Though it has proven useful for a number of low order systems, the identification of the ARMA model is often hampered by the sensitivity of parameter estimates to measurement noise bias. Modal methods and signal processing algorithms reduce the sensitivity to noise by using methods such as model overspecification or complex iterative procedures. Numerous algorithms and their effectiveness in reducing noise bias are presented. Finally, a two-stage identification technique is presented which uses overspecified models to estimate the poles of the ARMA model from system free vibration response data using a form of the Principal Eigenvectors Method. A Least Squares algorithm is then used to identify the transfer function zeroes from forced response records. Experimental response data for both single-degree-of-freedom and multiple-degree-of-freedom systems are used to evaluate the different methods of identification. An extension of the methods to nonlinear discrete time series models is also presented. These models are a logical extension of the linear models. The nonlinear model forms are discussed and both simulated and actual experimental data from an oleo-pneumatic landing gear strut are used to evaluate the model forms.

INTRODUCTION

Background

Dynamic system modeling of real structural systems is typically done for one of three reasons. The system model may be needed to determine whether the structure will have acceptable response to the variety of input forces that it will encounter during its lifetime. If the response is unacceptable, either the structure is modified, perhaps using some information extracted from the model, or the input forces have to be altered. The second reason is that a system model may be needed to implement a control algorithm. The required accuracy of the model depends on the sophistication of the algorithm. The third reason may be simply a verification of results developed from some other analysis.

Analytical or experimental procedures are used to develop the system model. The traditional analytical procedures involve the formulation of differential equations termed the equations of motion. Either numerical or analytical integration is used to determine the solutions of the differential equations of motion and thus the system response. One of the more popular approaches to develop the equations of motion for a structure is the Finite Element Method (FEM). The FEM can be used to develop a set of second order differential equations through discretization of the structure. The set of second order differential equations represents one form of a system model. Structural engineers usually prefer the system model in an alternative form termed the modal form. The modal form of the system model is comprised of the mode shapes, modal frequencies, and modal damping factors. The modal frequencies and modal damping factors can be determined from the characteristic equation of the structure. The mode shape defines the amplitude of response at given modal frequencies at the discretized points. The response at the discrete point is a summation of the scaled response at each modal frequency. The modal form of the model can be synthesized from the equations of motion and the equations of motion can be synthesized from the modal form of the model.

The traditional experimental procedure for the determination of a system model involves the modal form. The modal information is derived from experimentally acquired data. The structure must be excited at a point or a number of points and the response measured at a discrete set of points. Frequency domain methods of identification transform the time domain response measurements into the frequency domain in the form of Discrete Fourier Transforms (DFT) using a Fast Fourier Transform (FFT) algorithm. Frequency Response Functions (FRF) can be derived by dividing the DFT's of the response measurements by the DFT's of the input functions. Multiple data sets are acquired and the FRF's for each input-output pair are averaged to reduced leakage and measurement errors.

The modal information is then parameterized by curve fitting techniques performed on the ensemble of FRF's.

In the past decade, modal analysis techniques using time domain data have also become popular. These techniques use time domain data to parameterized the modal form of the model. Either a set of time domain free response data can be directly used or the ensemble of FRF's can be transformed back into the time domain providing impulse response functions. The major time domain methods include the Complex Exponential Method (CEM), Ibrahim's Time Domain technique (ITD), and the Eigensystem Realization Algorithm (ERA). The time domain methods involve the formulation of a coefficient matrix from the time domain data. The eigenvalues and eigenvectors of this matrix completely characterize the modal form of the model. The methods differ by the way in which the coefficient matrix is formed.

Time domain methods offer a higher resolution capability for closely spaced frequencies than the frequency domain methods. The major advantage of the frequency domain methods is that multiple sets of data can be used and the effect of noise can be greatly reduced. The time domain methods have to use overspecified model orders or iterative techniques to counter the effects of noise bias. The frequency domain methods are user intensive, requiring the user to distinguish between important and unimportant modes; the time domain methods are more automated. The time domain methods may therefore be better suited for rapid "on-line" modeling.

The frequency domain models can be represented by a matrix of transfer functions in the Laplace domain. The time domain models can be represented by a matrix of discrete time transfer functions. Response is determined, using the frequency domain models, by convolution integrals involving the elements of the matrix and the input function. Response is determined, using the time domain models, by recursive addition of state variables. The weights of the state variables in the addition process are defined by the parameters in the discrete time transfer function.

The Problem

During service, certain types of structures can assume many different "configurations" due to changes in mass loading, temperature changing the structural properties, or failure of localized components. If one is concerned with the prediction of the dynamic response of critical components of a complete structure when subjected to a specific loading condition, then a single structural model defined for the "ideal" structure may not prove suitable. The many possible structural "configurations" and inputs in the lifetime of some structures place limits on the usefulness of certain detailed analytic or

numerical modeling procedures such as Finite Element Analysis. It would be desirable to have techniques that would provide "on-line" or adaptive models that would be suitable for the rapid and accurate prediction of transient dynamic response for a specific set of loading conditions.

Consider the problem of an airplane about to traverse a rough or damaged runway. Prediction of peak acceleration levels at several critical locations on the structure could help to determine whether the aircraft would be damaged while using the runway or could help to determine the speed and path the aircraft should take to minimize the risk of damage. A model relating the vibration (peak displacement or acceleration) at the critical locations within the structure to the specific runway profile would be needed. However, each time the aircraft is used, its structural configuration may change; for example, the payload or fuel loading may be modified. When the structural configuration changes, the predictive model must change. Or consider future large space structures that will be fabricated in orbit. Dynamic models will be necessary to control these structures. The varying structural characteristics during assembly would outdate the baseline analytical or modal models used to predict dynamic response.

In both examples, input to the structure is provided at a discrete number of points, and knowledge of the system response may be necessary at only a finite number of points on the structure. It would be desirable to identify or update the structural characteristics every time the structure is used. Ideally, digital time histories of the input and system output would be acquired, and the system model or transfer function would be derived or updated automatically. For linear systems, discrete time transfer functions are well-suited for automatic digital identification. One form of a discrete time transfer function is the Autoregressive Moving Average (ARMA) model. The ARMA model can be used to predict response for Multiple Input Multiple Output (MIMO) systems as well as Single Input Single Output (SISO) systems.

Overview

This report is concerned with the suitability and identification of ARMA models for structural response prediction, and will be limited to SISO applications. The extension to MIMO systems seems to be direct. (More research in this area may be necessary.) This report presents a discussion of the suitability of using ARMA models for structural response prediction and an overview of the factors relating to the parameter identification process. The ARMA model was chosen because of its suitability to the digital environment and because time domain models can be identified in a more automated fashion than frequency domain models. These two factors are very important when considering the

ultimate goal of response prediction. For example, if an aircraft taxi response is desired, the data required to parameterize a model for the aircraft would be acquired as part of the digital instrumentation system planned for future aircraft systems, and the "model" for structural response prediction would have to be automatically synthesized so that "warnings" or operational instructions would be provided to the pilot.

In addition to the ARMA model, Autoregressive (AR) models and Moving Average (MA) models will be discussed. The major identification algorithms for the parameterization of the AR, MA, and ARMA models will be presented. A classical identification scheme, the single-stage-least-squares (SLS) algorithm, and a proposed modification, a two-stage-least-squares (2LS) algorithm, are the main algorithms presented. Results using the SLS and 2LS algorithms to parameterize single-degree-of-freedom (SDOF) and multiple-degree-of-freedom (MDOF) system models are presented. These results were achieved using simulated and actual experimental data and the models were then used to predict transient response for these systems. The final section will describe the extension of the discrete time series models to nonlinear models.

DYNAMIC SYSTEM MODELS

There are many different types of analytic or numerical models that can be used to predict vibration. The models can be developed from either basic physical principles or from the observed response of the system. This report will focus on the development of numerical models for complex structural systems by recording and analyzing the response of the system. The experimental model can be in the form of a parameterized set of differential equations, a modal model, or a parameterized set of difference equations. This section briefly presents the different forms of the system model and compares the requirements necessary to determine system parameters. A discussion at the end of the section will give some of the reasons why the ARMA model has been chosen as the focus of this report.

Differential Equations

The undergraduate engineer is taught in mechanics and vibration classes that complex structures can be modeled as discretized, linearized, multiple-degree-of-freedom systems. Newtonian mechanics can be used to write a system of differential equations to describe the dynamic behavior of the structure. The differential equations are typically written in the form of second order, linear, constant coefficient equations as

$$\mathbf{M} \ddot{\mathbf{y}} + \mathbf{C} \dot{\mathbf{y}} + \mathbf{K} \mathbf{y} = \mathbf{B} \mathbf{u} \quad (1)$$

where \mathbf{y} is a vector representing the position of n generalized discrete points representing the n degrees of freedom and \mathbf{u} is a vector of m inputs. The coefficient matrices \mathbf{M} , \mathbf{C} , \mathbf{K} and \mathbf{B} , which are referred to as system parameters, are used to describe the system. Some parameter identification techniques attempt to determine \mathbf{M} , \mathbf{C} , \mathbf{K} , and \mathbf{B} from experimental data. The estimation procedures, referred to as equation of motion methods, require that all inputs and the position, velocity, and acceleration at the generalized degrees of freedom be measured. Some methods use integration or differentiation to generate two of three measurement quantities (position, velocity, and acceleration), from one measurement (position, velocity, or acceleration) but the applicability of this approach to anything but the simplest of systems has not been demonstrated. Usually, the matrices in Eqn 1 can only be estimated to within a transformation unless a mass or stiffness perturbation method is used. If the parameters of the system can be determined and one wants to determine the response of the system to another input, the usual methods for the

solution of linear differential equations are sufficient. Given the model, the response of the generalized points to an arbitrary input can be predicted through numerical integration.

The set of differential equations can be reduced to a single differential equation of order $2n$ with a single dependent response variable. The dependent variable can be any linear combination of the n generalized degrees of freedom. The single differential equation can also be parameterized from experimental data. The estimation procedure requires that all inputs and the dependent response with all of its derivatives up to order $2n$ be measured or estimated. The differential equation can be used to predict the response of the single dependent variable to an arbitrary input. The reduction of the model given by Eqn 1 simplifies the estimation process, since the number of parameters of the model has been reduced. The reduced model gives response predictions of the one dependent variable and not at all the generalized coordinates.

Modal Models

Modal methods use the measured response to estimate vibration parameters such as the mode shape, natural frequencies, damping factors, and modal participation factors. The input to the system can take the form of an impulse, a "random" time history, or a periodic function of specific form, such as a sine wave. The modal method assumes that the actual system response is the superposition of a number of characteristic "modes" with specific frequencies and damping characteristics. The method is based on the measurement of the complex response of the system and then the processing of the response data to determine the contributing modal parameters.

The response of the system due to an impulse is the free response after the impulse has occurred. The solution of Eqn 1 due to an impulse is of the form $y(t) = p \exp(\lambda t)$. Substitution into Eqn 1 yields the eigenvalue problem

$$[\lambda^2 \mathbf{M} + \lambda \mathbf{C} + \mathbf{K}] \mathbf{p} = 0 \quad (2)$$

There exist $2n$ discrete time eigenvalues (poles), λ , representing the natural frequencies and damping factors. Here, \mathbf{p} represents the complex modes of vibration and is a scaled version of the mode shapes. The system response to the unit impulse is found by the summation

$$\mathbf{x}(t) = \sum_{j=1}^{2n} \mathbf{p}_j \exp(\lambda_j t) \quad (3)$$

Modal methods use time domain data or frequency domain data to identify the poles and the complex modes of vibration. The response at the measurement points due to an impulse at the other input locations is needed to identify the complex modes of vibration for each input; the scaling of the individual modes define the modal participation factors.

The identification of the modal model requires that the impulse response function, in the time domain, or the frequency response function, in the frequency domain, be "measured" at every output location for every input location. Whether the identification procedure is time or frequency based, the impulse response function is usually developed in the frequency domain using ensemble averages of the input and output frequency spectra. A measurement of the response at every location and a measurement of each input are required. The measurements can be made all at once or separately. But many measurements at many locations are usually needed. This method is very well-established and is very useful if a complete model of the structure is desired.

There are some advantages and disadvantages to the use of modal methods. The estimated frequencies, damping factors, and mode shapes from each impulse response will be slightly different. Global estimates have to be made through the use of some averaging procedure. Also, if there are n degrees of freedom, response measurements at n locations are required. Given frequency, damping factor, mode shape estimates, and modal participation factors, the generalized stiffness ($M^{-1}K$), generalized damping matrices ($M^{-1}C$), and generalized input matrix ($M^{-1}B$) can be estimated. Identification of the full modal model is equivalent to the identification of the differential equations when the generalized coordinates are the modes of vibration. The modal model can be synthesized from the differential equation model and vice versa.

Difference Models

The differential equation model can be transformed into a difference equation model by a number of differencing techniques. A form of the difference equation model is

$$y_k + A_1 y_{k-1} + A_2 y_{k-2} = B_0 u_k + B_1 u_{k-1} + B_p u_{k-2} \quad (4)$$

where y is a vector of n responses and u is a vector of m inputs at discrete times. Equation 4 is an ARMA model for an Multiple Input and Multiple Output (MIMO) system. The Autoregressive parameters are the A matrices and Moving Average parameters are the B matrices. Mode shapes, frequencies, and damping factors can all be derived from a MIMO ARMA model as described by reference 1. Identification of the ARMA model given by Eqn 4 would require the input at each location to be measured and the response at n

locations to also be measured, just as with the modal models. But unlike the modal models, the ARMA model can be identified without forming the impulse response functions. Reference 1 also shows that identification of the Autoregressive matrices from impulse response functions is equivalent to the time domain modal method known as the Ibrahim Time Domain Technique (reference 2). Unlike the differential equation models, no integration is necessary to predict response. But like the differential equation models, the ARMA model can be reduced if only a single response is measured. The resulting difference model would be

$$y_k + a_1 y_{k-1} + \dots + a_{2n} y_{k-2n} = b_0^T u_k + b_1^T u_{k-1} + \dots + b_{2n}^T u_{k-2n} \quad (6)$$

which is a Multiple Input Single Output (MISO) model; here the Moving Average parameters are row vectors and the Autoregressive parameters are constants. For a single input, the Moving Average parameters become scalars. The identification of the SISO ARMA model requires that only a single input and a single output be measured.

Overview

The goal of the research effort summarized in this report was to study methods that may be able to automatically parameterize a model for a complex structural system. The model would then be used to predict response for a specified system input. The Differential Equation methods are undesirable because the full state of the response (position, velocity, and acceleration) is required from measurements or from auxiliary estimations (integrations or differentiations). The modal methods are undesirable because multiple measurement locations are required. The ARMA model appears to present the best alternative. The size of the ARMA models is adjustable, depending upon how many response locations are required. In the aircraft taxi response example, if the predicted acceleration response at the wingtip and the pilot location are the only critical locations, the ARMA model can be developed for the response at just those locations. Only the acceleration at wingtip and pilot locations and the inputs have to be measured to identify the model. The ARMA model can also be identified without forming the impulse response in the frequency domain. The identification of the ARMA model can be accomplished entirely in the time domain. The next section will describe the ARMA model in depth, and the remaining sections deal with the identification of the discrete time series models.

DISCRETE TIME TRANSFER FUNCTIONS

The ARMA model is used in this report to predict structural vibration. Identification procedures, examined later in the report, will parameterize the ARMA model from input-output discrete time histories. Before proceeding to the identification procedures, background on the ARMA model is provided. This section describes, through the use of the z-transform, the discrete time transfer function and its relationship to the continuous time transfer function. Approximations are introduced that will allow the discrete time transfer function to be synthesized from the continuous time transfer function. Applications of the ARMA model are briefly discussed, and the advantages and disadvantages of ARMA models are presented. Examples using discrete time transfer functions to predict vibration are included. This section introduces the ARMA model, describes relationships to continuous transfer functions, and shows, by example, that the ARMA model can be used to accurately predict structural vibration.

The Z-transform

For linear systems the relationship between the input to the system and the system response or output can be expressed as transfer functions. The transfer functions can be determined by transforming the input and output time functions using Laplace transformations. The transfer function in the Laplace domain is found by dividing the Laplace transform of the output by the Laplace transform of the input,

$$G(s) = \frac{Y(s)}{U(s)} \quad (7)$$

The frequency domain transfer function is simply the Laplace domain transfer function evaluated along the complex axis ($s=j\omega$). The goal of frequency domain identification methods is to accurately determine a frequency domain transfer function for every input-output pair. There exists a discrete time equivalent of Eqn 7 that can be used in the time domain. The discrete time equivalent involves the use of the z-transform instead of the Laplace transform. The relationship between the s or Laplace domain and the z or discrete time domain is written as

$$z=e^{sh} \quad (8)$$

where s is the Laplace variable, z is the z-transform variable, and h the discrete time interval. Note that the stable region in the Laplace domain (that is the region in which the

real part of s in negative) is mapped inside the unit circle in the z -domain. Analytically, the discrete time transfer function is obtained by a straightforward procedure if the input and output time functions are known. Realistically, the time functions are *measured* at discrete time instances, and the exact input and output time functions are unknown. In practice, the discrete time transfer function has to be determined using a modified form of the z -transform.

Suppose that a function, $f(t)$, is known precisely at n discrete time instances, then the sampled function, $f^*(t)$, can be reconstructed as a summation of the discrete time values times the appropriate delta functions,

$$f^*(t) = \sum_{k=0}^{n-1} f(kh) \delta(t - kh) \quad (9)$$

Here, $f^*(t)$ is exactly equivalent to $f(t)$ at the n discrete time instances and is zero at every other time. The Laplace transform of Eqn 9 is

$$F(s) = \sum_{k=0}^{n-1} f(kh) e^{-ksh} \quad (10)$$

The z -transform of Eqn 9 is calculated by substituting Eqn 8 into Eqn 10 to obtain

$$F(z) = \sum_{k=0}^{n-1} f(kh) z^{-k} \quad (11)$$

The discrete time transfer function is simply the ratio between the z -transform of the output and the z -transform of the input;

$$G(z) = \frac{Y(z)}{U(z)} = \frac{\sum_{k=0}^{n-1} y(kh) z^{-k}}{\sum_{k=0}^{n-1} u(kh) z^{-k}} \quad (12)$$

If there is no noise or error in the measurements, Eqn 12 may reduce to a polynomial expression

$$G(z) = \frac{b_0 + b_1 z^{-1} + b_2 z^{-2} + \dots + b_p z^{-p}}{1 + a_1 z^{-1} + a_2 z^{-2} + \dots + a_p z^{-p}} \quad (13)$$

If there is noise, an identification algorithm must be used to estimate the parameters in Eqn 13. The discrete time transfer function shown in Eqn 13 is also called the Infinite Impulse Response (IIR) filter and can be written in the form of an ARMA model. The basic ARMA model is the SISO model which has the form

$$y(k) = -a_1 y(k-1) - a_2 y(k-2) - \dots - a_p y(k-p) + b_0 u(k) + b_1 u(k-1) + \dots + b_p u(k-p) \quad (14)$$

where $u(k)$ are the discrete values (at time kh) of the various input functions, and $y(k)$ are the discrete time values of the response. The variable z in Eqn 13 is also known as the forward-shift operator. The forward shift-operator shifts the discrete time index by 1,

$$z[y(k)] = y(k+1) \quad (15)$$

The discrete time transfer function is only an approximation to the continuous time transfer function. Variations in the input between sample instances do not affect the output according to the discrete time transfer function, although such variations will affect the output of the actual system. Notice that two different time functions can have exactly the same z -transform.

An alternative formulation of the discrete time transfer function is given in Appendix A. The derivation begins with the state space representation of a system and ends with the discrete time transfer function. The only approximation used in the derivation is the assumption that the input is constant over the sample interval.

Transformation to the Discrete time domain

Ideally, to transform a transfer function in the Laplace domain to the time domain, the substitution

$$s = \frac{1}{h} \ln z \quad (16)$$

would convert the Laplace transforms to z -transforms. The main difficulty with the conversion is that the transfer function will not reduce to a simple form. The resulting form will contain terms involving the logarithm of z , which do not have the convenient definition of the forward-shift operator, Eqn 7. One would like to have a substitution approximately

equivalent to Eqn 16 that would result in discrete time transfer functions that were ratios of polynomials in z . Such substitutions are commonly used in digital control engineering. The simplest are the forward rectangular rule,

$$s = \frac{z-1}{h} \quad (17)$$

and the backward rectangular rule,

$$s = \frac{z-1}{zh} \quad (18)$$

The most popular approximation is Tustin's rule,

$$s = \frac{2}{h} \frac{z-1}{z+1} \quad (19)$$

The forward rectangular rule is the Euler integration scheme. The backward rectangular rule corresponds to backward differencing and Tustin's rule is trapezoidal or Modified-Euler integration. The input is assumed to be constant in the forward and backward rectangular rules and varies linearly in Tustin's rule. The rules are approximations of Eqn 8, the expansion of Eqn 8 is

$$z = e^{sh} = \sum_{n=0}^{\infty} \frac{(sh)^n}{n!} = 1 + sh + \frac{(sh)^2}{2} + \frac{(sh)^3}{6} + \dots \quad (20)$$

The forward rectangular rule is the two-term approximation of Eqn 8. The backward rectangular rule is expressed as

$$z = \frac{1}{1-sh} = 1 + sh + \sum_{n=2}^{\infty} (sh)^n \quad (21)$$

which is a two-term approximation plus an over approximation of the remaining terms. Tustin's rule is expanded as

$$z = \frac{1 + \frac{sh}{2}}{1 - \frac{sh}{2}} = 1 + sh + \frac{(sh)^2}{2} + \sum_{n=3}^{\infty} \frac{(sh)^n}{2} \quad (22)$$

which is a three-term approximation plus an over approximation of the remaining terms.

The reason that Tustin's rule is the most popular approximation is that it maps stable poles in the Laplace domain to stable pole locations in the z -domain and it maps

unstable poles in the Laplace domain to unstable pole locations in the z-domain. The forward rectangular rule maps unstable poles in the Laplace domain to unstable pole locations in the z-domain but maps some stable poles in the Laplace domain to unstable pole locations in the z-domain. The backward rectangular rule maps stable poles in the Laplace domain to stable pole locations in the z-domain but maps some unstable poles in the Laplace domain to stable pole locations in the z-domain. References 3 and 4 describe these approximations in some detail.

Applications of ARMA models

The accuracy of the approximations discussed in the previous section improves as the sample rate increases. All three provide nearly the same discrete time transfer functions. The approximations have received extensive use in digital control engineering. A crude procedure in control engineering is to analytically design a compensator in the Laplace domain, transform it at a high sampling rate to the z-domain, and then use a controller to implement the discrete time transfer function of the compensator (reference 4).

The primary application of the methods discussed in this report is not system control but is focussed on the discrete time transfer functions or ARMA models when used for vibratory prediction of complex multiple-degree-of-freedom systems. The approximations are useful in discovering what considerations are necessary to make the discrete time transfer function an attractive and accurate means of predicting vibration. The approximations suggest that a high sample rate may be needed to increase the accuracy, although, a high sample rate increases the computational load of the prediction.

Other control-oriented applications of the ARMA model include digital filtering (references 5 and 6) and identification of chemical processes (reference 7). Structural applications of the ARMA model include substructure modelling (reference 8), probabilistic simulations (reference 9), spectral estimation (reference 10), and vibratory parameter extraction (reference 11).

Advantages and Disadvantages of the ARMA model

There are advantages to the use of the ARMA models in identification and prediction. The ARMA model is a minimum parameter model; it therefore requires the least number of parameters to characterize the system. Consider an N degree of freedom, linear dynamic system which can be modeled as N second order, ordinary differential equations. The $2N$ states of this model can be expressed as the generalized coordinates and their first time derivatives. A fully coupled system with viscous damping would require $3(N^2+N)/2$ parameters (assuming symmetric mass, damping and stiffness matrices) to completely

define the system. Solution of this system of equations would provide the complete spatial distribution for the structure at any instant in time. An alternate form of the system model could be a single ordinary differential equation of order $2N$. The states of this model would be a single generalized coordinate and all of its derivatives up to order $2N$. For free vibration response, this equation could be characterized using only $2N-1$ parameters. The solution would yield a single state and all of its derivatives up to order $2N$. The second form is a minimum parameter model. An equivalent ARMA model would also be a minimum parameter model.

The SISO ARMA model's states are discrete time values of a single input and single output at a given instance in time and at a finite number of previous instances. The model state for a p th order model contains the system output at p previous time instances and the system input at $p+1$ time instances. The model state at the next time instance is found by incrementing all the states at the current time by 1. The identification and prediction procedures for the ARMA model require the minimum number of measured quantities. Only the system input and response need be measured. For instance, if the response is acceleration at some location, velocity at that location need not be known to identify the model. Once the parameters of the model are known, prediction can be quickly accomplished, given the input time history and the initial state of the model. The disadvantages of ARMA models are their limited accuracy, it is an approximation, and the identification problems associated with time domain procedures.

Examples

In the following examples, a single-degree-of-freedom (SDOF) base motion problem and an arbitrary multiple-degree-of-freedom (MDOF) system are used to examine the effect of sample rate upon the accuracy of the discrete time transfer function. Consider the SDOF spring-mass-damper base motion problem shown in Figure 1, the input is provided by the base mass and the output is the response of the free mass. The transfer function of this simple linear system is

$$G(s) = \frac{2\zeta\omega s + \omega^2}{s^2 + 2\zeta\omega s + \omega^2} \quad (23)$$

A discrete time transfer function can be found through any of the approximations discussed above. Tustin's rule (Eqn 19) will be used for the example presented here. The parameters

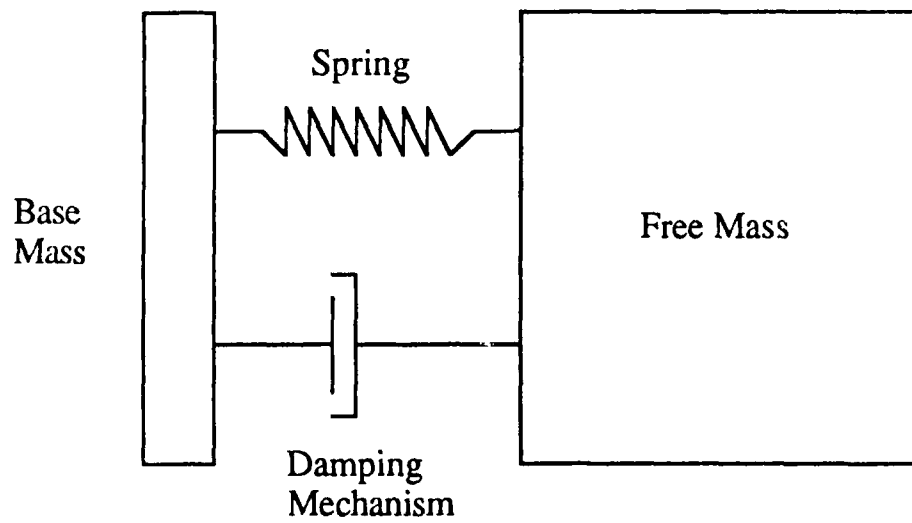


Figure 1: Schematic of the SDOF base motion system.

and accuracy of the discrete time transfer function depend upon the sample rate. It is convenient to compare the different transfer functions through the use of the magnitude frequency response plot. The frequency response is found by the substitution of $s=j(2\pi f)$ into the transfer function. The magnitude frequency response plot is found by plotting the magnitude of resulting complex expression versus frequency, f . The magnitude frequency response plot shows graphically the output gain of the system versus the input frequency. The phase of the frequency response also contains valuable information, but the meaning of the magnitude plot is easier to interpret and will be used for illustrative purposes. Note that the magnitude frequency response plot of the discrete time transfer function requires the substitution of Eqn 2 prior to the substitution of $s=j(2\pi f)$. The transformation from the discrete time domain to the s domain is not an approximation. Also the frequency response function for the discrete time equivalent can be evaluated at any frequency value by the computer.

The natural frequency of 10 Hz and damping factor of 1 percent critical were used in Eqn 23 for the example. The magnitude frequency response plot of the transfer function is shown in Figure 2 along with the magnitude frequency response plots of the discrete time equivalents obtained through the use of Tustin's rule at two different sample rates. The discrete time equivalents using the higher sample rate (200 Hz) is approximately equivalent to the transfer function from 0 to 20 Hz. The discrete time equivalent using the lower sample rate (50 Hz) is approximately equivalent to the transfer function from 0 to 5 Hz. This would imply that the sample rate of the discrete time approximation would have to be at least 10 to 20 times the base bandwidth of input signal to get accurate vibratory predictions.

An arbitrary MDOF system was also used to compare the effect of sampling rates upon the accuracy of the discrete time model for a more complex system. The arbitrary system was generated by randomly placing poles and zeros of the transfer function in the Laplace domain. Figure 3 shows the magnitude frequency response of an arbitrary system (a 4 DOF system) along with the magnitude frequency response plots of the discrete time equivalents obtained through the use of Tustin's rule at two different sample rates. The discrete time equivalent at the 1 kHz sampling rate is approximately equivalent to the arbitrary transfer function over the entire frequency range plotted (0 to 75 Hz). The discrete time equivalent at the lower sampling rate (200 Hz) is only accurate up to about 20 Hz. Predictions of system response to simulated inputs using the discrete time equivalents in the form of ARMA models (Eqn 8) were compared to those calculated through standard numerical integration (fourth order Runge-Kutta). A periodic input comprised of three unit amplitude sinusoids at frequencies of 2, 30, and 50 Hz is shown in Figure 4. Inspection of

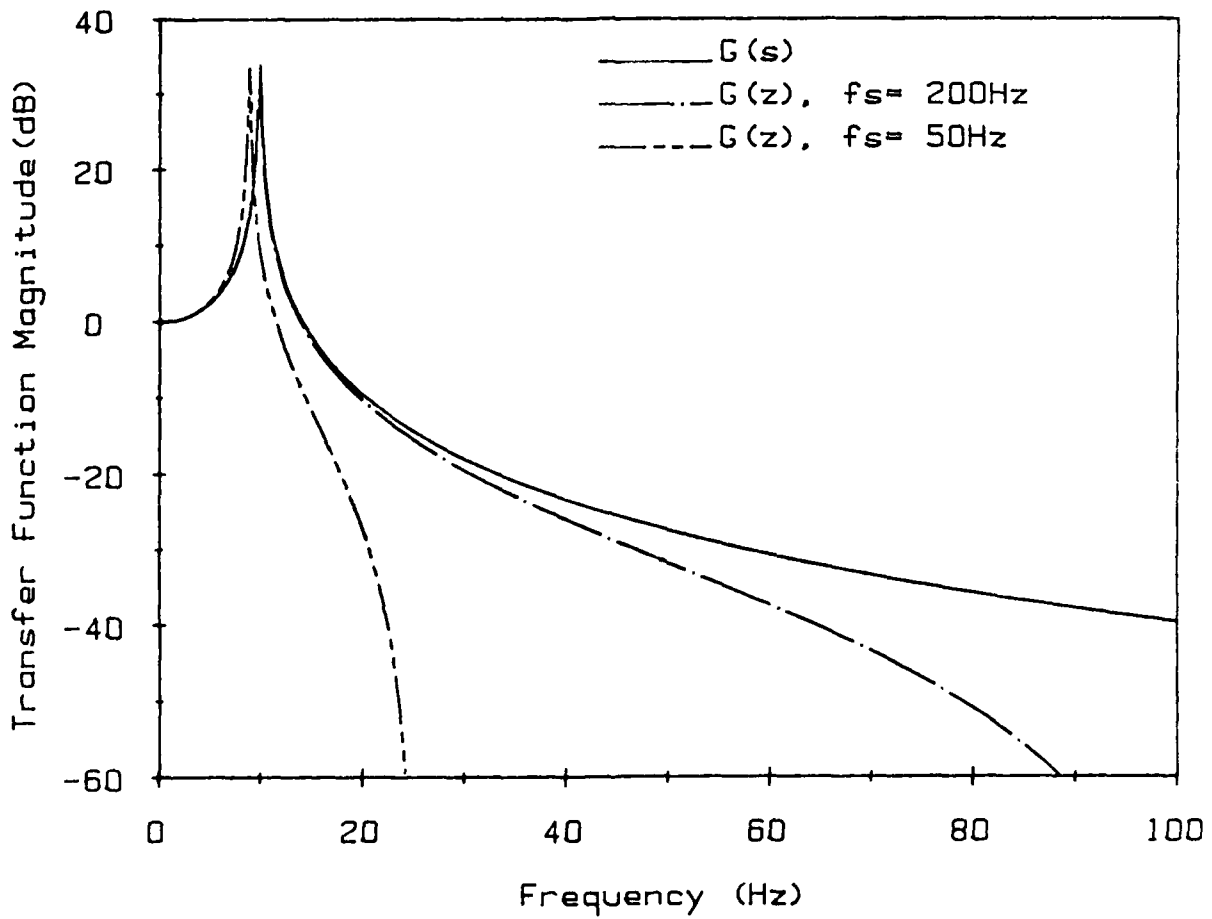


Figure 2: Tustin's Rule used to approximate a SDOF system transfer function.

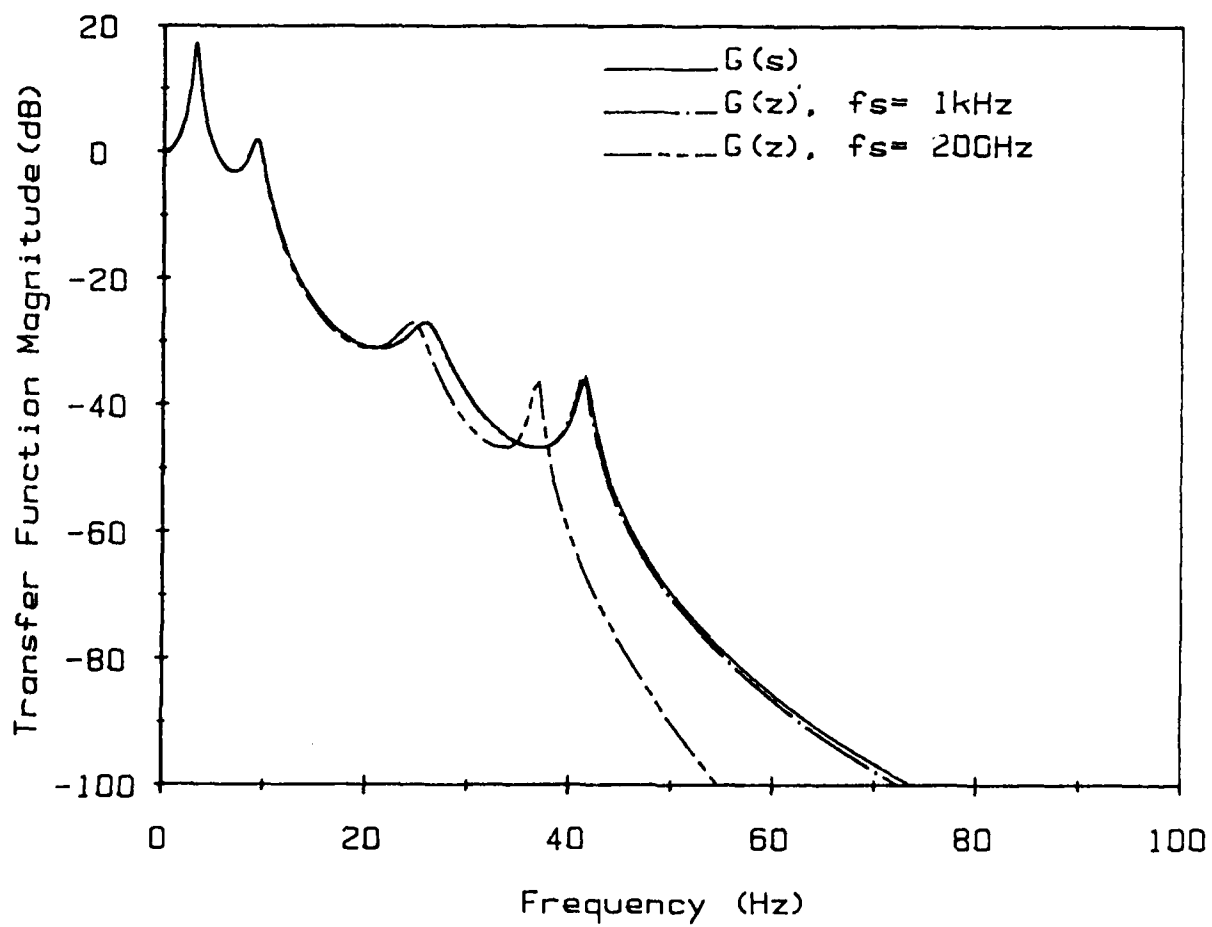


Figure 3: Tustin's Rule used to approximate a MDOF system transfer function.

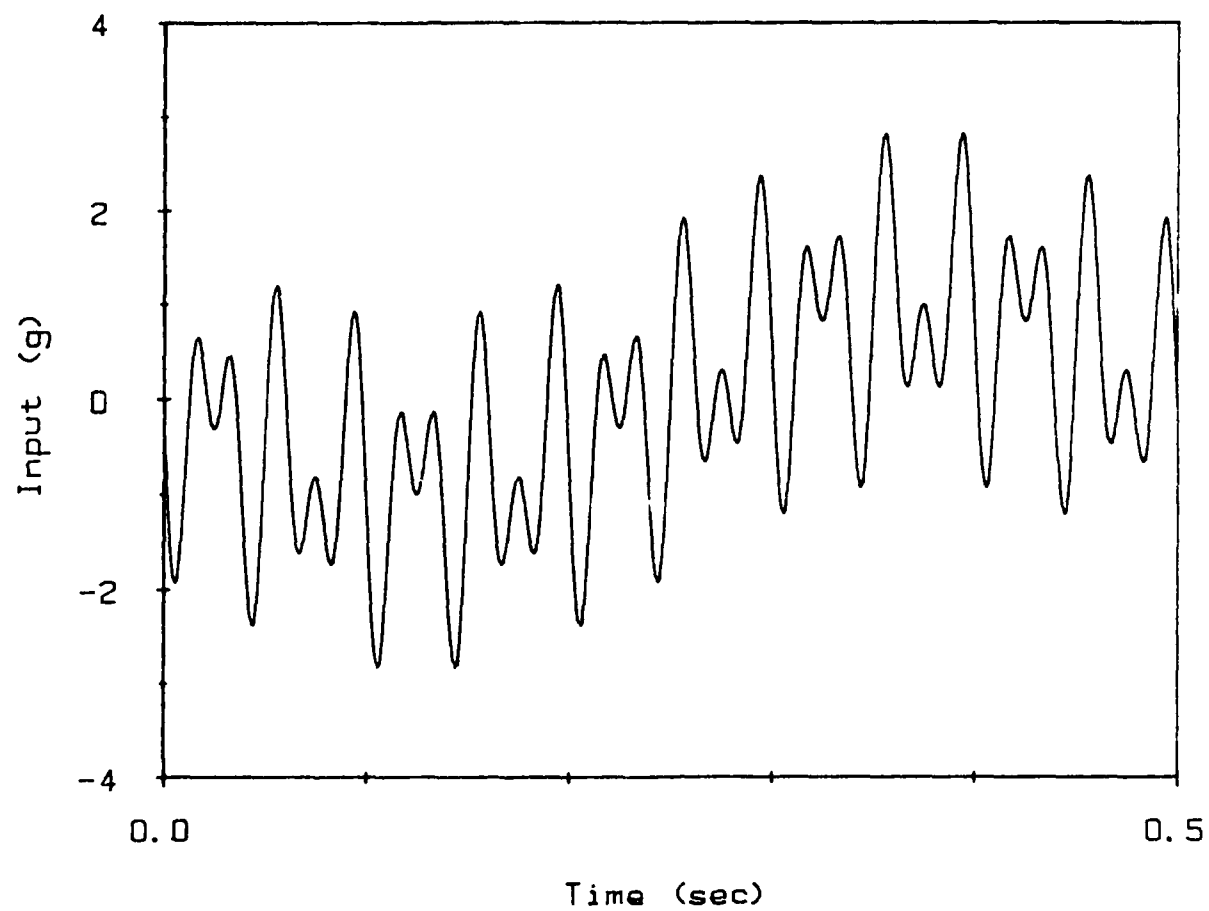


Figure 4: Periodic input to the MDOF system.

the magnitude frequency response plots indicates that the discrete time equivalent sampled at 1 kHz should have virtually the same response as the continuous time system at these frequencies and the discrete time equivalent sampled at 200 Hz will not be as accurate at the higher frequencies. Figure 5 shows the response predicted by the ARMA models in comparison to the numerically integrated response. (The predictions are determined through knowledge of the input and model parameters only; the response is calculated recursively and the initial conditions are assumed to be zero.) Figure 5 shows that both predictions are highly accurate. One would have expected the discrete time equivalents at the higher sampling rate to be accurate, and the errors of the discrete time equivalent at the lower sampling rate to be small, since the magnitude of the response is so low at the higher input frequencies.

Figure 6 shows a pseudo-random input (Gaussian noise with a unit variance) which should provide a very broadband excitation for this system. The bandwidth of the signal was reduced to approximately 0-50 Hz through the use of a digital filter (an 8th order ARMA approximation of an 8 pole Butterworth filter). The magnitude frequency response of the filter is shown in Figure 7. The filtered broadband input is shown in Figure 8. The filtered input was then applied to the system. The predicted responses, based on the discrete time equivalents, are shown in comparison to the numerically integrated response in Figure 9. The ARMA approximation prediction at the high sampling rate follows the numerically integrated response very closely (within the resolution of the plot). The ARMA prediction for the lower sample rate is not quite as accurate, but for many applications it would be considered to be an adequate representation of the system response.

Overview

The discrete time transfer function has been shown to provide an accurate prediction of simulated response when the sampling rate is at least 10 to 20 times larger than the bandwidth of the input. The discrete time transfer functions used in the examples were developed through analytical approximations and the errors are due to those approximations. The discrete time transfer function assumes that the input is constant over the sampling interval. Even if a discrete time transfer function could be found that did not use the approximations, the sampling rate would conceivably have to be at least 10 times higher than the bandwidth of interest to realistically represent the input function. Although Shannon's Sampling Theorem (reference 4) states that only two points per cycle are needed to reconstruct a signal, it is well known that the sampling rate needs to be 10 to 20 times the bandwidth upper limit to accurately perform numerical integration for most numerical

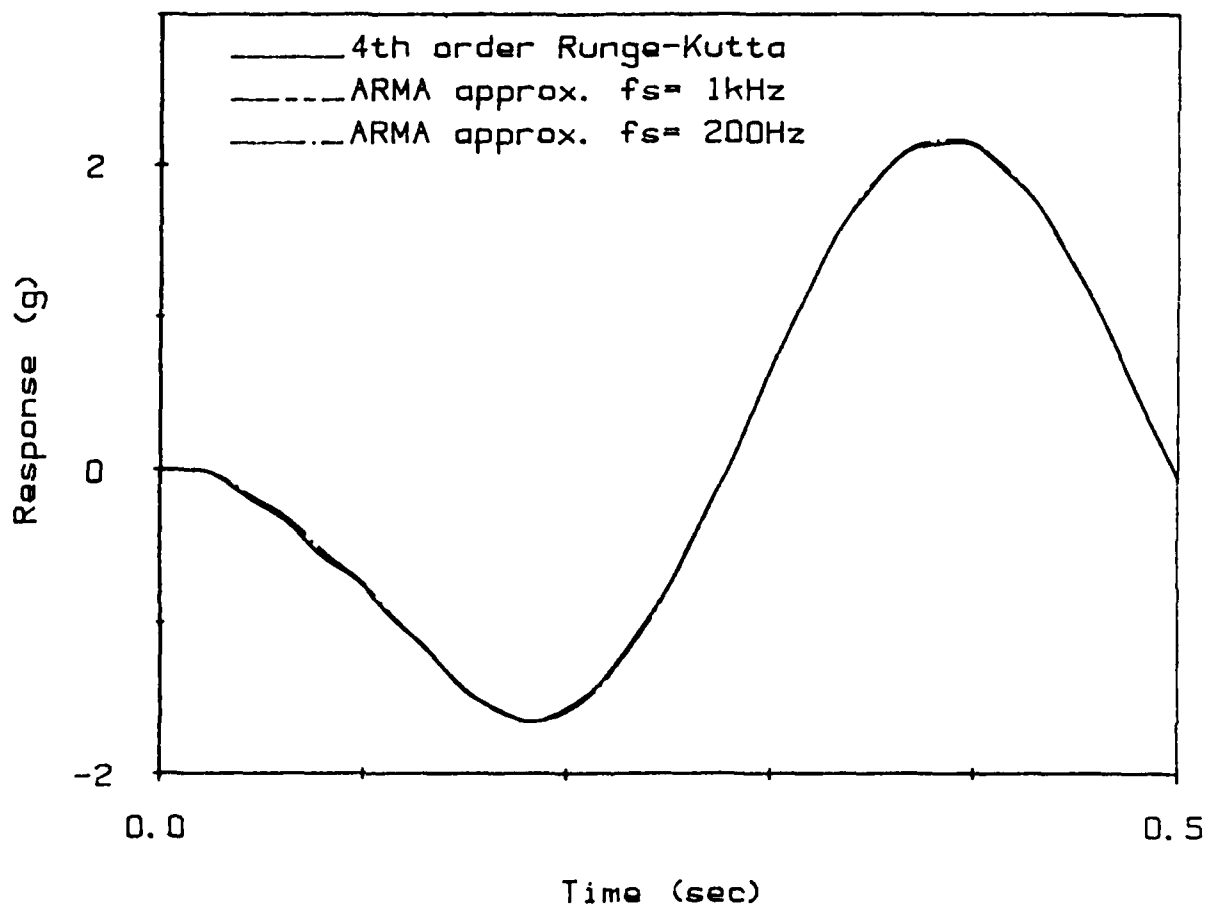


Figure 5: Simulated response of the MDOF system to the periodic input.

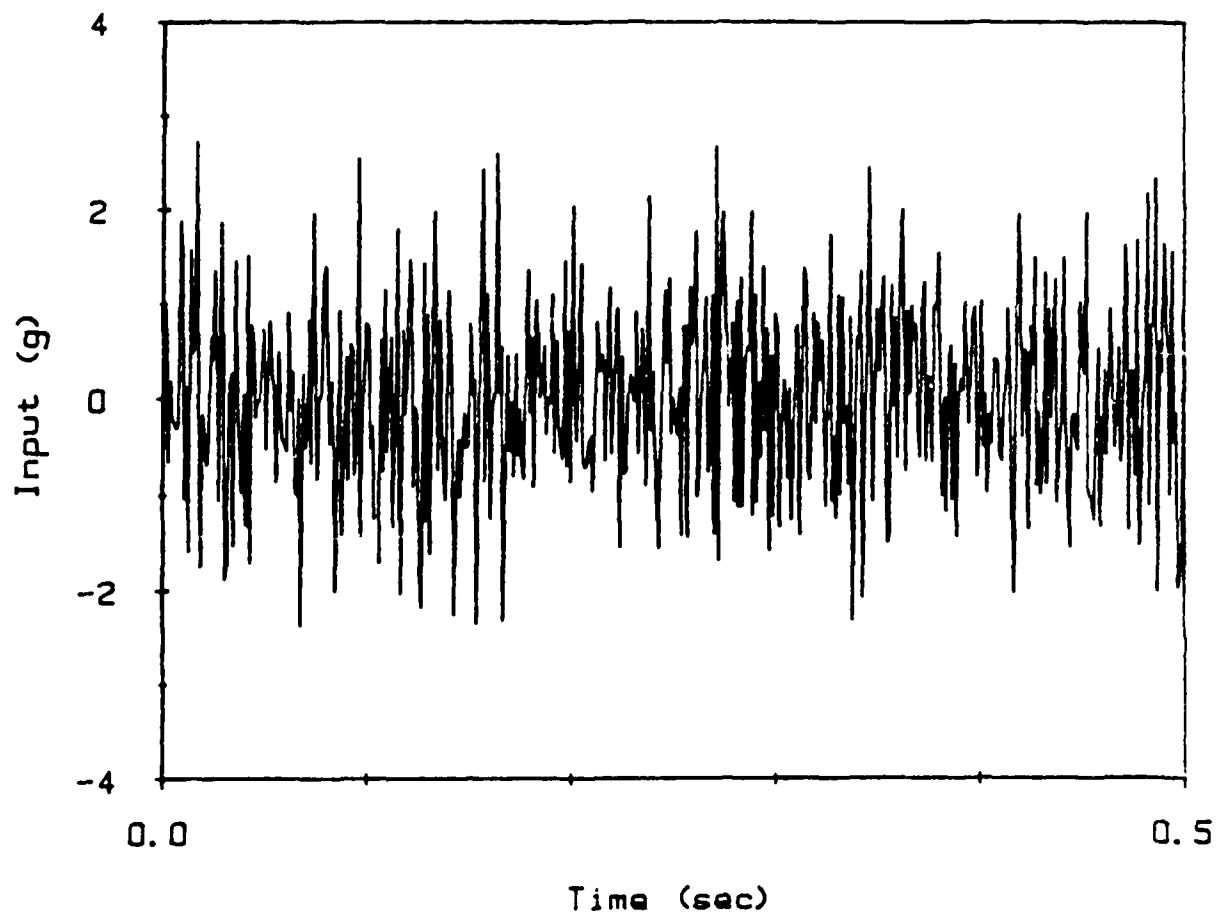


Figure 6: Pseudo-random input to the MDOF system.

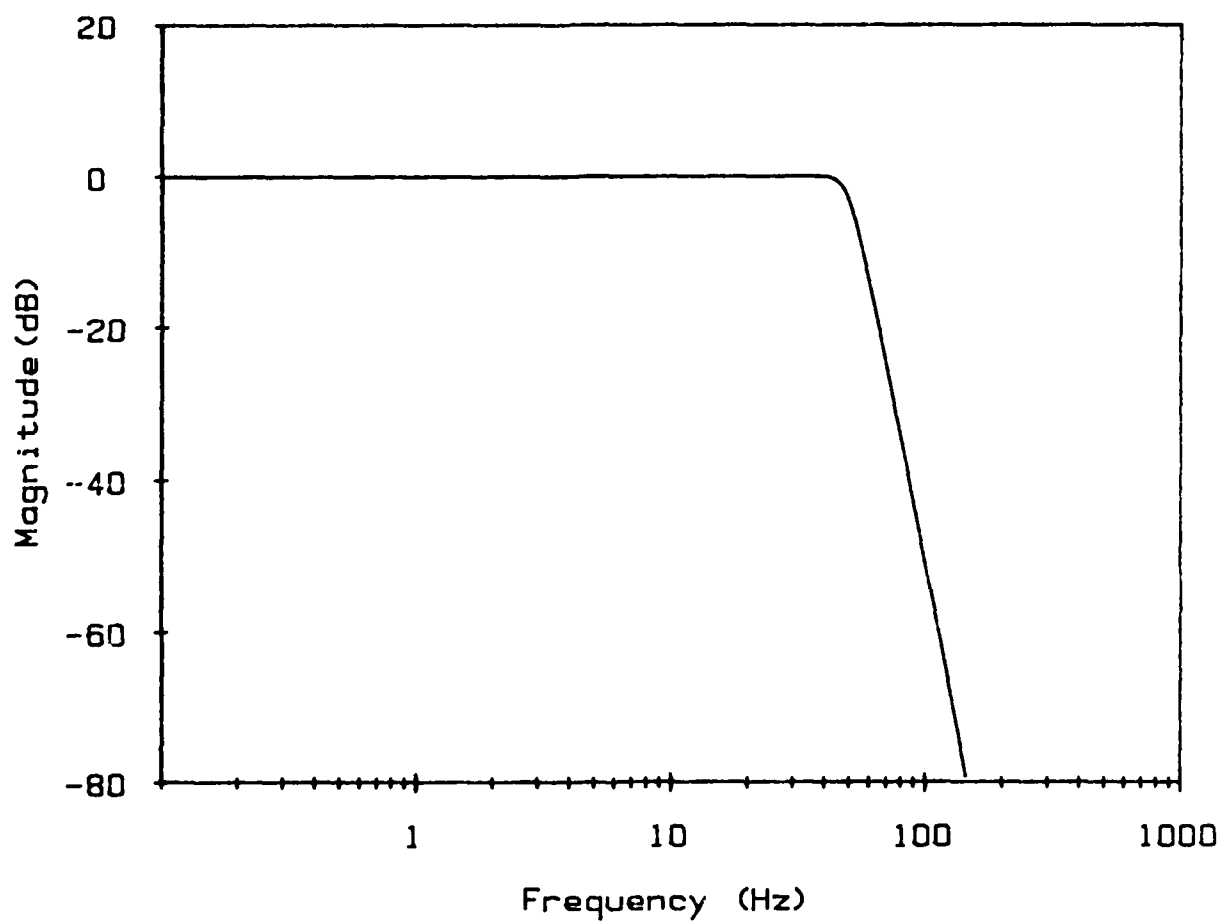


Figure 7: Frequency response of digital filter.

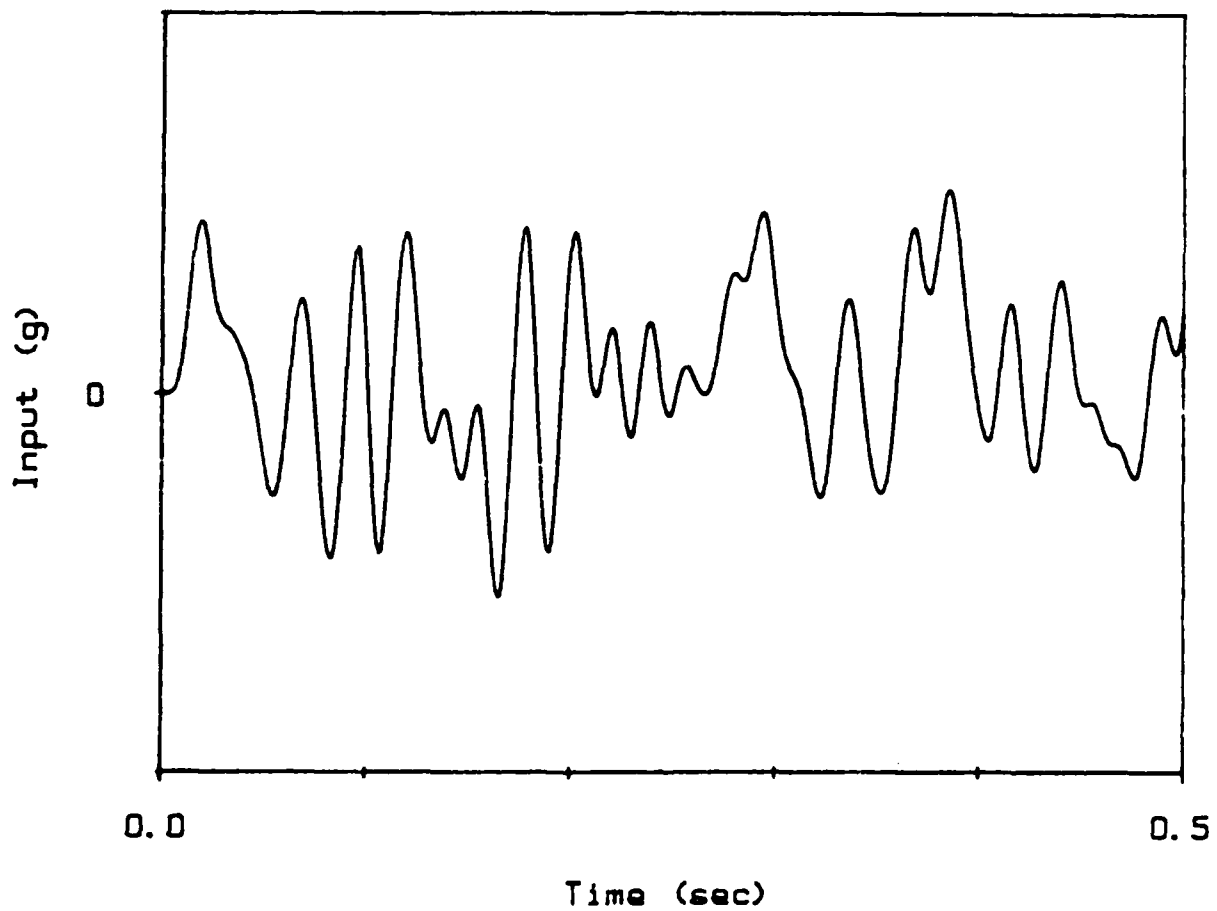


Figure 8: Filtered pseudo-random input to the MDOF system

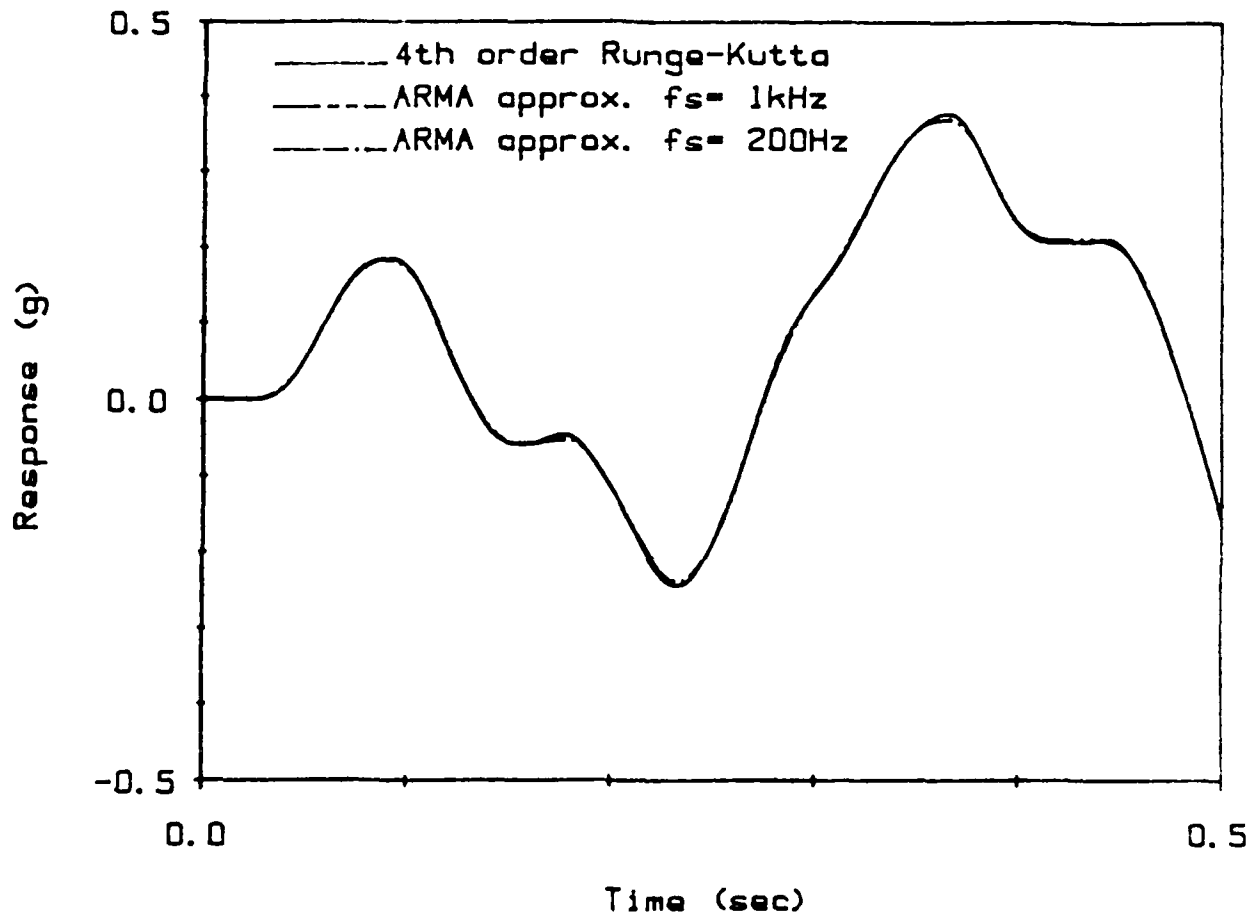


Figure 9: Simulated response of the MDOF system to the filtered pseudo-random input.

integration algorithms. The discrete time transfer function in the form of an ARMA model is a numerical integration scheme requiring similar sampling rates. The parameters of the ARMA model are just weights of the numerical integration scheme. The goal of this report is to investigate methods for determining these weights from real experimental structural response data, so that the ARMA model can be determined from experimental measurements and then used to predict vibration response. The following sections describe numerical methods that can be used to estimate the parameters of the ARMA model.

PARAMETER IDENTIFICATION

The goal of system modeling and parameter identification is to decide on the form of the model and then identify the parameters of the model. Often the choice of the model form and parameterization of the model are done at the same time. Here, the focus is on the use of the discrete time transfer function or the ARMA model for structural vibratory prediction. The model form is fixed except for the choice of the size (or order) of the model. Experimental data from the structure itself are needed to determine the proper order. Once the order is selected, experimental data are used to parameterize the ARMA model. Some consideration must be made of the choice of experimental data and the data acquisition procedures. Once data are collected, an identification algorithm must be chosen to parameterize the model. This section describes some of the difficulties in data acquisition procedures and model order selection based upon the free response autocorrelation matrix.

Data Acquisition and Filtering

In order to parameterize a SISO ARMA model, one needs to simultaneously measure the input and output time series. Usually the data is acquired with the aid of anti-aliasing filters. The anti-aliasing filters are low pass filters which are used to limit the bandwidth of the experimental signals. They are helpful in eliminating high frequency noise and high frequency modes. The filters truncate a high or infinite degree of freedom system to a lower order system with modal frequencies in the allowable, selectable bandwidth. An ideal low pass filter causes no phase or magnitude distortion of the sinusoidal components of the signal below the cutoff frequency and truncates the sinusoidal components of frequencies above the cutoff frequency. Practical low pass filters distort the phase and magnitudes of the sinusoidal components of the signal below the cutoff frequency and only attenuate the higher frequency components. Low pass filters distort the signal frequency according to the filter's transfer function. The Fourier transform of the signal prior to filtering ($X_{in}(\omega)$) is altered to yield,

$$X_{out}(\omega) = F(\omega) X_{in}(\omega) \quad (24)$$

where $F(\omega)$ is the frequency response of the low pass filter. The z-transform is analogously altered by the filter

$$X_{out}(z) = F(z) X_{in}(z) \quad (25)$$

where $F(z)$ is the discrete time equivalent of $F(\omega)$. When both the measured input and the output time series have been conditioned by filters, the discrete time transfer function between the measured input and the output time function is

$$G(z) = \frac{Y(z) F_y(z)}{U(z) F_u(z)} \quad (26)$$

where $F_u(z)$ and $F_y(z)$ are the discrete time transfer functions of the input and output anti-aliasing filters. The discrete time transfer function, $G(z)$, will be unaffected by the filters when the two anti-aliasing filters have the same frequency response function. Thus, if filters are identical and are set at the same cutoff frequency, the identification procedure can treat the measured response as if it had not been filtered.

If the filters are not identical, then the measured data must be corrected so that the filters do not affect the transfer function. The correction takes place in the frequency domain using the convolution properties of the Discrete Fourier Transform (DFT) (reference 12). The measured time series is first converted into the frequency domain using an FFT. The DFT of the signal is corrected to compensate for the filter and the corrected frequency domain response is converted back into the time domain using an inverse-FFT. The difficulties with the procedure is that the DFTs have leakage and aliasing errors that may result in a further noise corruption of measured data. Also the transfer function of the filter must be known precisely to compensate in the frequency domain.

There is also resolution noise introduced by the digitization of the signal. The analog-to-digital converters have a finite number of values to assign the infinite possibilities of a voltage range. For example, 4096 values may be assigned by the computer to voltages between +1 and -1 Volt. If only 10 percent of the voltage range is used, only 410 different values would be used to define the continuously varying signal. The resolution noise is reduced by using as much of the entire voltage range as possible, thus amplifiers may be needed. The amplifiers may introduce more noise but, one hopes, not as much as the resolution noise. Also, the amplifiers may introduce additional distortion of the signal, since the amplifiers have a transfer function of their own. The goal of the data acquisition process is to digitize the input and output time functions while minimizing the noise and distortion.

System Order

Once data are taken, the ARMA model can be parameterized. The order of the ARMA model has to be selected for a given system. The order of the ARMA model given in Eqn 14 is the size of the integer p . If the system order is unknown apriori, it has to be arbitrarily selected or determined from experimental data. The free response can be used to determine order. Consider what happens to Eqn 14 when there is no input: the model reduces to

$$y(k) = -a_1 y(k-1) - a_2 y(k-2) - \dots - a_p y(k-p) \quad (27)$$

where the parameters, the a 's, are known as the Autoregressive parameters of the ARMA model. Equation 27 can be put in the form

$$[z^p + a_1 z^{p-1} + \dots + a_{p-1} z + a_p] y(k) = C(z) y(k) = 0 \quad (28)$$

Processes, like $y(k)$, that satisfy Eqn 22 are called Autoregressive (AR) processes. The model given by Eqn 27 is called an AR model. Note that the order of the AR model for system free response is identical to the order of the ARMA model for system forced response.

A summation of damped sinusoids, the free response of linear structural systems, can be modeled exactly as an AR process. (See Appendix B.) Furthermore, the order of the AR model is twice the number of modal frequencies or number of degrees of freedom in the system. The modal frequencies and damping factors can be extracted from the roots of $C(z)$, termed the characteristic equation in the time domain.

A crude procedure for determining system order is to count the number of peaks or modes in the the power spectrum of the system's free response or count the number of peaks in the system's frequency response plot (often automatically displaced on a spectrum analyzer). Problems occur when the signal is too noisy, the modes are too closely space to distinguish separate peaks, or one or more of the modes is highly damped, reducing the size of one or more peaks. Though the procedure can be effective for selecting order, it is not well-suited for digital automation. A method better suited for automation depends upon the discrete time free response autocorrelation matrix. Consider an AR process of order p given by Eqn 28 rearranged as

$$\sum_{k=0}^p a_k y(m-k) = 0, a_0 = 1. \quad (29)$$

If Eqn 29 is multiplied by $y(q-m)$ and the expected value taken, the result is the well known autocorrelation relation (reference 13)

$$\sum_{k=0}^p a_k R_{yy}(q+k) = 0 \quad (30)$$

The autocorrelation matrix, arbitrarily dimensioned $m \times m$,

$$\mathbf{R}_{yy} = \begin{bmatrix} R_{yy}(0) & \dots & R_{yy}(-m) \\ \vdots & \ddots & \vdots \\ R_{yy}(m) & \dots & R_{yy}(0) \end{bmatrix} \quad (31)$$

only has p linearly independent columns (if $m > p$). Thus it is possible to determine system order by determining the rank of the autocorrelation matrix. The only difficulty is in accurately estimating the autocorrelation matrix. Consider the measured time series

$$x(k) = y(k) + n(k) \quad (32)$$

where y is the signal, n is the noise, and x is the measured signal. The autocorrelation matrix of the signal is estimated by the autocorrelation matrix of the measured signal whose autocorrelation matrix is

$$[\mathbf{R}_{xx}]_{ij} = \frac{1}{N-m} \sum_{k=1}^{N-m} x(k+i)x(k+j) \quad (33)$$

where N is the number of data points and m is the size of the autocorrelation matrix. The rank of a matrix can be evaluated using its singular value decomposition. (See Appendix C.) A matrix of size m and rank p will have $m-p$ zero singular values. The autocorrelation matrix of $y(k)$ will have rank p , but the matrix is unavailable since $y(k)$ is not a measurable value. The autocorrelation of matrix of the measured signal $x(k)$ is available and will have full rank due to effect of the noise present in the signal. Consider the expected value of \mathbf{R}_{xx} when the noise process is statistically independent from the signal $y(k)$ and is an independent identically distributed process (reference 14) with variance σ^2

$$E [R_{xx}] = R_{yy} + \sigma^2 I \quad (34)$$

An independent identically distributed process, $n(t)$, has statistically independent realizations at different times but each realization comes from the same parent distribution. The rank of R_{xx} is thus full and not equal to the rank of R_{yy} . Some properties of the Singular Value Decomposition (SVD) and symmetric matrices can be used to reduce Eqn 34 to a useable form. The Singular Value Decomposition of R_{yy} , since it is symmetric, is

$$R_{yy} = U \Sigma U^T \quad (35)$$

where U is an orthonormal matrix. The identity matrix can be represented by UU^T , reducing Eqn 34 to

$$E [R_{xx}] = U (\Sigma + \sigma^2 I) U^T \quad (36)$$

The rank of R_{yy} can be determined by counting the number of singular values of R_{xx} above the variance of the noise. There are at least three possible problems with such a procedure. First, the variance of the noise is unknown. Second, Eqn 36 represents the expected value of R_{xx} which can only be estimated. Third, the noise may not be an independent identically distributed process. In fact, the expected value of the noise autocorrelation may not be a diagonal matrix. Though there are some limitations in the use of Eqn 36 to determine the system's order, it is a useful relation which has proven helpful in evaluating system order.

Examples

The *expected value* of the autocorrelation matrix for a independent identically distributed noise process is equal to the variance times the identity matrix. One expects a flat singular value "spectrum" of the autocorrelation matrix. The singular value (SV) spectrum is merely a plot of the singular values of a matrix (in decreasing order) against the index of the singular values. Figure 10 shows the singular value spectra of unity variance Gaussian noise for a varying number of points developed using Eqn 33. The size of the autocorrelation matrix (20x20) was arbitrarily chosen. The figure shows that the spectrum becomes flatter as the number of points used to estimate the autocorrelation matrix increases. When the noise SV spectrum is not flat, it is roughly linear with the central signal value (in this case, value number 10) roughly equal to the variance of the noise.

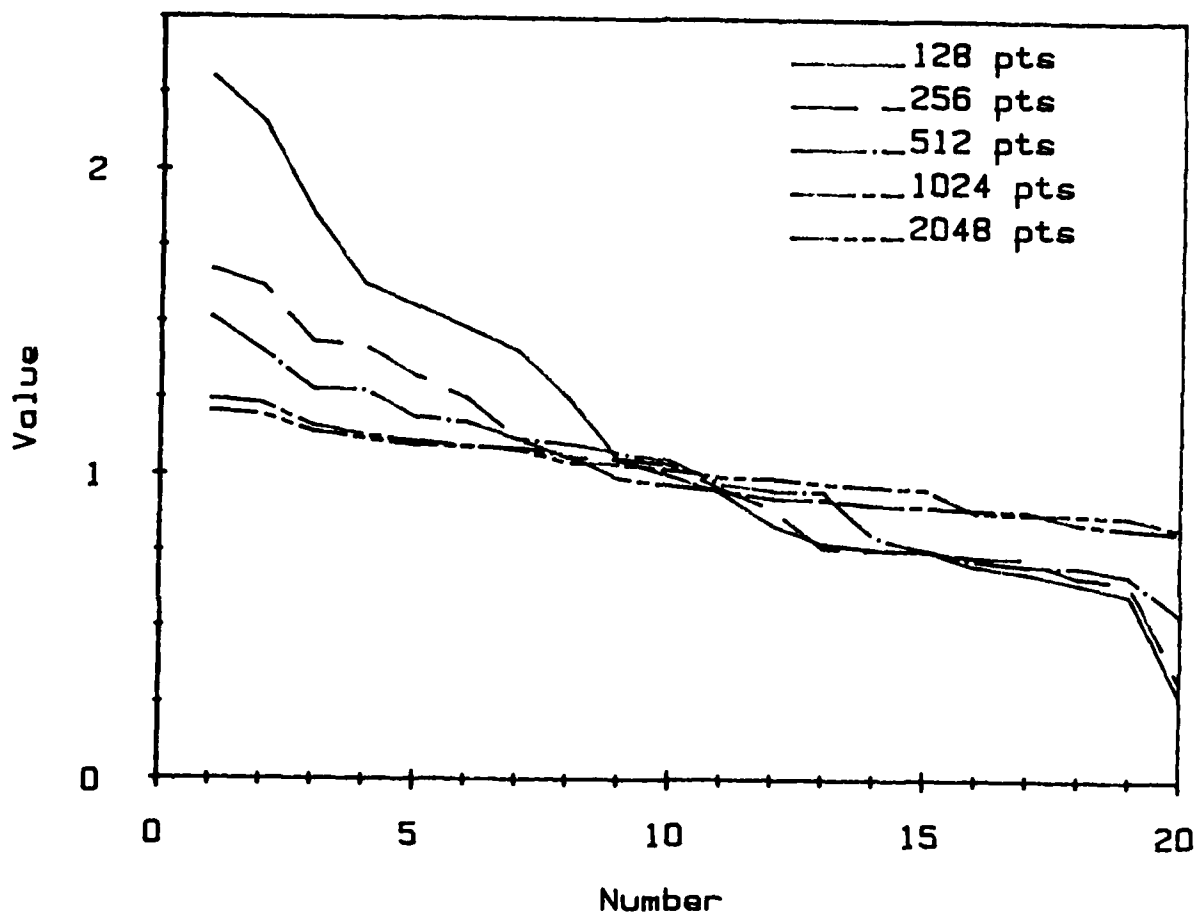


Figure 10: Singular Value Spectra of the autocorrelation matrix of unity variance gaussian noise.

Figure 11 shows the spectrum for a noiseless 6th order AR process (512 pts). The signal is composed of three damped sinusoids; it is therefore a simulated free response. There should be only 6 non-zero singular values. The spectrum does drop from roughly 10 for the sixth singular value to $2\text{E-}14$ for the seventh singular value. The seventh to the twentieth singular values range from $2\text{E-}14$ to $2\text{E-}15$, approximately equal to zero on the computer used for these calculations. Figure 11 indicates that the rank of the autocorrelation matrix is six.

Determining the rank of the autocorrelation matrix when there is no noise is relatively simple, but when noise is present in the signal, Eqn 36 can be used. Equation 36 says that the singular value spectrum of a noisy signal is the addition of the noise and the signal spectra. Figure 12 shows the spectra of the noise, the signal, and the noise plus the signal. The figure demonstrates that Eqn 36 is approximately true. With the knowledge that the noise spectrum is roughly linear, one would be able to surmise that the order of the system is six. Compare the ease of order determination using the singular value spectrum versus the use of the Power Spectrum shown in Figure 13. A structural dynamicist would be able to recognize that there are three significant peaks, but automating such a decision might be rather difficult. The problem is aggravated when there are closely spaced modes. Figure 14 shows the singular value spectra of a sixth order system with a pair of closely spaced modes (specifically at 14.6 and 15.0 Hz, which are roughly one DFT frequency bin apart) when the random noise is added. Extending the linear noise portion of the spectrum back indicates that a sixth order model is appropriate. The power spectrum shown in Figure 15 is ambiguous. It is very difficult to tell if there are three modes present or if the spectrum is noisy. The singular value spectrum may not be a "foolproof" method to select the system order, but the decision process when using the singular value spectrum is less subjective and more automated. If there is some doubt, the higher order model should be used because overspecification of the system order is not disastrous. An overspecified model may perform as well as a model with the proper order, but an underspecified model will not.

Overview

The problems of data acquisition and order selection were briefly discussed in this section. Free response can be used to determine system order through inspection of the singular value spectra. It must be noted that often it may be difficult or impossible to obtain

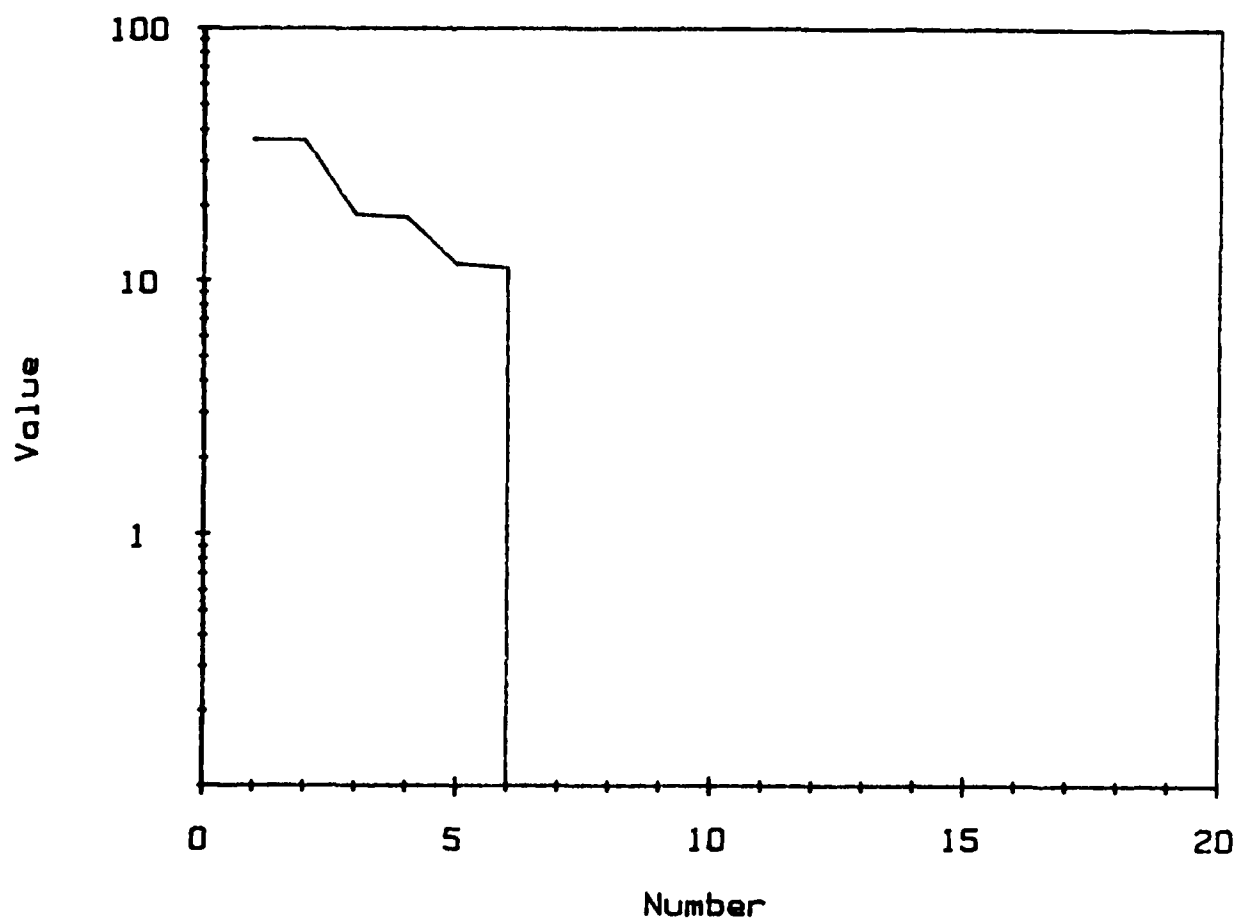


Figure 11: Singular Value Spectra of the autocorrelation matrix of a signal containing three damped sinusoids.

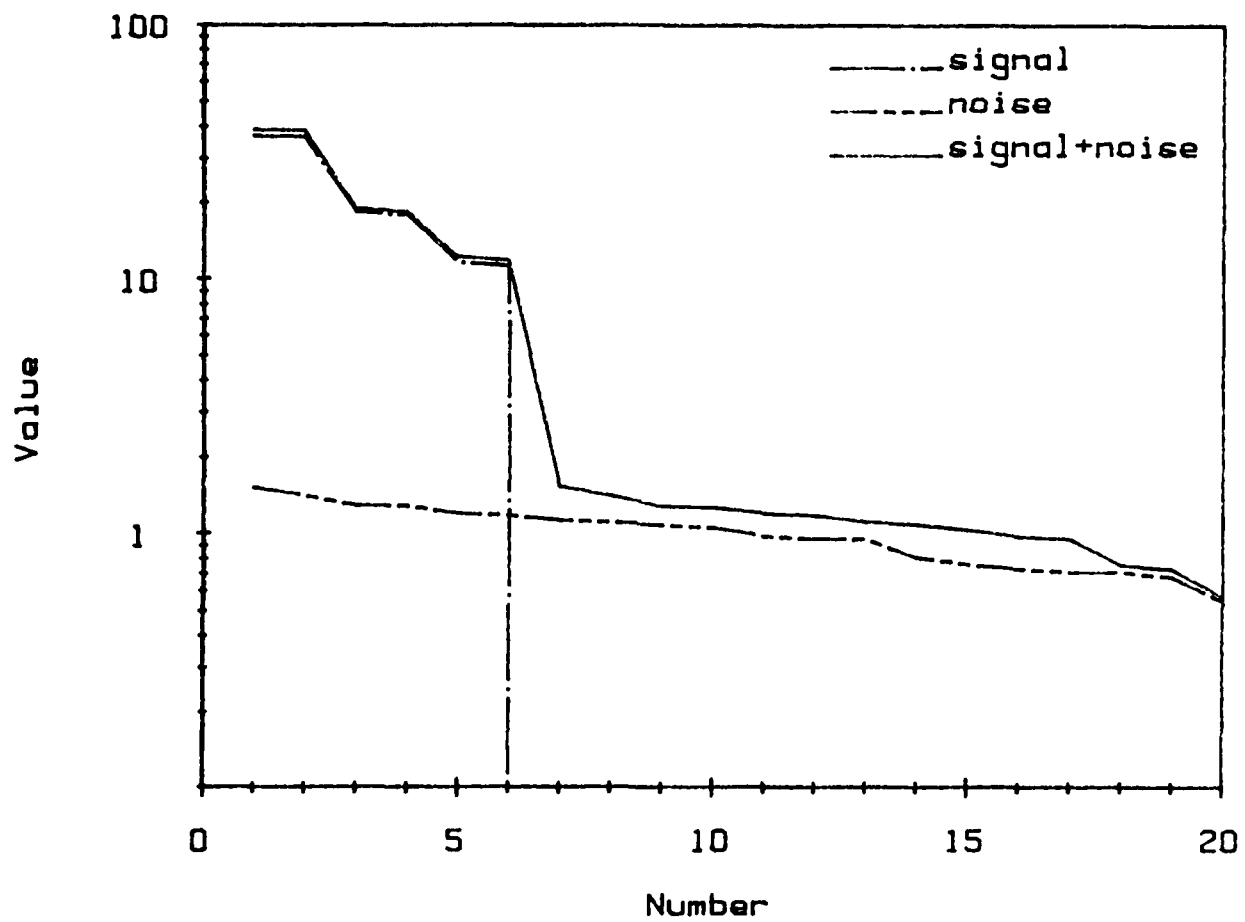


Figure 12: Singular Value Spectra of the autocorrelation matrices.

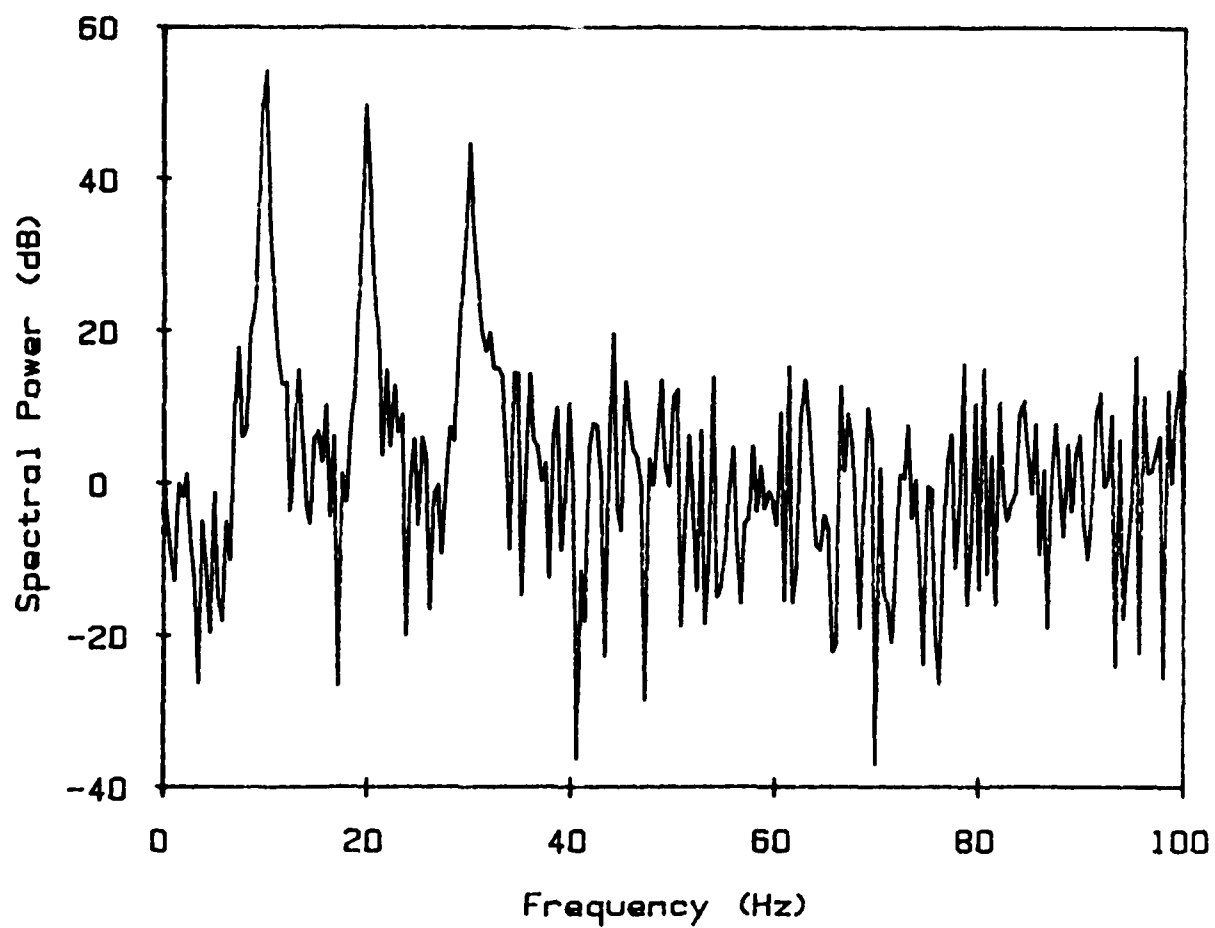


Figure 13: Power Spectrum of a noisy signal.

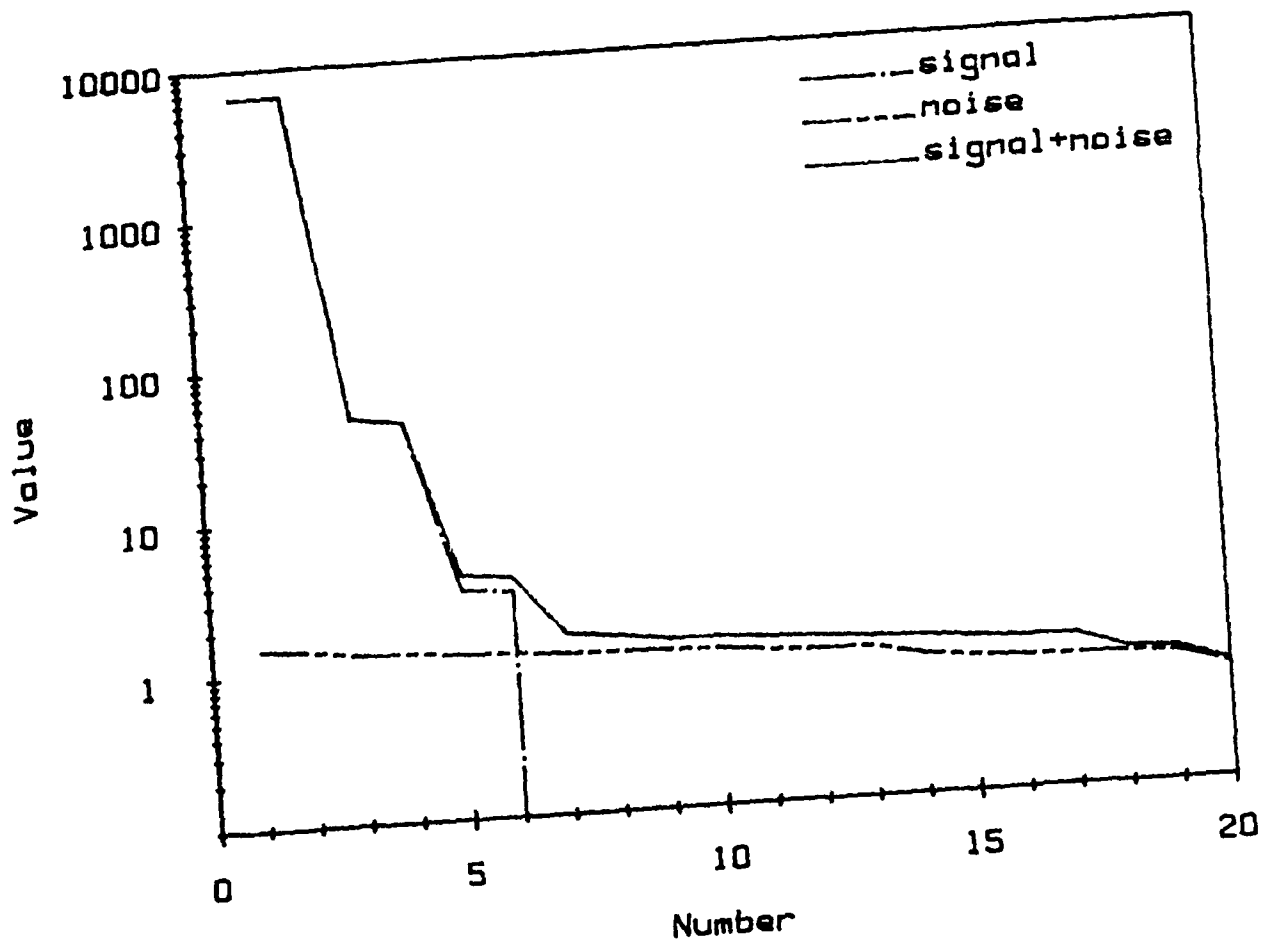


Figure 14: Singular Value Spectra of the autocorrelation matrices.

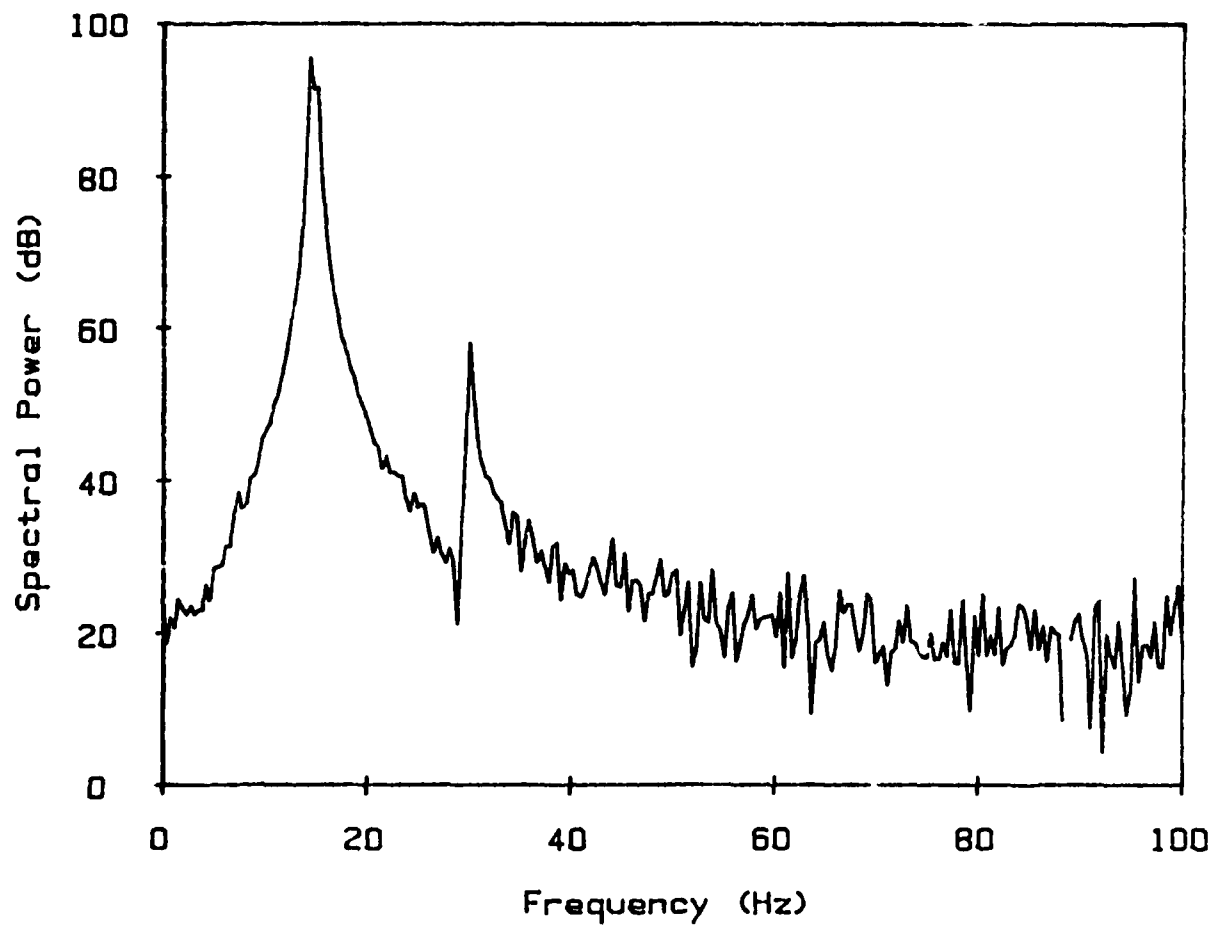


Figure 15: Power Spectrum of a noisy signal.

free response or the impulse response data. The system order may have to be selected while parameterizing the ARMA model. This can be accomplished by increasing the order of the ARMA model during the identification procedure until the estimated model is acceptable, by some measure. The resulting order of the ARMA model may not be the same as it would be using free response, and the ARMA model may end up being excessively large. Even if the free or impulse response is available, the proper order may not be selected as shown by the examples. Given an estimate of the ARMA model order and experimental data, the next step is to estimate the ARMA model. The next section presents identification procedures to do the ARMA parameter estimation.

IDENTIFICATION OF THE ARMA MODEL

This section presents some classical time domain identification methods that use experimental data to estimate the parameters of the ARMA model. The experimental data is used to write an overdetermined set of equations. The most straightforward way of solving these equations is the Least Squares method. Unfortunately, the Least Squares method produces biased parameter estimates. Many other methods exist that attempt to reduce the bias in some fashion. Some of these methods are included here.

The ARMA model

The ARMA model contains transient response terms, the AR part of the model, and forced response terms, the MA part of the model. The model can be written in vector form as

$$y_m(k) = [-y_m(k-1) -y_m(k-2) \dots -y_m(k-p) \quad u_m(k) \quad u_m(k-1) \quad u_m(k-p)]\theta + e(k) \quad (37)$$

where the subscript m denotes measured quantities, $e(k)$ denotes a residual or error, and

$$\theta = [a_1, a_2, \dots, a_p, b_0, b_1, \dots, b_p]^T \quad (38)$$

Identification algorithms are used to estimate the parameter vector, θ , by some criteria given multiple equations produced by varying the index k in Eqn 37. In order to identify the parameters of the ARMA model, Eqn 37 must be written for at least $2p+1$ different time instances. If the data is exact and from an ARMA process, the exact parameters can be found by solving the $2p+1$ equations. When noise corrupts the measured input and output discrete time histories, it is impossible to determine the ARMA model parameters exactly. An estimate of the parameters can be made by solving an overdetermined set of equations (more than $2p+1$ equations). There are various methods to solve this set of equations. The methods have varying criteria and will be presented in the following sections.

The Least Squares (LS) algorithm

The Least Squares algorithm solves the overdetermined set of equations by minimizing the sum of the squares of the residuals. If there are N data points in each time history, $N-p$ equations can be written, where p is the model order. The equations in matrix form are

$$\mathbf{A}_m \theta = \mathbf{g}_m + \mathbf{e} \quad (39)$$

where $\mathbf{g}_m = [y_m(p+1), y_m(p+2), \dots, y_m(N)]^T$ (40)

$$\mathbf{e} = [e(p+1), e(p+2), \dots, e(N)]^T \quad (41)$$

and

$$\mathbf{A}_m = \begin{bmatrix} -y_m(p) & \dots & -y_m(1) & u_m(p+1) & \dots & u_m(1) \\ -y_m(p+1) & \dots & -y_m(2) & u_m(p+2) & \dots & u_m(2) \\ \vdots & \dots & \vdots & \vdots & \dots & \vdots \\ -y_m(N-1) & \dots & -y_m(N-p) & u_m(N) & \dots & u_m(N-p) \end{bmatrix} \quad (42)$$

Solving Eqn 39 by minimizing the sum of the squares of the residual is equivalent to solving a set of equations termed the normal equations,

$$(\mathbf{A}_m^T \mathbf{A}_m) \theta_{LS} = \mathbf{A}_m^T \mathbf{g}_m \quad (43)$$

The solution of the normal equations is

$$\theta_{LS} = (\mathbf{A}_m^T \mathbf{A}_m)^{-1} \mathbf{A}_m^T \mathbf{g}_m \quad (44)$$

where the term $(\mathbf{A}_m^T \mathbf{A}_m)^{-1} \mathbf{A}_m^T$ is referred to as the pseudo-inverse of \mathbf{A}_m . The normal equations become highly ill-conditioned as either the sample rate or the number of parameters increase. One method to reduce the ill-conditioning problem is to solve the overdetermined set of equations through a technique termed singular value decomposition. Solving the equations by singular value decomposition will result in a LS estimate, but the equations are solved in a different fashion. (See Appendix D.)

The bias in the Least Squares estimate is apparent when Eqn 39 is premultiplied by the pseudo-inverse of \mathbf{A}_m , resulting in

$$\theta_{LS} = \theta - (\mathbf{A}_m^T \mathbf{A}_m)^{-1} \mathbf{A}_m^T \mathbf{e} \quad (45)$$

Taking the expectation of Eqn 45, yields

$$E [\theta_{LS}] = \theta - E [(A_m^T A_m)^{-1} A_m^T e] \quad (46)$$

Equation 45 shows that the LS parameter estimates are biased by the $E[(A_m^T A_m)^{-1} A_m^T e]$ term. It has been widely recognized that the LS estimates are biased (references 15 and 16). This sensitivity of the LS estimates to noise often makes the estimates unreliable. Usually an overspecification of the model order, which will be discussed later, or an iterative technique to improve the estimates can be used to reduce the bias.

Generalized Least Squares

The Generalized Least Squares (GLS) algorithm is an iterative technique used to improve the biased LS parameter estimates. The algorithm attempts to reduce the noise bias by modelling the residuals. The residual process is modeled as an Autoregressive (AR) process

$$0 = C(z) e(k) - \epsilon(k) \quad (47)$$

where $\epsilon(k)$ is another residual process. The model of the system is an ARMA model

$$A(z) y_m(k) = B(z) u(k) + e(k). \quad (48)$$

Multiplying Eqn 48 by $C(z)$ and using Eqn 47, yields

$$A(z) C(z) y_m(k) = B(z) C(z) u_m(k) + \epsilon(k). \quad (49)$$

If one defines $C(z) y_m(k)$ as $x(k)$ and $C(z) u_m(k)$ as $z(k)$, then the new system model is

$$A(z) x(k) = B(z) z(k) + \epsilon(k) \quad (50)$$

which is the basis for the GLS algorithm. The GLS estimate of the system model is the LS estimate using the transformed processes $x(k)$ and $z(k)$. The GLS algorithm in step form is:

1. Estimate θ_{LS} (Eqn 44).
2. Calculate the residual sequence $e(k)$.
3. Model the residual sequence as an Autoregressive Process.
4. Generate $x(k)$ and $z(k)$.
5. Compute θ_{GLS} : the LS estimate of (Eqn 50).
6. Go to Step (2) until θ_{GLS} converges.

The GLS algorithm replaces the residual process of the LS estimate, $e(k)$, by the residual process of the Generalized Least Squares estimate. The bias of the GLS estimate is hopefully smaller than the bias of the LS estimate because $\epsilon(k)$ will be of smaller magnitude than $e(k)$.

Reference 17 proposed a modification of the GLS algorithm called Modified Least Squares (MLS) estimation algorithm. The MLS algorithm also models the residual process as an Autoregressive process. The algorithm is noteworthy because it readily demonstrates the effect of the residual model. Equation 44 is rewritten as

$$\theta = \theta_{LS} + (A_m^T A_m)^{-1} A_m^T e \quad (51)$$

If e is estimated as an AR process, then there is a set of overdetermined equations based upon the residual sequence

$$e = \Omega c + \epsilon \quad (52)$$

The residual of Eqn 52, ϵ , is neglected and the Modified Least Squares estimate is written from Eqn 51 as

$$\theta_{MLS} = \theta_{LS} + (A_m^T A_m)^{-1} A_m^T \Omega c \quad (53)$$

The Generalized Least Squares algorithms model the bias term and add the result to the LS estimate in order to improve the estimate. The difficulties of the GLS algorithms are that they are iterative (and thus prone to computational stability concerns) and the size of the residual model has to be specified.

Instrumental Variables

The GLS method relies upon the AR model of the residuals to, in a sense, estimate the bias of the LS estimates and therefore better estimate the parameters. The Instrumental Variable (IV) technique attempts to force the bias towards zero by proper selection of a different "pseudo-inverse." Suppose that a matrix, Z , could be found so that

$$E[Z^T e] = 0$$

and

$$E[Z^T A_m] = R \quad (54)$$

where R is a non-singular matrix. The "pseudo-inverse" of $(Z^T A_m)^{-1} Z^T$ can be formed. Premultiplying Eqn 41 by this "pseudo-inverse" yields

$$\theta_{iv} = \theta - (Z^T A_m)^{-1} Z^T e \quad (55)$$

where

$$\theta_{iv} = (Z^T A_m)^{-1} Z^T g_m \quad (56)$$

Here the expected value of the IV estimate is the parameter vector. The main problem with the IV method is the selection of Z . The matrix Z is comprised of instrumental variables and is structured similar to A_m . The instrumental variables should be correlated to the noise-free signal and uncorrelated to the noise. The perfect set of instrumental variables is the noise-free signal itself which is unavailable. An auxiliary model can be used to generate the instrumental variables and hence the matrix Z . Reference 18 has shown that any stable model of the same order as the system provides consistent unbiased IV estimates, when there is no noise in the input measurements. The Z matrix is constructed from the instrumental variables by substituting Z for A_m and the output of the auxiliary model for the output of the system. Reference 15 has also assumed that the input is free of noise. The assumption that the input is noise free may be valid in control engineering where the input can be a reference voltage but the input will surely contain noise in structural applications.

Maximum Likelihood Method

The Maximum Likelihood Method (MLE), like the GLS algorithm, assumes that the residual sequence is an AR process and uses the model

$$\epsilon(k) = \sum_{i=0}^p a_i y_m(k-i) + \sum_{i=0}^p b_i u_m(k-i) + \sum_{i=0}^p c_i e(k-i) \quad (57)$$

The parameters, the a_i , b_i , and c_i , are estimated to maximize the probability of the $\epsilon(k)$ sequence under the normal probability density function. References 3 and 19 give an iterative algorithm to perform the estimation. The major difficulties with the MLE method are that the method is iterative and the assumption of normal residuals may not be valid in many cases.

The Overspecified LS model

The main difficulty with the time domain estimation of the ARMA model is the estimation bias. The LS algorithm has been modified to produce the other major algorithms in hopes of reducing or eliminating the bias. The major difficulties of the algorithms are

that they are iterative in nature and lack the simplicity of the LS algorithm. In order to implement the LS algorithm one needs to "measure" the time series data, form matrices of the proper order, and invert a single matrix. There are no convergence considerations. An alternative way to reduce the bias is to overspecify the LS model. The additional parameters serve as additional modes which may be used to effectively model the noise. If the noise is adequately modeled, the residuals are reduced and the estimation bias is reduced. However, the overspecified model will contain extra poles and zeroes related to the noise. If the overspecified model is used to predict vibration, the noise modes will still be present. Usually the noise modes in the overspecified model are of such a low magnitude that the prediction is unaffected.

Examples

Four computer programs based on the LS, the GLS (actually the MLS form of the GLS algorithm), the IV (as proposed in reference 18), and the MLE (according to reference 19) were completed and simulated data contaminated with noise was used to test the algorithms. The Laplace domain model of the test system was

$$G(s) = (2s+100) / s^2+2s+100 \quad (58)$$

which was transformed by Tustin's Bilinear rule (sampled at 400 rad/sec) to

$$G(z) = \frac{0.02141 z^2 + 0.01207 z - 0.009335}{z^2 - 1.945 z + 0.969} \quad (59)$$

in the discrete time domain. Input time histories were developed to model random input to the system. Random numbers (uniform distribution) were determined to represent the input time increments. The magnitude of the input was gaussian. If the input time increment was greater than the system sample time, the input was assumed to vary linearly between input specification times. This was a simple attempt to set the "wave" length and spectrum of the input time series. The random time series was used as input to Eqn 59 to produce a noise-free system output time series. The output was then contaminated with simulated Gaussian noise at an signal-to-noise ratio (SNR) of 40 dB. The signal-to-noise ratio is defined as

$$SNR = 20 \log_{10} \frac{A_{rms}}{\sigma_{noise}} \quad (60)$$

where A_{rms} is the root mean square amplitude of the noise-free signal. Figures 16, 17, and 18 show three different random inputs that were used in the numerical experiments. Table 1 shows the parameter estimates of the four algorithms for each case.

It is clear that the IV method gives the best estimates of the AR parameters. The MA parameters are difficult to obtain and the estimation success is dependent upon the excitation (the input). The third input, which has the widest excitation range, appears to provide the best parameter estimates. This is related to the concept of persistent excitation and has not been discussed as yet. A persistent excitation is an input that provides enough information so that the Moving Average parameters can be accurately estimated. Though all three inputs appear to be persistently exciting, there seems to be an optimal input among the three. The concept of optimal input is discussed in reference 20.

The LS estimates are biased when noise is present. System parameters developed using a non-overspecified LS approach would not be suitable for predicting vibratory response. Among the three iterative methods, the IV method was the most accurate method, the easiest to program, the quickest computationally, and the most stable method. The main difficulty with the IV algorithm is the generation of the instrumental variable. The method suggested in reference 15 requires that the input must be noise-free to insure convergence. If the input is a control system reference voltage, the assumption of noise-free input is valid. If the input is a structural measurement, the assumption is invalid.

Overview

A number of parameter identification algorithms have been discussed. All the algorithms are schemes to solve an overdetermined set of equations in order to estimate the parameters of a model. The key difficulty to be overcome is the effect of noise bias. Many of the algorithms utilize an iterative scheme to model the noise and improve the parameters. Other non-iterative algorithms simply overspecify the model order and use the additional modes of the model as a noise outlet. Usually the overspecified algorithms out-perform the iterative schemes both in computer cost and accuracy. The difficulty with the overspecified algorithms is the sorting of the noise modes from the true modes of the model. Time domain modal techniques such as the ITD and the ERA also use overspecification to reduce noise bias. These techniques use modal confidence factors

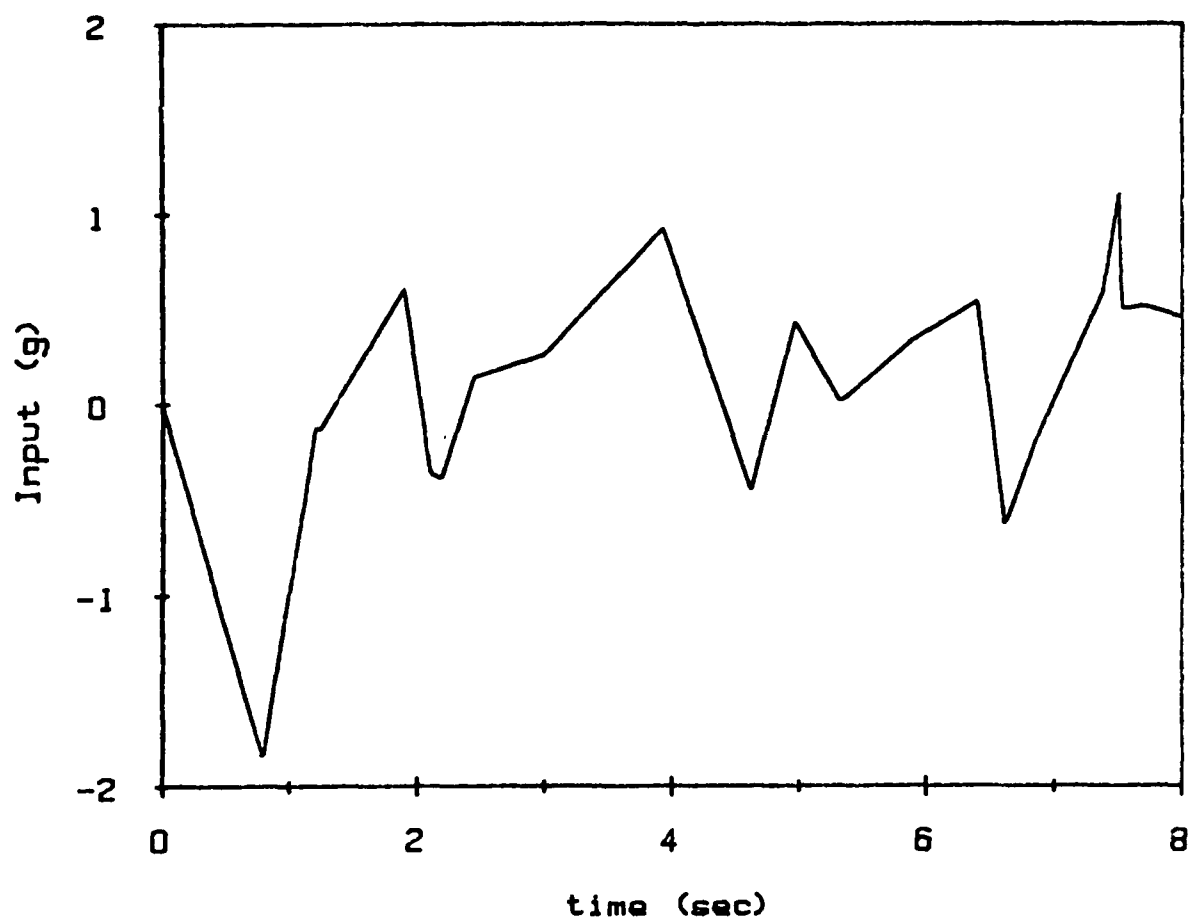


Figure 16: Input Case 1.

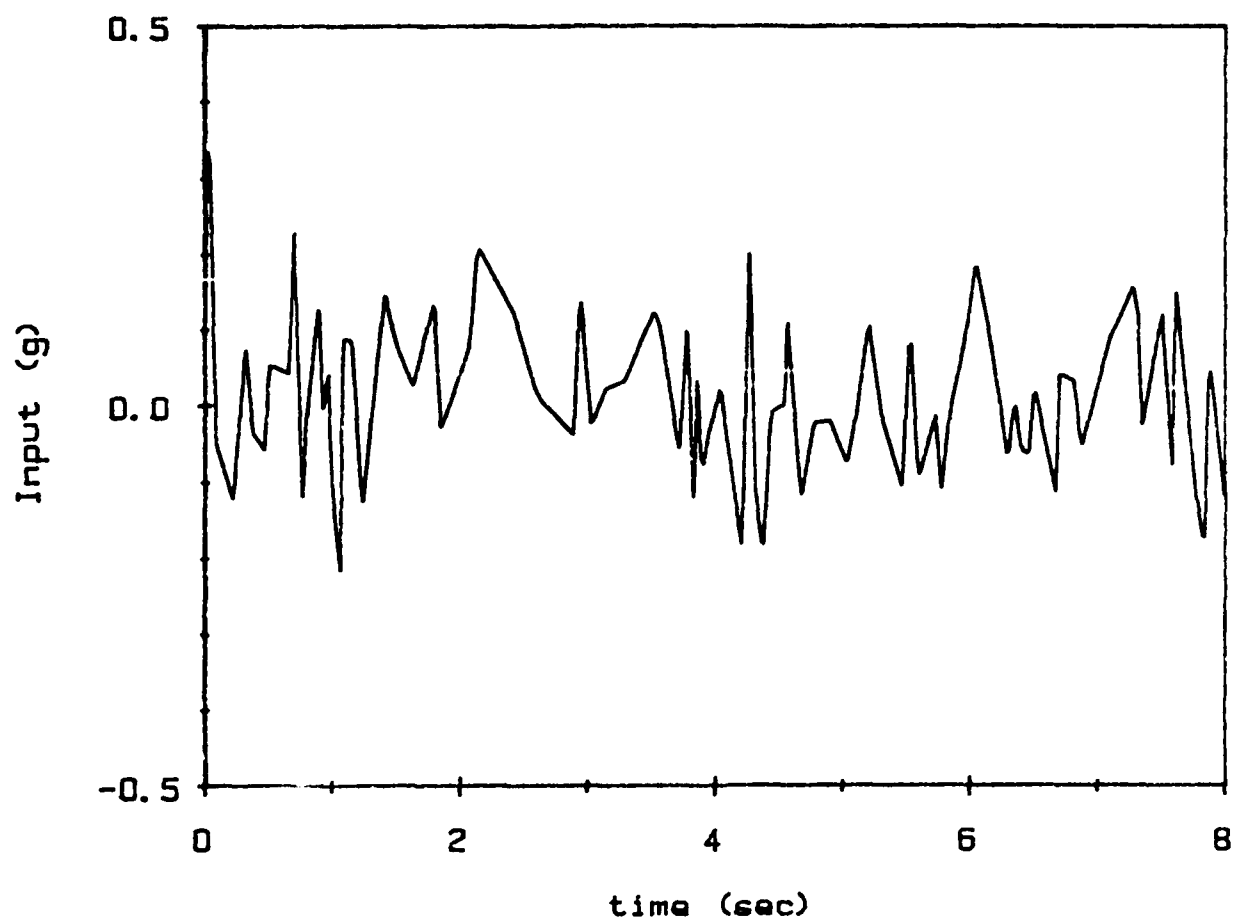


Figure 17: Input Case 2.

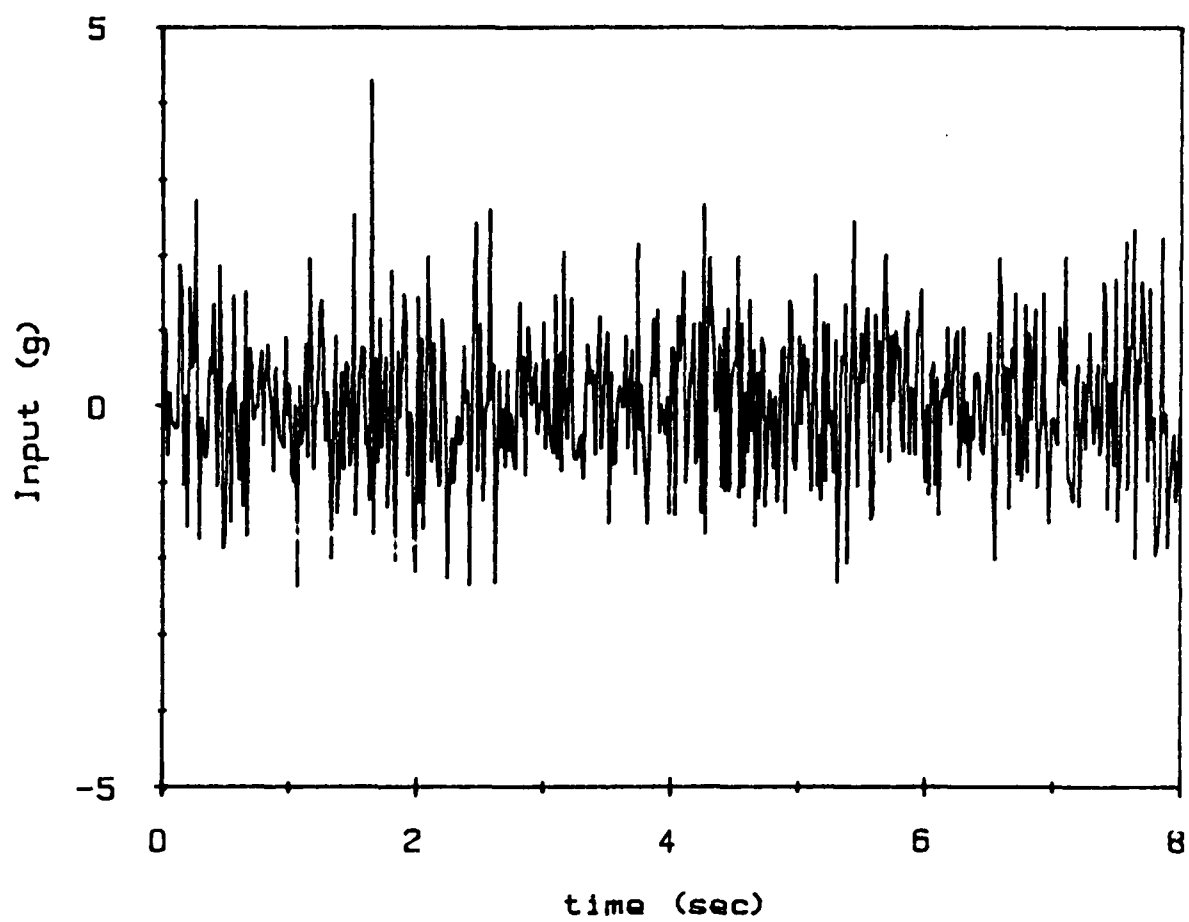


Figure 18: Input Case 3.

Table 1: Parameter Estimates

	a1	a2	b0	b1	b2
True values:	-1.945	0.969	0.0214	0.0121	-0.00934
Input = Case 1					
LS	-1.740	0.769	0.148	-0.116	0.00016
GLS	-1.875	0.892	0.135	-0.143	0.0238
IV	-1.947	0.971	0.128	-0.196	0.0929
MLE	-2.802	1.654	0.383	-0.712	0.176
Input = Case 2					
LS	-1.829	0.858	0.040	-0.024	0.0190
GLS	-1.860	0.884	0.034	-0.012	0.0085
IV	-1.942	0.967	0.040	-0.022	0.0094
MLE	-2.674	1.745	0.064	-0.070	-0.0307
Input= Case 3					
LS	-1.788	0.812	0.0194	0.0154	-0.0041
GLS	-1.857	0.877	0.0208	0.0138	-0.0059
IV	-1.941	0.966	0.0197	0.0128	-0.0082
MLE	-1.924	0.949	0.0207	0.0116	-0.0087

developed from mode shape information to sort the noise modes. The simplest and most efficient technique to identify an SISO ARMA model is to overspecify the model order before using the LS algorithm. But since there is no method at present to reduce the overspecified model once it has been estimated, the predictive model would be excessively large and contain noise-related modes.

FREE RESPONSE METHODS

The ARMA model can be identified in a single stage using the algorithms discussed in the previous sections or in two separate stages. In a two-stage method, the AR parameters are identified separately from the MA parameters. The AR parameters can be identified from free or impulse response records. Also, if the frequencies and damping factors are known, the AR parameters can be indirectly identified. All of the algorithms in the preceding section can be modified slightly to identify the AR model from free response. In addition, there are many time domain procedures that are used to estimate structural frequencies and damping factors. Among these are the Ibrahim Time Domain Technique (ITD), the Eigensystem Realization Algorithm (ERA), and the Complex Exponential Method (CEM). Essentially, these algorithms identify the pole locations in the z-plane. The poles locations can be used to identify an AR model. The algorithms can also be used to identify the complex mode shapes of the structure. These methods require free response or impulse response of the structure measured at many locations on the structure. Ideally, the AR model can be identified from a single signal. The structural identification techniques require more data and produce more information than might be desirable for the transient response prediction problem which this report addresses. There exists many algorithms in the signal processing field such as Prony's method, the Pisarenko Method, and the Principal Eigenvectors Method (PEM) which identify the frequencies and damping factors from a single response record. Recently, these signal processing techniques have made inroads into the structural identification field. The signal processing and the time domain modal methods are all linear prediction methods (reference 13) and are non-iterative. The major means of reducing bias errors using linear prediction is to overspecify the system order. The overspecification produces extraneous poles which must be distinguished from the signal poles. The time domain modal methods are able to distinguish the poles by building modal confidence factors. The modal confidence factors are determined by comparing the mode shapes of the two separate identifications. The signal processing techniques do not identify mode shapes and the extraneous poles must be distinguished from the signal poles by some apriori knowledge. The PEM can be modified slightly to automatically determine which poles correspond to the signal and which correspond to the noise.

The AR model

The Autoregressive model given by Eqn 27 can exactly model a signal comprised of damped sinusoids (Appendix B). The roots of the time domain characteristic, Eqn 28, are

directly related to the frequencies and damping factors by Eqn 8, where z and s are complex numbers. The frequencies and damping factors are related to the roots of the characteristic equation by

$$s_i = -\zeta \omega \pm j \omega_d \quad (61)$$

when substituted into Eqn 8 yields

$$z_i = e^{sh} = e^{-\zeta \omega h} (\cos \omega_d h + j \sin \omega_d h) \quad (62)$$

Thus, if one is able to model a signal as an AR process, a characteristic equation can be written using the AR parameters. The roots of the characteristic equation define the frequencies and damping factors of the sinusoids present in the signal. Conversely, if the frequencies and damping factors are known, the AR model can be determined using the approximations outlined above.

The locations of the poles, roots of the characteristic equation, in the z -plane are defined by the frequencies, damping factors, and sample rate in Eqn 62. One sees that the stability region ($\zeta > 0$) in the z -plane is inside the unit circle. Lines of constant damping are decaying spirals and lines of constant damped natural frequencies are straight lines as shown by Figure 19. According to Figure 19, the root locations get closer to the (1,0) point in the z -plane as the sample rate increases. As the root locations get closer to the (1,0) point, perturbations in the root locations result in greater errors in frequency and damping estimates. Figures 20 to 25 show the error envelopes for frequency and damping estimates for various root location perturbations. For instance, Figures 21 and 22 show that the identified damped natural frequency will be in error by around 10% as the root location travels to the (1,0) point (for a perturbation radius of 0.01) and the damping estimate will be in error over 400%. The figures show that damping error is much more sensitive to the exact damping value than is the frequency estimate and the size of the frequency envelope is approximately linear with respect to the perturbation size (See Appendix E.) The figures are different from those calculated in reference 2. The figures illustrate that when the sample rate is high and the damping factor is low (as with most identified structural systems), the roots of the characteristic equation must be identified very accurately for reliable estimates of frequency and damping factors and hence reliable vibratory response prediction. This means that the identification scheme must be accurate in the parameterization of the characteristic equation.

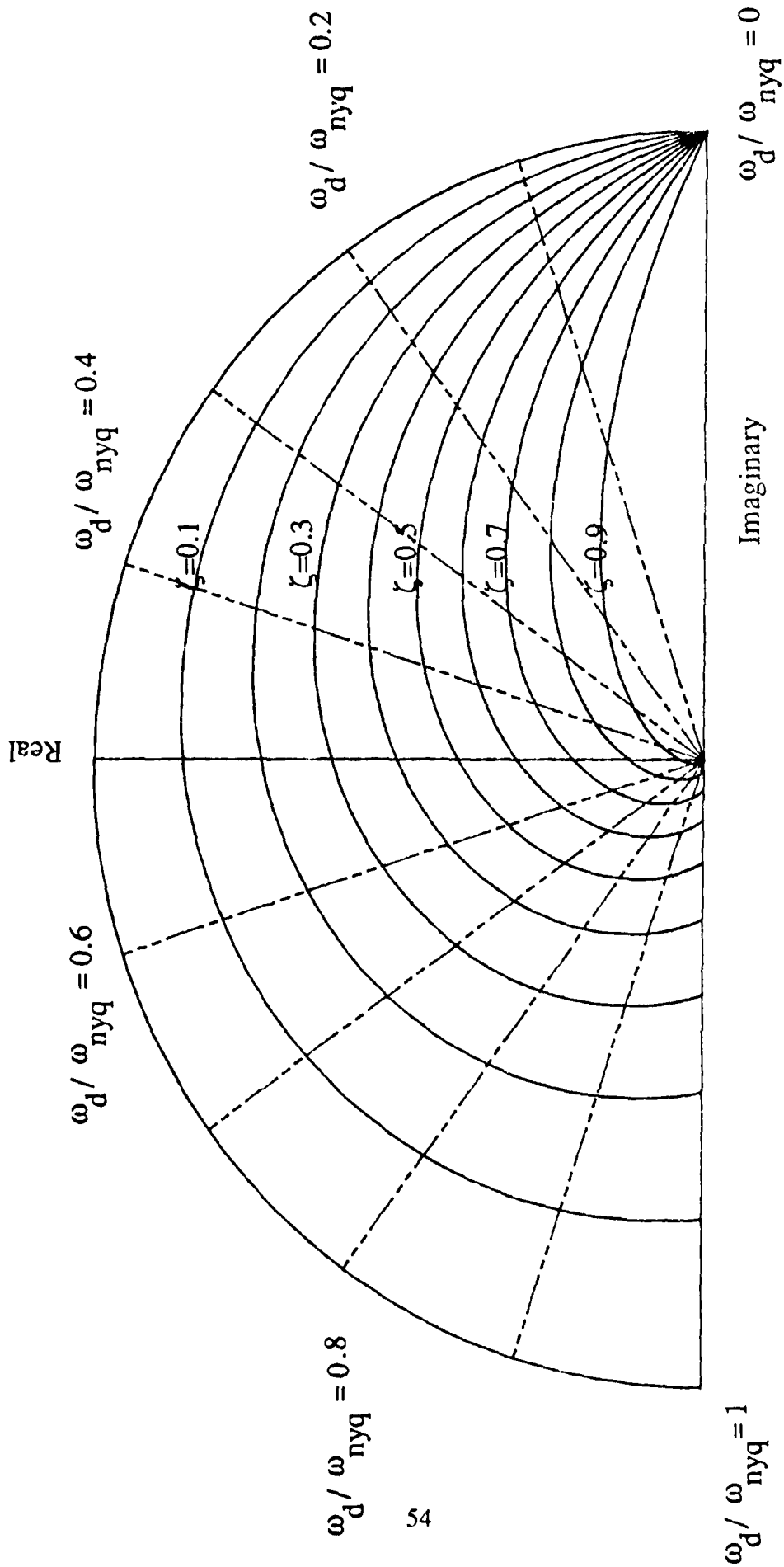


Figure 19: Contour map of discrete time transformation.

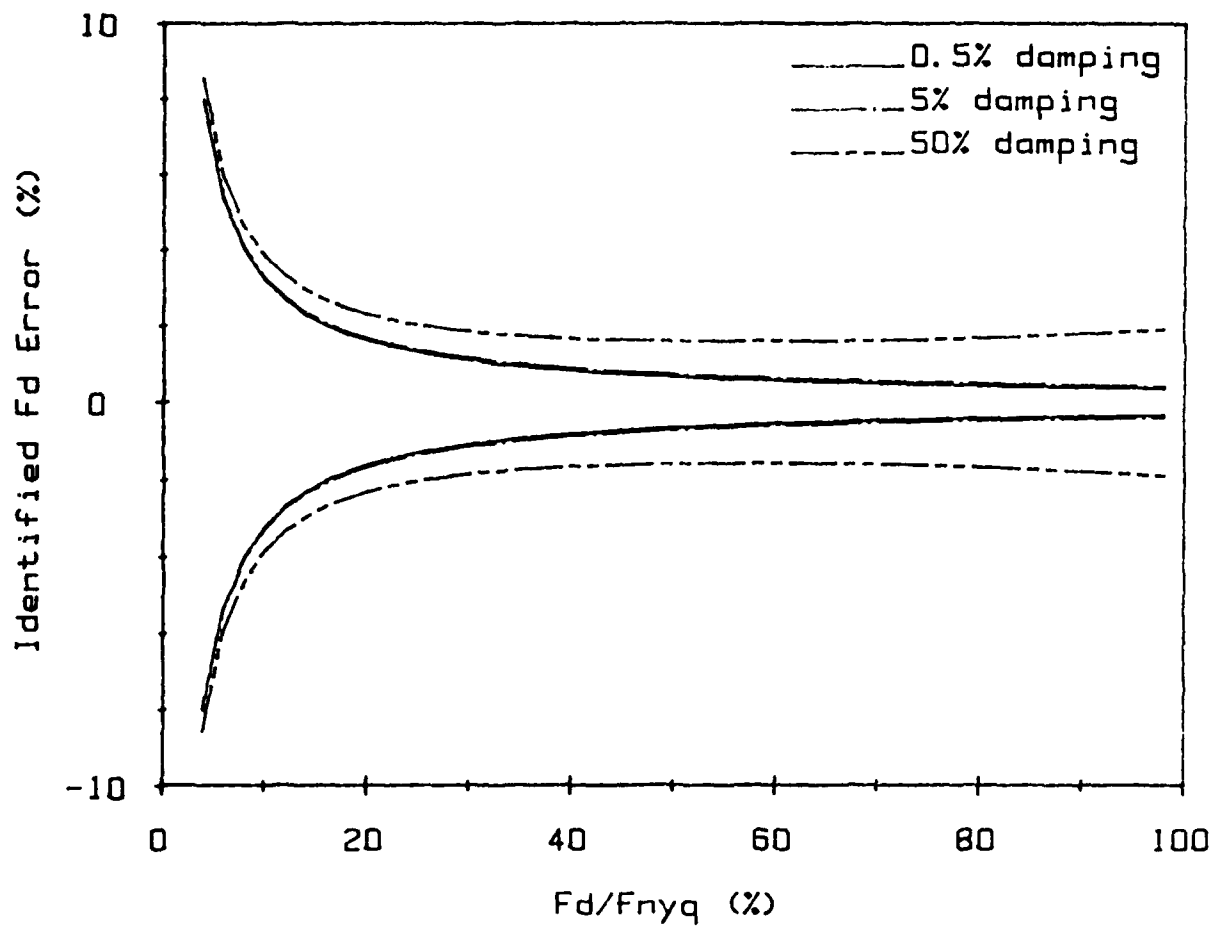


Figure 20: Envelope of percent damped frequency error
(radius of uncertainty =0.01).

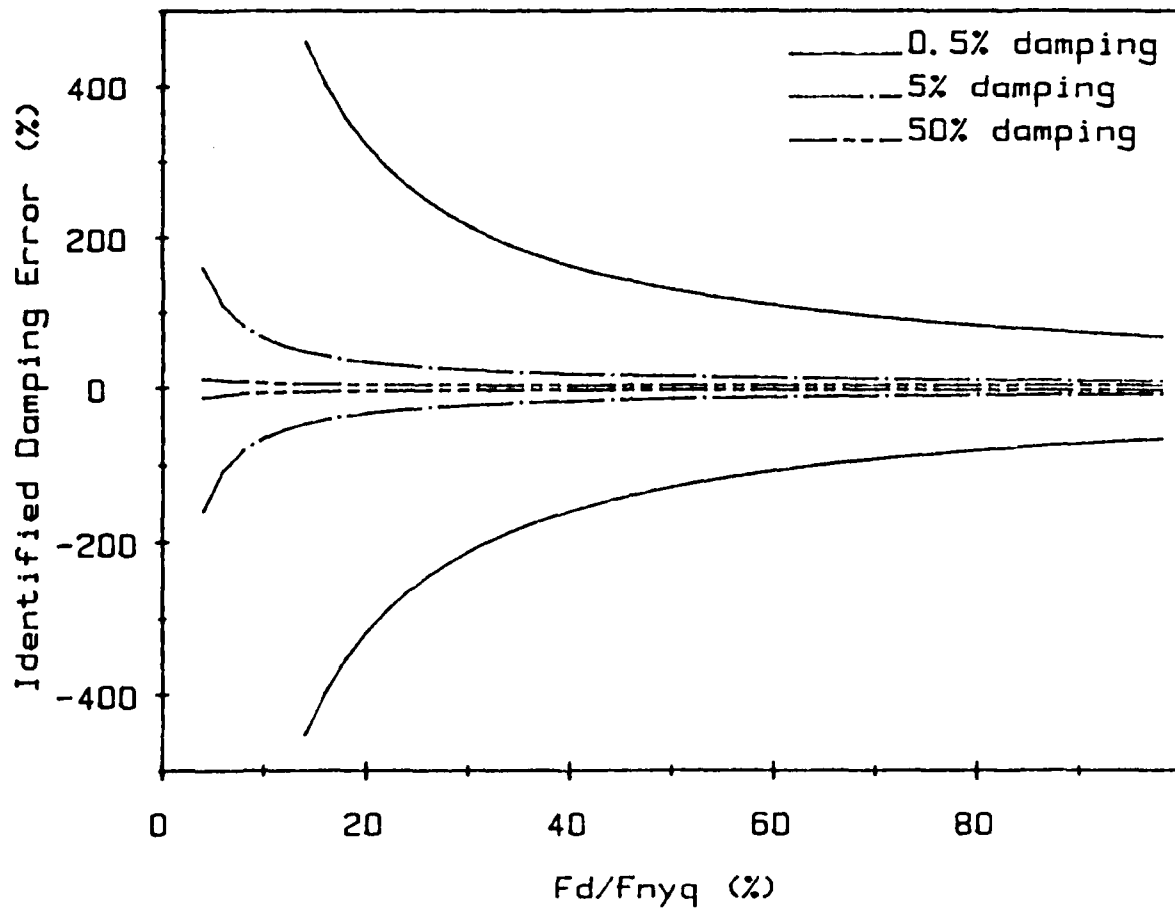


Figure 21: Envelope of percent damping error
(radius of uncertainty=0.01).

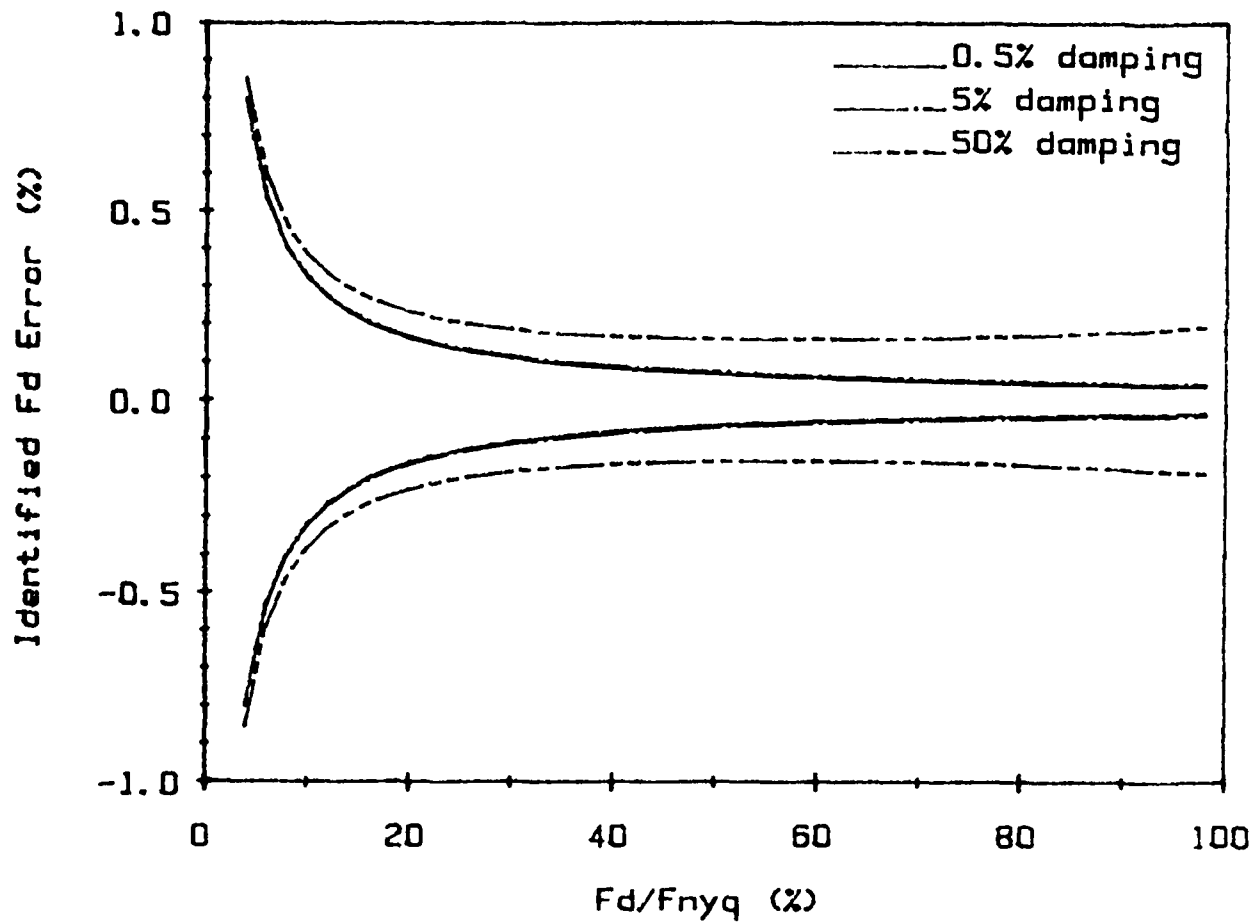


Figure 22: Envelope of percent damped frequency error
(radius of uncertainty =0.001).

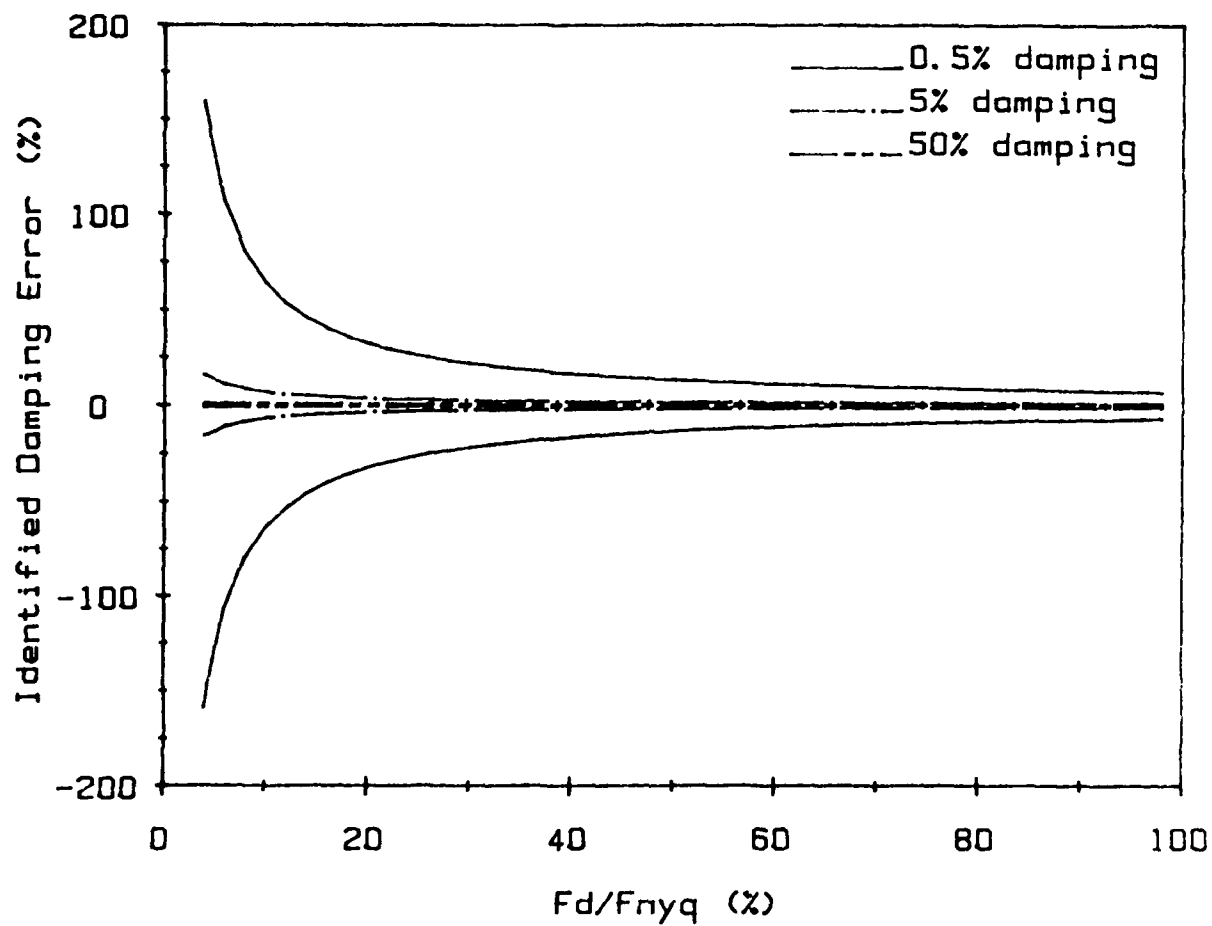


Figure 23: Envelope of percent damping error
(radius of uncertainty=0.001).

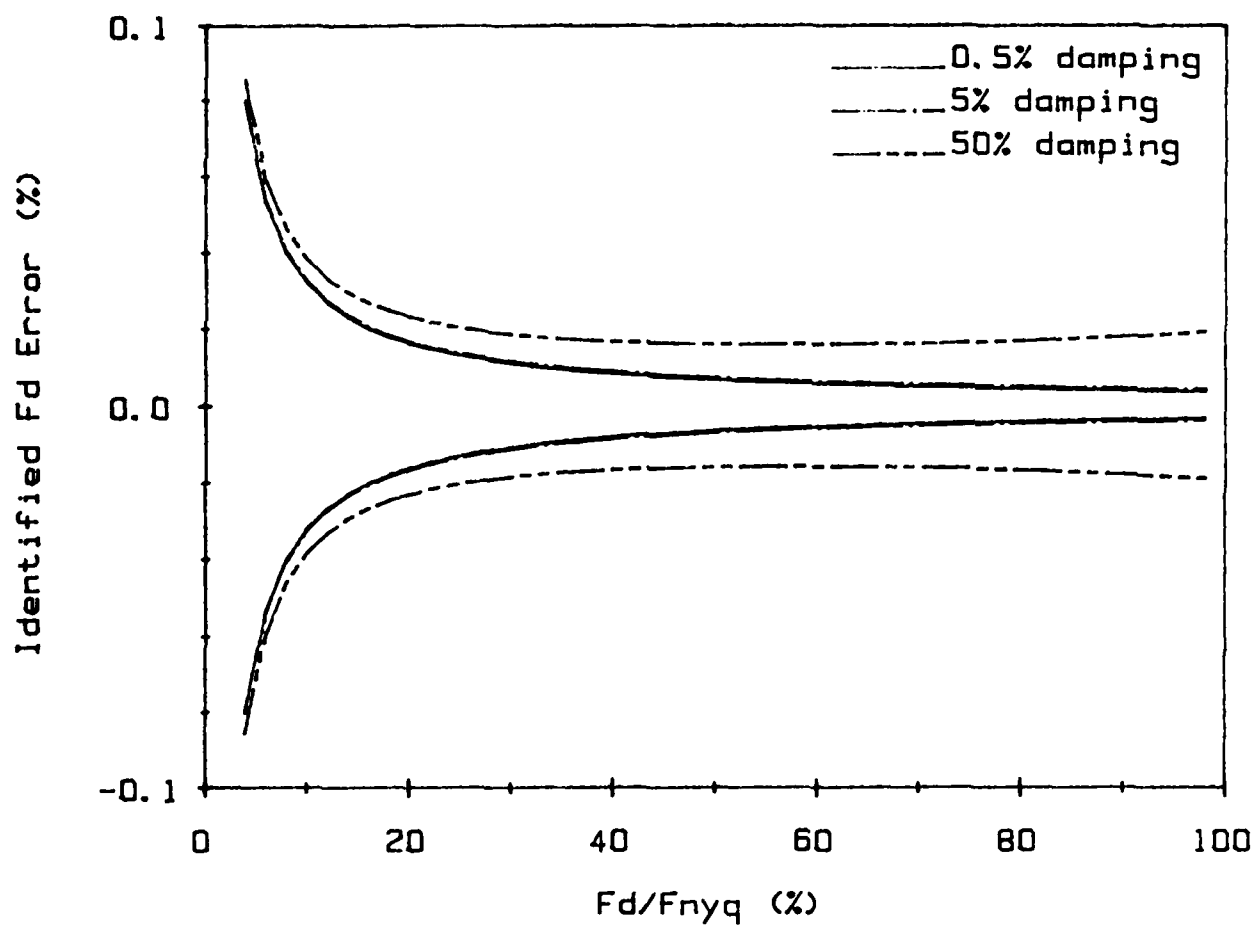


Figure 24: Envelope of percent damped frequency error
(radius of uncertainty = 0.0001).

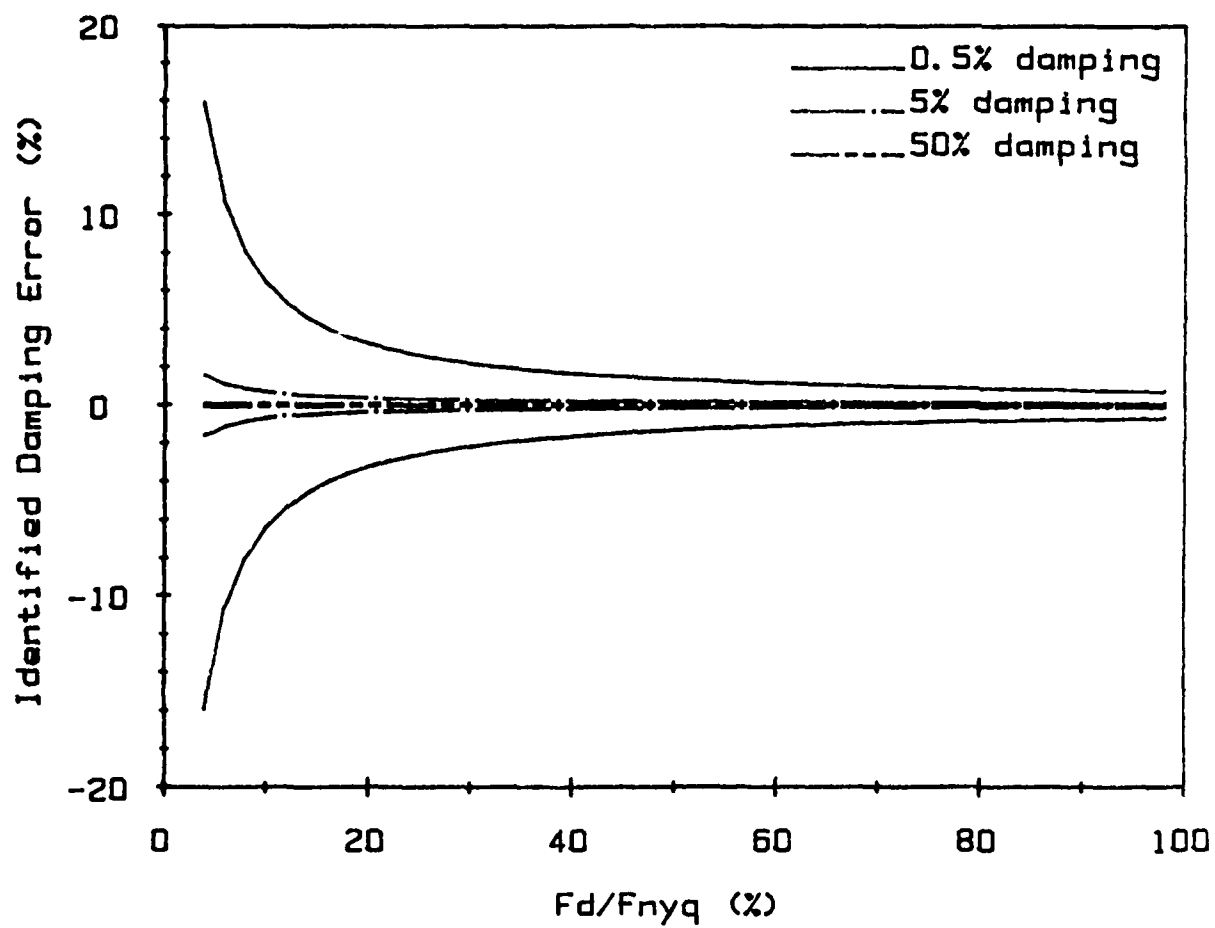


Figure 25: Envelope of percent damping error
(radius of uncertainty ≈ 0.0001).

Pisarenko Harmonic Decomposition

The first method discussed is the Pisarenko Harmonic Decomposition Method (PHD) and is also called the Total Least Squares (TLS) algorithm (reference 21). The PHD method is based upon the autocorrelation of an AR process. Equation 30 is written $p+1$ times and the AR coefficients are determined through an eigensolution.

$$\begin{bmatrix} R_{yy}(0) & \dots & R_{yy}(-p) \\ \cdot & \cdot & \cdot \\ \cdot & \cdot & \cdot \\ R_{yy}(p) & \dots & R_{yy}(0) \end{bmatrix} \begin{bmatrix} 1 \\ a_1 \\ \cdot \\ a_p \end{bmatrix} = 0$$

or

$$R_{yy} \theta = 0 \quad (63)$$

But R_{yy} is unavailable and R_{xx} must be used instead. Substitution of Eqn 34 into Eqn 63 yields

$$(R_{xx} - \sigma^2 I) \theta = 0 \quad (64)$$

which is an eigenvalue problem. The parameter vector is the eigenvector of R_{xx} which corresponds to the eigenvalue equal to the variance of the noise. Since the variance of the noise is not known apriori, one of the eigenvalues has to be chosen as the noise eigenvalue. Typically, the signals have a signal-to-noise ratio greater than 1, and the noise eigenvalue will be the eigenvalue with the lowest magnitude.

The Correlation Fit

Reference 21 suggests another methods based upon the autocorrelation relationship. The method is called the Correlation Fit (CF). In the CF method, Eqn 30 is written more than p times

$$\begin{bmatrix} R_{xx}(0) & \dots & R_{xx}(1-p) \\ \cdot & \cdot & \cdot \\ \cdot & \cdot & \cdot \\ R_{xx}(q-1) & \dots & R_{xx}(q-p) \end{bmatrix} \begin{pmatrix} a_1 \\ \cdot \\ \cdot \\ a_p \end{pmatrix} = - \begin{pmatrix} R_{xx}(1) \\ \cdot \\ \cdot \\ R_{xx}(q) \end{pmatrix} \quad (65)$$

with R_{xx} used as an estimate of R_{yy} . The $R_{xx}(0)$ term in the autocorrelation matrix is the most corrupt with noise because its expected value contains the variance of the noise, while the expected value of the other R_{xx} terms are the corresponding R_{yy} terms. The CF eliminates the first p equations in Eqn 65 because these equations contain the $R_{xx}(0)$ terms. The remaining $q-p$ equations can then be solved in a Least Squares fashion. Reference 21 compares the CF to other methods.

Overspecification of the AR model

Reference 21 also discusses some of the advantages of overspecification of the AR model. The process $y(t)$ was assumed to be an AR model of order p

$$A(z) y(k) = 0 \quad (66)$$

where $A(z)$ is a p th order polynomial in z . Multiplying Eqn 66 by an arbitrary polynomial in z of order q yields

$$D(z) A(z) y(k) = C(z) y(k) = 0 \quad (67)$$

or

$$[1 + c_1 z^{-1} + \dots + c_{p+q} z^{-p-q}] y(k) = 0 \quad (68)$$

The parameters of $C(z)$ can be determined by any of the other methods described. However, R_{yy} is singular for orders greater than p , so there are an infinite number of solutions to Eqn 68. But, $A(z)$ is a factor of $C(z)$, and therefore the AR parameters can be uncovered in any particular $C(z)$. The infinite number of possibilities for $C(z)$ are manifested by an infinite number of possible $D(z)$.

The Principal Eigenvectors Method

The Principal Eigenvectors Method (PEM) of identification is a simple modification of an overspecified LS solution. The PEM finds the unique overspecified parameter vector with a minimum norm. The PEM sets up the LS solution from an overspecified model

$$(A_m^T A_m) \theta = A_m^T g_m + e \quad (69)$$

The $A_m^T A_m$ matrix is a scaled version of R_{xx} and as such its rank is full (from the noise contributions) even in the overspecified form. However, the first p singular values

correspond to signal-plus-noise and the $q-p$ remaining singular values correspond to just noise. The matrix can be split by Singular Value Decomposition into a signal subspace,

$$(\mathbf{A}_m^T \mathbf{A}_m)_{\text{signal}} = \sum_{i=1}^p \sigma_i \mathbf{u}_i \mathbf{v}_i^T \quad (70)$$

and into a noise subspace

$$(\mathbf{A}_m^T \mathbf{A}_m)_{\text{noise}} = \sum_{i=p+1}^q \sigma_i \mathbf{u}_i \mathbf{v}_i^T \quad (71)$$

where the singular values are ordered from largest magnitude to the smallest. Since, a singular or ill-conditioned solution of the normal equations is expected and the factor $A(z)$ of the overspecified model $C(z)$ is desired, the noise subspace of $\mathbf{A}_m^T \mathbf{A}_m$ can be zeroed to reduce the effects of noise. The remaining solution is a singular solution with the useful property of being a minimum norm solution. (The length of the the overspecified parameter vector is the shortest of all the singular solutions.) The remaining noise in the matrix will affect the factor $D(z)$ and not greatly affect $A(z)$. The PEM effectively modifies the autocorrelation matrix and reduces the effects of the noise. The penalty paid for the modification is that the AR model had to be overspecified and will contain signal poles and extraneous poles. The only remaining difficulty is how to sort the roots of $A(z)$ from the roots of $D(z)$.

The Modified PEM

The estimates of the frequencies and damping factors are improved when the model is overspecified, but it is often difficult to distinguish the system frequencies and dampings from the extraneous ones introduced by the overspecified model. The Modified Principal Eigenvectors Method (MPEM) for damped exponentials (reference 22) addresses this problem. The MPEM solves a set of LS equations using the PEM, but, because of the way the equations have been written, the signal poles can be distinguished from the extraneous poles. The MPEM uses the mapping in Eqn 8 to estimate the frequencies and damping factors. The singular values of the discrete time autocorrelation matrix are obtained in the MPEM and the order of the system can be identified in an automated fashion.

The MPEM requires expressing the AR model in the backward direction and thus places stable poles outside the unit circle. The overspecified model is used to increase the

accuracy of the estimation in the presence of noise. The overdetermined equations for a Lth order backward linear prediction can be written in matrix form as

$$\begin{bmatrix} y_m(2) & y_m(3) & \dots & y_m(L+1) \\ y_m(3) & y_m(4) & \dots & y_m(L+2) \\ \vdots & \vdots & \ddots & \vdots \\ y_m(N-L-1) & y_m(N-L) & \dots & y_m(N) \end{bmatrix} \begin{pmatrix} c_1 \\ c_2 \\ \vdots \\ c_L \end{pmatrix} = - \begin{pmatrix} y_m(1) \\ y_m(2) \\ \vdots \\ y_m(N-L) \end{pmatrix} + \begin{pmatrix} e(1) \\ e(2) \\ \vdots \\ e(N-L) \end{pmatrix} \quad (72)$$

or

$$\mathbf{Q}_m \mathbf{c} = -\mathbf{d}_m + \mathbf{e} \quad (74)$$

The backward polynomial, the polynomial corresponding to the overspecified backward AR model, can be written as

$$C(z) = 1 + c_1 z + c_2 z^2 + \dots + c_L z^L \quad (75)$$

There are p roots of Eqn 75 located outside the unit circle representing the poles associated with the system frequencies and damping factors. There are L-p extraneous poles. The normal equations are

$$\mathbf{Q}_m^T \mathbf{Q}_m \mathbf{c} = -\mathbf{Q}_m^T \mathbf{d}_m = \mathbf{f} \quad (76)$$

Again the matrix on the left hand side, $\mathbf{Q}_m^T \mathbf{Q}_m$, is split into a signal subspace and a noise subspace, and the noise subspace is zeroed. This solution of the normal equations forces the extraneous poles inside of the unit circle, thereby allowing the system poles to be distinguished from the extraneous ones (reference 22). The solution is

$$\mathbf{c} = \sum_{k=1}^p \sigma_k^{-1} [\mathbf{u}_k^T \mathbf{f}] \mathbf{v}_k \quad (77)$$

where σ_k , \mathbf{u}_k , \mathbf{v}_k are p principal eigenvalues and eigenvectors of the singular value decomposition of $\mathbf{Q}_m^T \mathbf{Q}_m$. Reference 22 has shown that the MPDM does achieve the Cramer-Rao lower bound for the variance of the frequency and damping estimates. Once

the system frequencies and dampings are estimated from the MPEM, Eqn 8 can be used to estimate the AR parameters at any sampling rate.

Examples

1. Simulated Free Response

Simulated free response records were generated and corrupted with various kinds of noise. The major signal processing algorithms were used to estimate the damped natural frequencies and damping factors from the corrupted response. The types of corruption ranged from gaussian noise to correlated noise to constant bias. The simulated signals contained one, two, or three sinusoidal components and 256 points sampled at 2 kHz. The SDOF simulated data's natural frequency was 1 Hz with 1 percent damping. The two DOF simulated data contained frequency components at 1 and 10 Hz, with 1 percent damping. The three DOF simulated data contained frequency components at 1, 10, and 25 Hz, all damped at 1 percent. The sample rate was two thousand times greater than the first system frequency which placed the pole location very close to the (1,0) point. According to the error envelopes discussion at the beginning of this section, at such a high sampling rate the identification routines would have to estimate the pole location very accurately in order to accurately estimate the frequency and damping factor. In order to represent a system with natural frequencies such as these, one would need a sample rate of at least 500 Hz (twenty times the highest frequency). The sample rate that was used is four times greater than 500 Hz and represents an extremely difficult identification problem.

The algorithms used in the simulation were the LS, IV, PHD, MLE, GLS, CF, and MPEM. The LS algorithm was used in the classical form and in the overspecified form. The overspecified LS estimate required the apriori knowledge of the true frequency values to sort the signal frequency from the extraneous frequencies, knowledge that may not be available in an automated method. The IV technique is an iterative technique that uses the past iteration's estimation to generate an improved set of instrumental variables. Instead of iterating to improve the instrumental variables, fixed sets of instrumental variables were used in this example. The two sets of instrumental variables are labelled as IV_{perfect} and IV_{poor} in the following tables. The IV_{perfect} used the exact signal as the instrumental variables and represents the best set of instrumental variables possible. The IV_{poor} used data generated with nine-tenths of the exact frequency and represents an acceptable set of instrumental variables. The other iterative algorithms, MLE and GLS, were limited to two and a single iteration, respectively. The number of iterations were

limited because the autoregressive model of the residuals often were identified as unstable and the algorithms diverged. The MPEM was overspecified so that there would be four extraneous poles for every signal pole.

The SDOF data was first corrupted with gaussian random noise at a signal-to-noise ratio (SNR) of 40 dB. Table 2 shows the results from the identification algorithms. The iterative techniques (GLS and MLE) failed to estimate the frequency and damping factors locating the estimated poles on the real axis in the z-plane. The instrumental variables and Pisarenko methods estimated the damping factor as negative (unstable). The better estimates are the overspecified LS estimate and the Correlation Fit. The MPEM method estimated the damping factor as slightly negative which would not have been identified as a signal pole.

Next, correlated noise was added to the signal in the form of a 60 Hz noise and constant bias. The correlated noise required additional modes to model the noise. In the case of the 60 Hz signal one addition mode is required. In the case of a constant term, half a mode or an increase of the order by one was needed. Each root of the AR model is equivalent to an exponential in the signal. An added sine wave requires the addition of two complex exponentials; an added constant requires a single real exponential. Table 2 shows that the MPEM and the overspecified LS estimates are exact when the model was overspecified.

An additional frequency was added to the signal and the same types of noise were also added. Tables 3 and 4 show the frequency and damping estimates from the seven algorithms. Again the best estimates were from the overspecified LS algorithm and the MPEM. Since the LS algorithm requires apriori knowledge to distinguish noise and true modes and the MPEM does it automatically, the MPEM is considered the better method.

The third set of numerical experiments compared the MPEM to the LS and CF methods when the third frequency of 25 Hz was added. The LS and CF methods represent the best non-iterative methods *without* overspecification. The overspecified LS method was not considered because of the inability to distinguish modes without apriori knowledge. The added noise was uncorrelated gaussian noise and a higher *signal* frequency of 50 Hz with an amplitude two orders of magnitude less than signal amplitudes. The higher frequency represents a higher mode whose amplitude has been attenuated by a low pass filter. The final simulation contained the higher mode noise, uncorrelated gaussian noise at 40dB, and a constant bias. The final simulation represents real life data, a higher mode, uncorrelated noise at a reasonable level, and an slight error in balancing

Table 2: One DOF Simulated Data
 $(f_d=1.0 \text{ Hz}, \zeta=0.01, \text{Amp}=1., \phi=10^\circ, 256 \text{ pts}, f_s=2000 \text{ Hz})$

Algorithm	grv noise		60Hz noise		constant bias		constant bias	
	40dB rms		Amp=0.01		Amp=0.01		Amp=0.5	
	f_d	ζ	f_d	ζ	f_d	ζ	f_d	ζ
LS								
n=2	.*	.*	.*	.*	0.999	.012	0.793	.054
n=10	1.002	.023	1.000	.010	1.000	.010	1.000	.010
IV								
poor	1.012	-.011	0.942	.002	1.000	.011	0.974	.060
perfect	1.008	-.006	0.911	-.023	0.999	.012	0.958	.084
PHD	0.972	-.002	1.002	-.029	0.999	.012	0.793	.051
MLE (2 iter)	.*	.*	.*	.*	0.999	.012	0.797	.083
GLS(1iter)	.*	.*	.*	.*	0.999	.012	0.793	.054
CF	0.999	.011	1.005	.010	0.999	.007	1.077	.238
MPem (L=10)								
p=2	0.994	-.000**	0.997	.001	0.999	.011	0.791	.034
p=3	.†	.†	.†	.†	.†	.†	1.000	.010
p=4	.†	.†	1.000	.010	.†	.†	.†	.†

* unable to identify

** identified as extraneous

† case not considered

Table 3: 2DOF Simulated Data Results for 1st Mode
 $(f_d=1.0 \text{ Hz}, \zeta=0.01, \text{Amp}=1., \phi=10^\circ, 256 \text{ pts}, f_s=2000 \text{ Hz})$

Algorithm	grv noise		60Hz noise		constant bias		constant bias	
	40dB rms		Amp=0.01		Amp=0.01		Amp=0.5	
	f_d	ζ	f_d	ζ	f_d	ζ	f_d	ζ
LS								
n=4	.*	.*	.*	.*	0.999	.012	0.791	.052
n=10	1.003	.014	1.000	.010	1.000	.010	1.000	.010
IV								
poor	1.065	-.612	0.432	.915	1.000	.011	0.976	.057
perfect	1.040	-.595	1.033	.672	0.999	.012	0.959	.083
PHD	.*	.*	4.627	0.066	0.999	.012	0.790	.049
MLE (2 iter).	.*	.*	.*	.*	0.999	.012	0.797	.111
GLS (1iter)	.*	.*	.*	.*	0.999	.012	0.791	.052
CF	.*	.*	.*	.*	0.999	.007	1.096	.217
MPER (L=20)								
p=4	0.997	.006	0.998	.006	0.999	.011	0.788	.027
p=5	.†	.†	.†	.†	.†	.†	1.000	.010
p=6	.†	.†	1.000	.010	.†	.†	.†	.†

* unable to identify

† case not considered

Table 4: 2DOF Simulated Data Results for 2nd Mode
 $(f_d=10.0 \text{ Hz}, \zeta=0.01, \text{Amp}=1., \phi=20^\circ, 256 \text{ pts}, f_s=2000 \text{ Hz})$

Algorithm	grv noise 40dB rms		60Hz noise Amp=0.01		constant bias Amp=0.01		constant bias Amp=0.5	
	f_d	ζ	f_d	ζ	f_d	ζ	f_d	ζ
LS								
n=4	10.001	.070	.*	.*	10.000	.010	9.999	.010
n=10	10.000	.010	10.000	.010	10.000	.010	10.000	.010
IV								
poor	10.370	.020	9.636	.051	10.000	.010	9.994	.010
perfect	9.939	.013	9.958	.016	10.000	.010	9.999	.010
PHD	9.904	.012	14.969	0.002	10.000	.010	9.999	.010
MLE (2 iter)	8.870	.108	9.880	.172	10.000	.010	10.000	.010
GLS (1iter)	10.002	.070	9.885	.173	10.000	.010	9.999	.010
CF	10.002	.015	9.9971	.0166	10.000	.010	10.000	.010
MPem (L=20)								
p=4	9.998	.010	10.000	.010	10.000	.010	10.000	.010
p=5	.†	.†	.†	.†	.†	.†	10.000	.010
p=6	.†	.†	10.000	.010	.†	.†	.†	.†

* unable to identify

† case not considered

strain-gage accelerometers. Table 5 shows the results from the simulated experiments. The MPEM estimates were quite accurate.

2. Experimental Free Response

The time domain experimental free response from a SDOF system and a cantilever beam cited by reference 23 was used to further compare the algorithms. The SDOF system was similar to the base motion system shown in Figure 1, except the base mass was constrained. The other mass was constrained to a motion along a single axis. The damping was primarily provided by the bearing friction and was definitely non-viscous. The cantilever beam was made from steel and was 37.25 inches long with a cross section of 1.5 by 0.0625 inches. The damping was structural. All of the algorithms except the IV estimation were used.

The results are shown in Table 6. All of the methods were able to estimate the natural frequency of the SDOF system reasonably well, but there were considerable errors in the damping estimation when overspecification was not used. Log decrement procedures in reference 23 estimated the damping factor to be around 2%. The MPEM, the overspecified LS, the PHD, and CF damping estimates were all quite good.

Only the CF, the classical (non-overspecified) LS, and the MPEM were used to identify the cantilever beams natural frequencies and damping factors. The LS method failed to identify the first mode. The CF and the MPEM estimated the natural frequencies well, but the MPEM estimate of the damping in the first mode was lower than the CF method and on the same order of magnitude as the other modes. The MPEM estimate is probably the better of the two (the true values are unknown, since the data is experimental and a log decrement could not be performed).

3. Overspecification Example

The results from the simulated and experimental data show the need for overspecification and the MPEM method to get an accurate estimate of the natural frequencies and damping factors and hence an accurate estimate of the AR parameter vector. An additional set of simulations were conducted using one simulated free response record to show the effect of overspecification. The overspecification size was varied with the LS algorithm; and the PEM and MPEM algorithms were used to demonstrate the effects of overspecification and the minimum norm solution in the z-plane. The signal contained frequencies at 10, 20, and 30 Hz all damped at 1%. The sample rate was chosen to be 100

Table 5: 3DOF Simulated Data
 $(f_d=1,10,25; \zeta=.01,.01,.01; \text{Amp}=1,1,1; 256 \text{ pts}, f_s=2000 \text{ Hz})$

Algorithm	grv noise		higher mode		grv, 4th mode, bias	
	40 dB rms		Amp=.01		40 dB, A=.01, A=.01	
	f_d	ζ	f_d	ζ	f_d	ζ
LS (n=6)						
mode 1	*	*	*	*	*	*
mode 2	5.242	.362	9.974	.144	5.207	.369
mode 3	24.741	.032	25.066	.012	24.729	.032
CF						
mode 1	*	*	*	*	*	*
mode 2	9.814	.019	10.032	.016	9.822	.020
mode 3	24.988	.010	25.013	.010	24.992	.010
MPeM (L=30, p=6)						
mode 1	1.001	.010	1.000	.010	1.000	.011
mode 2	10.000	.010	10.000	.010	10.000	.010
mode 3	25.001	.010	25.000	.010	25.001	.010

* unable to identify

† case not considered

Table 6: Experimental Data (512 pts, fs=1000 Hz)

Algorithm	SDOF		MDOF: cantilever beam					
			1st mode		2nd mode		3rd mode	
	f_d	ζ	f_d	ζ	f_d	ζ	f_d	ζ
Analytical			1.45		9.10		25.49	
Estimated	~1.8	~.020						
LS								
n=2	1.797	.156	.†	.†	.†	.†	.†	.†
n=6	.†	.†	.*	.*	8.789	.003	24.64	.003
n=10	1.806	.022	.†	.†	.†	.†	.†	.†
PHD	1.809	.023	.†	.†	.†	.†	.†	.†
MLE (2 iter)	1.922	.008	.†	.†	.†	.†	.†	.†
GLS	(1iter)	1.797	.156	.†	.†	.†	.†	.†
CF	1.804	.021	1.515	.075	8.805	.002	24.66	.002
MPEM								
L=10, p=2	1.805	.020	.†	.†	.†	.†	.†	.†
L=30, p=6	†	†	1.512	.004	8.804	.002	24.66	.002

* unable to identify

† case not considered

Hz (512 points) so that the system poles would be well separated in the z-plane. Random gaussian noise was added to make the SNR equal to 20 dB.

Figure 26 shows the z-plane with the unit circle drawn. The true locations of the poles are shown as the circles in the figure and the estimated pole locations from a sixth order LS estimation are drawn as cross hairs. The estimated poles are very inaccurate. The estimated frequencies are therefore inaccurate as summarize in Table 7. Figure 27 shows what happens when the order of the LS estimation is increased to twelve. There are estimated locations very close to the true locations. Note that if the true locations were not known, there would be no way to distinguish the noise poles from the signal poles. The frequency estimates are reasonably accurate (1-2.5% error) but the damping estimates are inaccurate (200-400% error). The damping error envelopes given in Figures 21, 23, and 25 confirm that slight perturbation in the estimated locations will cause the large error in damping estimation when the damping is low (1% in this case). The order of the estimation is increased further to 30 to increase the accuracy. Figure 28 shows the resulting estimated pole locations and Table 7 shows that both the frequency and damping estimates are very accurate. Notice in Figure 28 that the extraneous roots are scattered about the unit circle. When the PEM is used with the same order, the frequency and damping estimates are about the same, but Figure 29 shows that the extraneous roots are scattered in a more orderly fashion. Still there is no way to distinguish poles with apriori knowledge; even with the "orderly" position of the poles, it would be impossible to separate the signal poles. Figure 30 shows what happens when the MPEM is used. The true locations of the poles are placed outside the unit circle, and the estimated signal pole locations are placed outside also, but the minimum norm solution places the extraneous poles all inside the unit circle. Thus, the signal poles can be differentiated from the extraneous poles and the high accuracy of overspecification is achieved.

4. Example: Closely Spaced Frequencies

The MPEM allows for overspecification, system order determination, and automatic sorting of signal and extraneous poles. In practice, one would input the free response data to a MPEM program, grossly overspecify the system order, evaluate the singular values of the $Q_m^T Q_m$ matrix and specify how many of the principal eigenvectors to use. The MPEM should locate the signal poles outside the unit circle. The number of principal eigenvectors (PE) should be the same number as the true order of the system, in the frequency range of interest, and the number of signal poles. But if the number of principal eigenvectors is slightly overspecified, the MPEM should determine the true order by

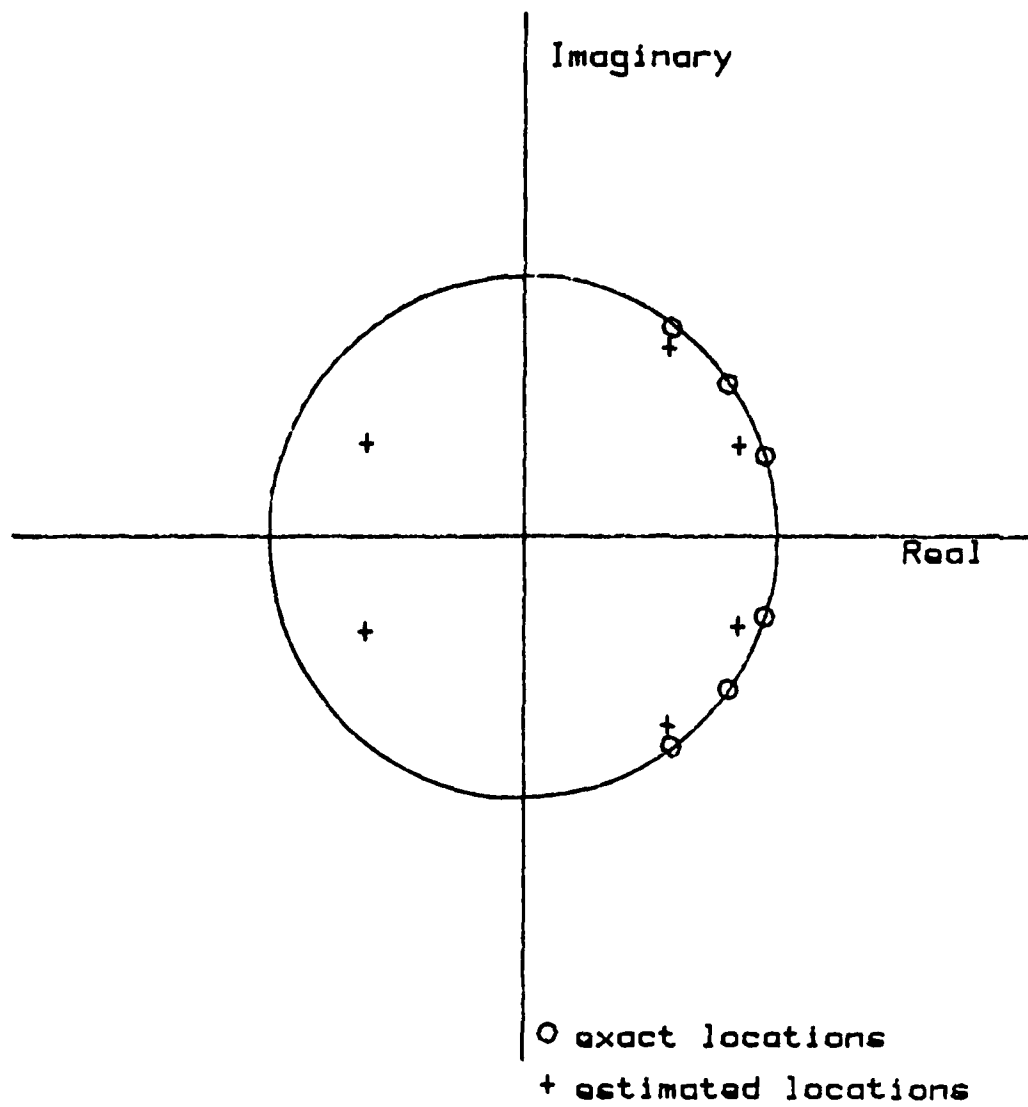


Figure 26: Estimated pole location from the LS algorithm ($n=6$).

Table 7: Simulated Data (512 pts, $f_s=200$ Hz)
($f_d = 10, 20, 30$ Hz, 1% damping 20 dB grv noise added)

Algorithm	1st mode		2nd mode		3rd mode	
	f_d	ζ	f_d	ζ	f_d	ζ
LS						
n=6	12.38	.227	28.38	.092	83.21	.128
n=12	10.08	.038	20.48	.039	30.36	.021
n=30	10.00	.010	20.01	.010	30.00	.010
PEM (L=30, p=6)						
	10.00	.010	20.01	.010	29.99	.010
MPEM (L=30,p=6)						
	10.00	.010	20.00	.010	29.99	.010

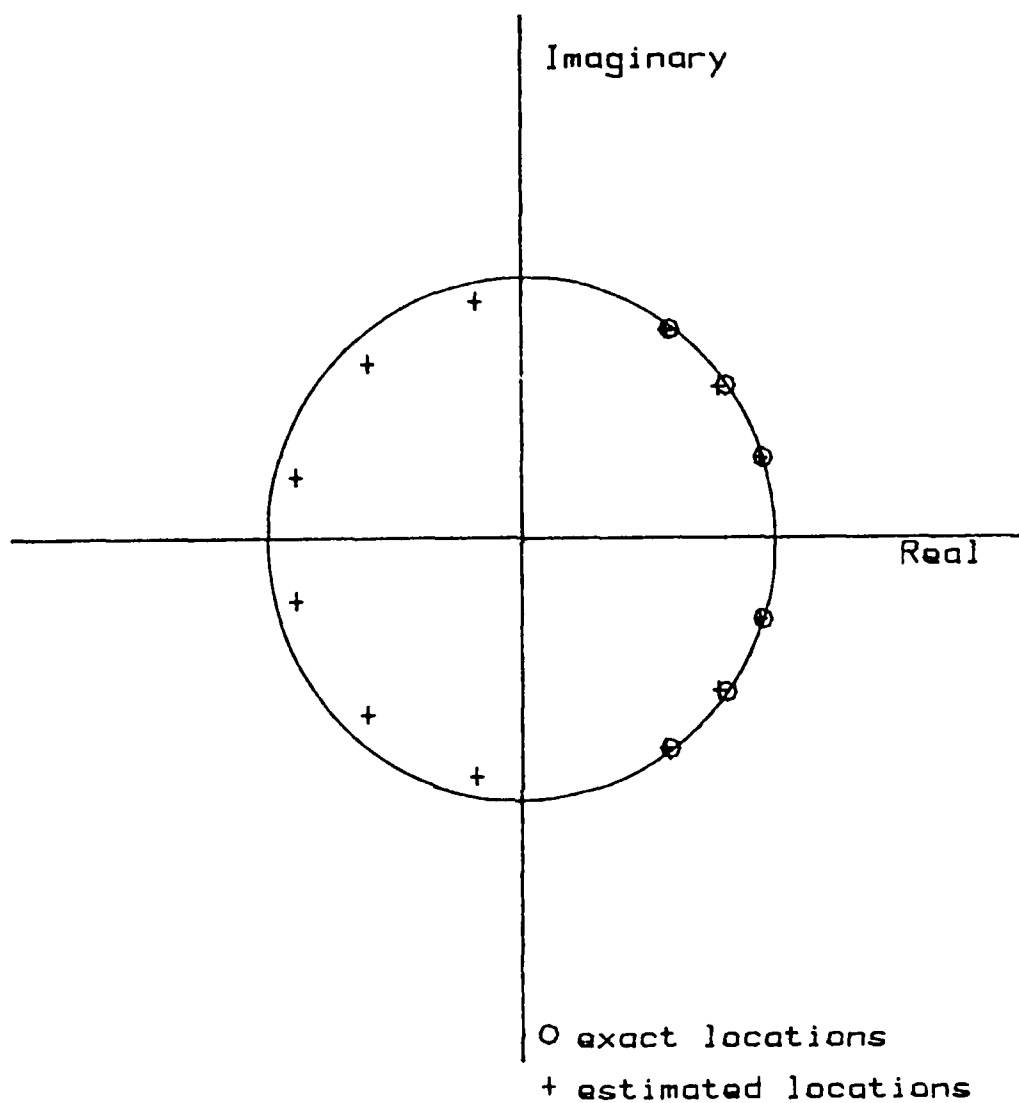


Figure 27: Estimated pole location from the overspecified LS algorithm($n=12$).

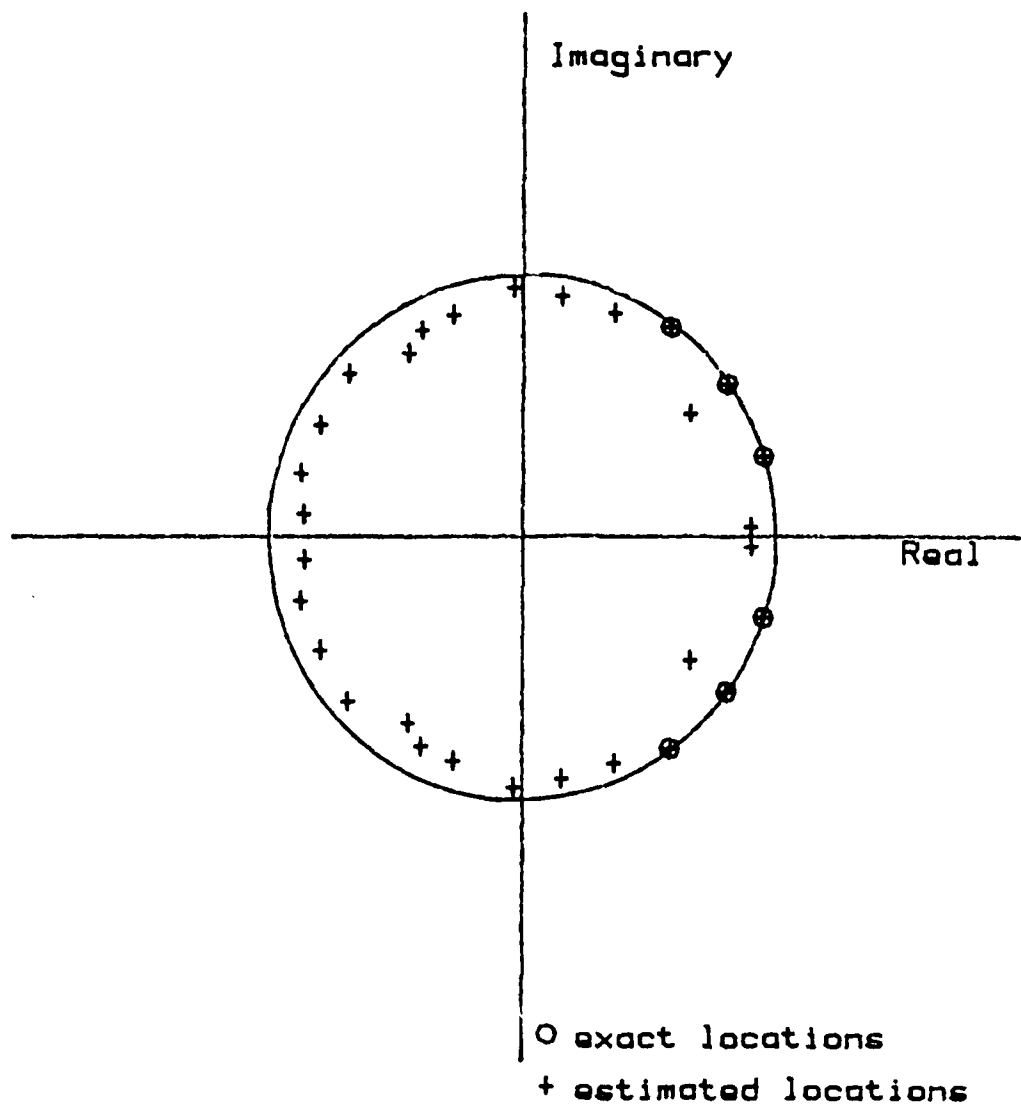


Figure 28: Estimated pole location from the overspecified LS algorithm($n=30$).

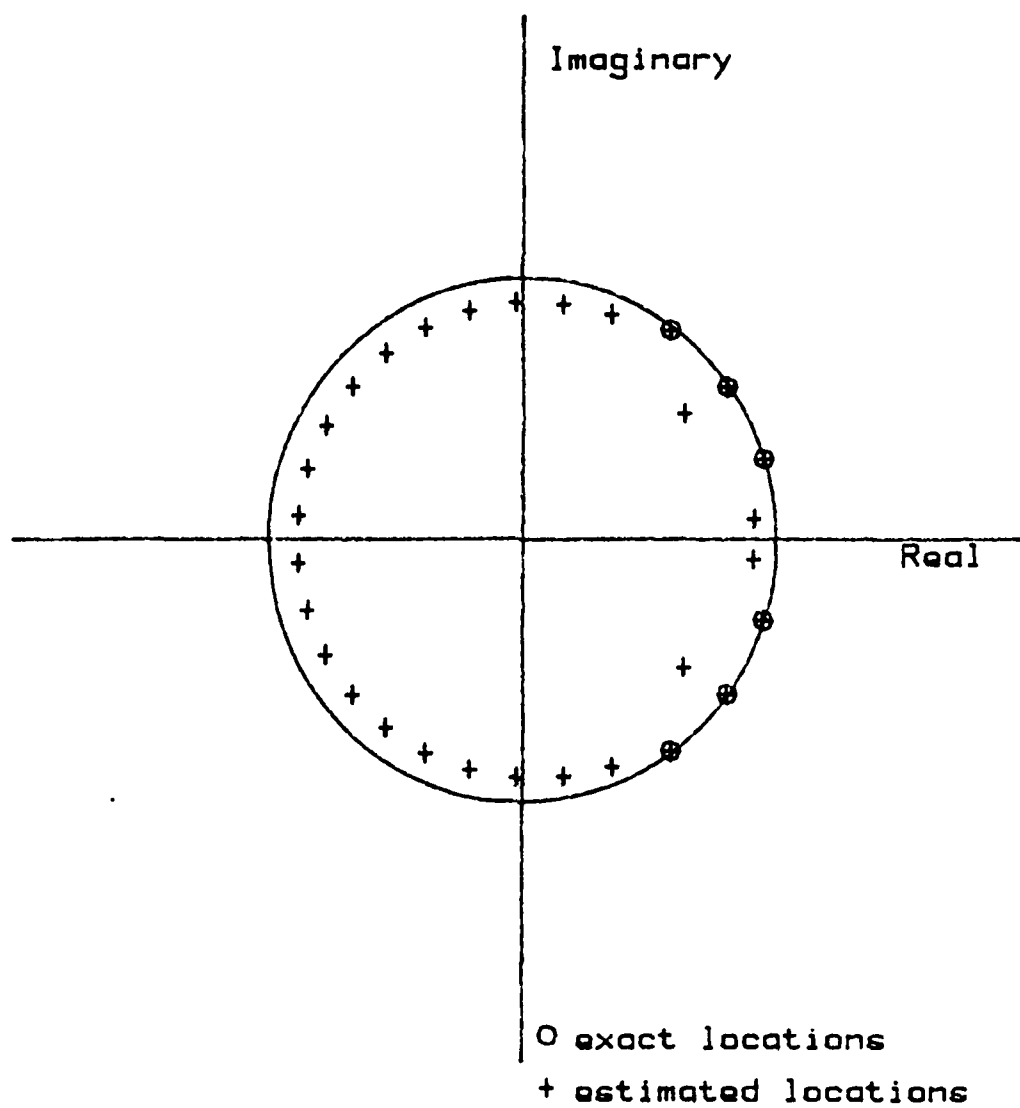


Figure 29: Estimated pole location from the PEM algorithm ($n=30$).

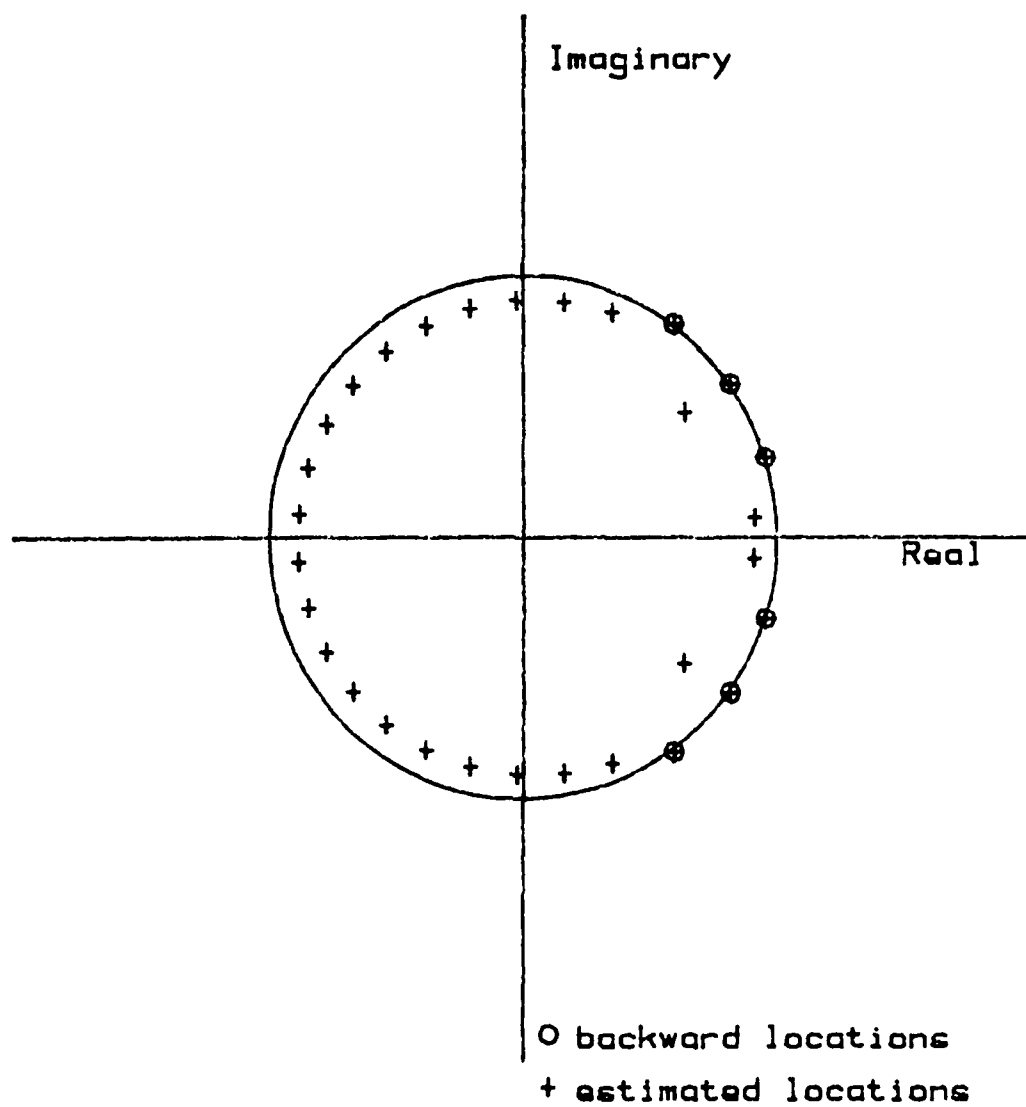


Figure 30: Estimated pole location from the MPEM algorithm ($n=30$).

locating the proper number of poles outside the unit circle. If there is too much noise, and the order has not been overspecified to a large enough value, the MPEM method may fail. Recall the example of the two closely spaced frequencies and the singular value spectrum shown in Figure 14. One may choose either 4, 6, or 8 as the system order after viewing the spectrum. Also, the noise singular values are very close in magnitude to the signal singular values and one would expect that the effect of the noise would be great even if the proper order was chosen. Figure 31 shows the singular value spectra of the $Q_m^T Q_m$ matrix for overspecification orders of 30 and 50. The spectra shown in the figure are intermediate results from the MPEM. Table 8 shows the frequency and damping estimates from the MPEM when the number of principal eigenvectors are chosen as 4, 6, or 8 for overspecification orders of 30 and 50. When the overspecification order is too low ($L=30$), the MPEM averages the two closely spaced modes regardless of the selection of the number of principal eigenvectors. The numerical difference between the signal singular values and the noise singular values is low with the low overspecification order. When the order is higher ($L=50$), the selection of the number of principal eigenvectors does have an effect upon the estimates. Notice that the numerical difference between the signal singular values and noise singular values is higher. The closely spaced modes are averaged as one value when four principal eigenvectors are used. The correct number of modes are identified when 6 or 8 is chosen as the number of principal eigenvectors. Theoretically, the number of principal eigenvectors should not be estimated too high, since the mechanism for distinguishing the signal and extraneous poles may be lost.

Overview

The key difficulty in estimating an AR model and equivalently estimating the frequencies and damping factors of a system is the effect of noise bias. In the examples, the effect of overspecification upon discrete time series models, in this case the AR model, is shown. The difficulty with the overspecified algorithms is the sorting of the noise modes from the true modes of the model. The MPEM is able to provide the benefits of overspecification and distinguish between the signal poles and the extraneous poles. An accurate low-order AR model can be developed from the MPEM estimates of signal poles. However, the goal of this report is to identify the means of constructing the whole discrete time transfer function. One method to deal with estimation bias is to simply identify the overspecified ARMA model in a single stage. The alternate is a two-stage procedure. The first stage would use free or the impulse response and the MPEM to identify order and produce an accurate AR model containing signal frequency components only. The second stage would then have to identify the MA parameters given the AR model and the input-

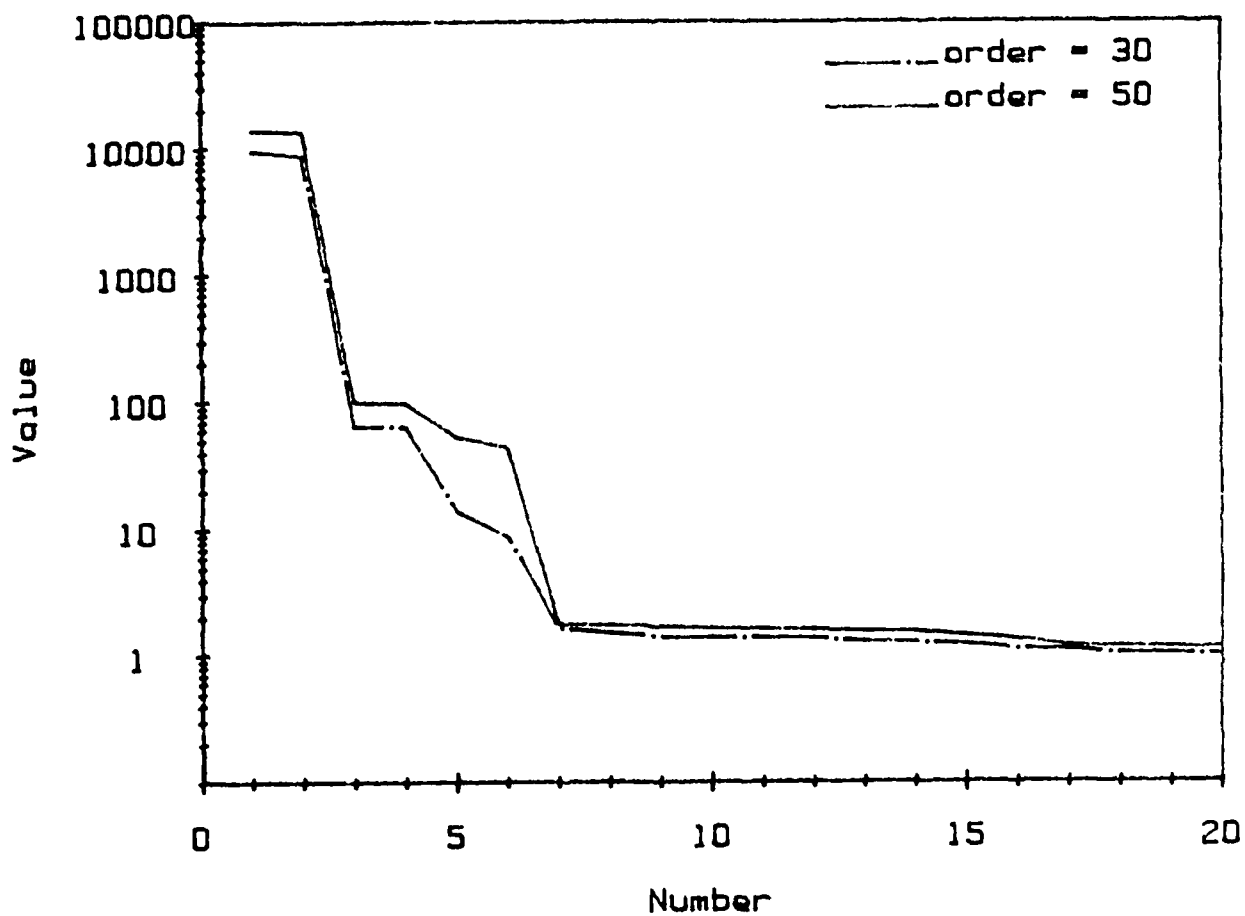


Figure 31: Singular Value Spectra of the backward autocorrelation matrix for two closely spaced modes.

Table 8: MPED estimates for MDOF data with closely spaced modes

Trial #	L	p	mode 1		mode 2		mode 3	
			freq	damp	freq	damp	freq	damp
			Hz	%	Hz	%	Hz	%
1	30	4	14.79	1.25	*	*	30.01	0.88
2	30	6	14.79	1.25	*	*	30.01	0.88
3	30	8	14.80	1.54	*	*	29.88	0.57
4	50	4	14.79	1.59	*	*	29.61	0.54
5	50	6	14.63	0.84	14.98	0.72	30.01	0.90
6	50	8	14.63	0.84	14.98	0.72	30.01	0.91
True Values			14.60	1.00	15.00	1.00	30.00	1.00

* unable to identify

output time history set. The next section explores the two methods using simulated and experimental data.

APPLICATIONS

In this section two algorithms used to parameterize a full ARMA model are compared. The first algorithm is a single-stage, possibly overspecified, Least Squares algorithm and will be denoted as the SLS (for single-stage least-squares) algorithm. The other is a two stage procedure that uses free response and the MPEM to identify system order and produce an accurate AR model containing signal frequency components only, and an MA LS procedure to identify the MA parameters. The two-stage algorithm will be denoted by 2LS. The 2LS algorithm will produce a lower order model without noise modes. The SLS algorithm will provide higher order models, due to overspecification, and requires less information since a free response record is not needed. The 2LS algorithm requires additional data and provides more information about the system. It identifies the signal frequencies and dampings along with providing a reduced order model which will allow for more rapid calculation of the system response. Simulated MDOF data and experimental SDOF and MDOF data will be used to compare the algorithms. Since the second stage of the 2LS algorithm has not yet been discussed, it will be presented here.

MA Parameter Identification

The ARMA model consists of two parts, the Autoregressive part and the Moving Average part. While the Autoregressive part of the ARMA has an easily interpreted physical meaning, the Moving Average (MA) part of the model does not. The MA part of the ARMA model relates the input directly to the output. It is the nonhomogeneous part of the ARMA model. A Moving Average process may be modeled as

$$y(k) = (b_0 + b_1 z^{-1} + \dots + b_p z^{-p}) u(k) \quad (78)$$

A Moving Average process is a weighted average of another process.

If the AR parameters for a given ARMA model are known, then the MA parameters can then be identified in a separate set of calculations or "second stage." Any of ARMA identification algorithms can be modified to identify the MA parameters. But, for simplicity in this report, the MA parameters are determined by a modified form of the LS algorithm. Given the input-output time histories and the AR parameters, the ARMA model can be reduced to a MA form. In order to identify the MA parameters, an overdetermined set of simultaneous equations is written in matrix form as

$$\begin{bmatrix} u_m(p) & u_m(p-1) & \dots & u_m(1) \\ u_m(p+1) & u_m(p) & \dots & u_m(2) \\ \vdots & \vdots & \ddots & \vdots \\ u_m(N) & u_m(N-1) & \dots & u_m(N-p+1) \end{bmatrix} \begin{pmatrix} b_0 \\ b_1 \\ \vdots \\ b_p \end{pmatrix} = \begin{pmatrix} z_m(p) \\ z_m(p+1) \\ \vdots \\ z_m(N) \end{pmatrix} + \begin{pmatrix} e(p) \\ e(p+1) \\ \vdots \\ e(N) \end{pmatrix} \quad (79)$$

or

$$U_m \mathbf{b} = \mathbf{z}_m + \mathbf{e} \quad (80)$$

where

$$z_m(k) = y_m(k) - \sum_{i=1}^p a_i y_m(k-i) \quad (81)$$

The LS solution of Eqn 79 is

$$\mathbf{b} = (U_m^T U_m)^{-1} U_m^T \mathbf{z}_m \quad (82)$$

Here the notation of persistent excitation is clearly demonstrated. If the scaled discrete time input autocorrelation matrix, $U_m^T U_m$, is singular, then the MA parameters can not be determined. A persistent excitation provides full rank of the input autocorrelation matrix (reference 16).

The second stage of the 2LS algorithm solves the set of equations through the use of a LS algorithm. It should be noted that any of the major algorithms could be used to estimate the MA parameters. The MA LS parameter estimates are biased, just as the full model LS estimate is biased. Other algorithms were considered for estimation of the MA parameters, but since the LS algorithm is the simplest of the major algorithms to implement, it was chosen for this sample study.

Examples

A series of experiments were performed to illustrate the application of the proposed two-stage approach. Simulated data for a MDOF system was used to compare the algorithms. Also, data for a SDOF and a MDOF system were acquired experimentally from actual structural systems and used to examine the 2LS algorithm. Results show that a model developed using single-stage LS parameter estimates (without overspecification) fails to predict response adequately for both the SDOF and MDOF system, while the model developed using the 2LS algorithm parameter estimates provides very good response predictions. Overspecified models can be identified using the SLS algorithm that can be

used to accurately predict response. All measured quantities cited in the following discussion are accelerations measured in g's.

1. Simulated Data

Input and output time histories were simulated to compare the two candidate algorithms, the 2LS and the SLS. The input was a pseudo-random binary input as shown in Figure 32. A sixth order arbitrary ARMA model was used to generate the system output time history for this input. The output was corrupted with gaussian random noise at a signal-to-noise ratio of 40 dB. The corrupted response is shown in Figure 33. The SLS algorithm was used to identify a sixth and twelfth order ARMA model. The FRF magnitudes of the identified and exact ARMA models are shown in Figure 34. The Figure illustrates that even a modest level of noise effects the SLS. The the first mode of the exact transfer function is accurately modeled by the twelfth order model and second mode is modeled but not as accurately. The sixth order model, recall the actual order of the system is six, is not represented accurately. Notice the strange behavior in the FRF magnitude plot of the 12th order model past 30 Hz. The extraneous modes are the cause of this behavior.

The noise used in the example has a flat spectral density over the entire frequency range. If these data were experimentally acquired, low pass filters would have limited the bandwidth of the signal and the bandwidth of the noise. The equivalent digital filter of a four pole low pass Butterworth filter (reference 5) was used to simulate the effect of actual low pass filters. The frequency response of the digital filter is shown in Figure 35. If the input and output are filtered by similar low pass filters, the transfer function (within the bandwidth) will be unaffected by the filters, but the filters will truncate the high frequency noise. Figures 36 and 37 are the simulated filtered input and output produced when the input and output time histories are modified by the digital filter (actually an ARMA model). When the SLS algorithm is used with the filtered input-output data sets, the results are much better. Figure 38 shows the FRF magnitude plots of the 6th and 12th order models. Both models follow the first two modes closely, but the third mode is not identified.

The FRF of the 2LS models identified using the filtered and unfiltered data are shown in Figure 39. The 2LS models are 6th order and were obtained by assuming that the AR part of the model is known precisely. The model obtained from the unfiltered data is inaccurate. The model obtained from the filtered data is accurate for the first two modes and third mode is identified but not very accurately. Certain characteristics of the two algorithms are readily illustrated by the example. First, the SLS models improve as the order is increased, and secondly, the algorithms work best when the noise is band-limited.

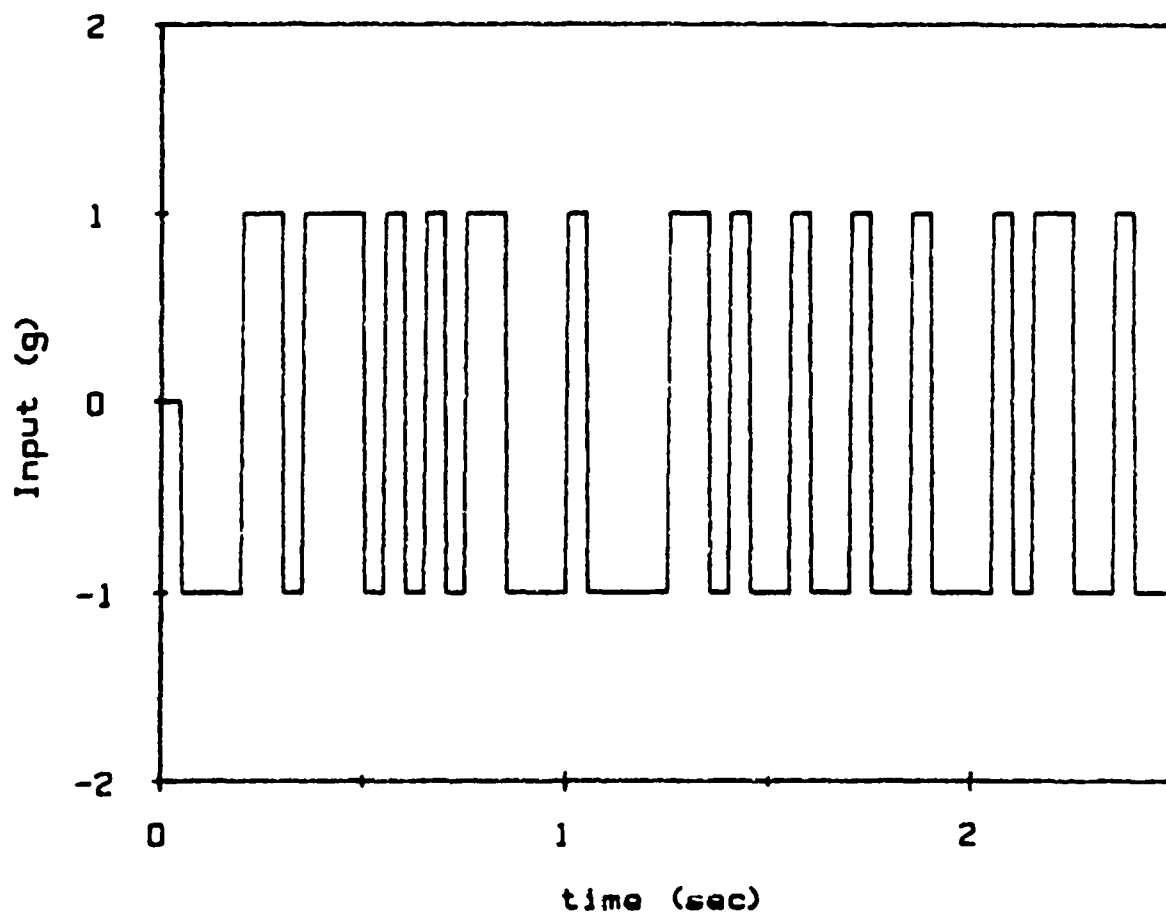


Figure 32: Pseudo-random binary input.

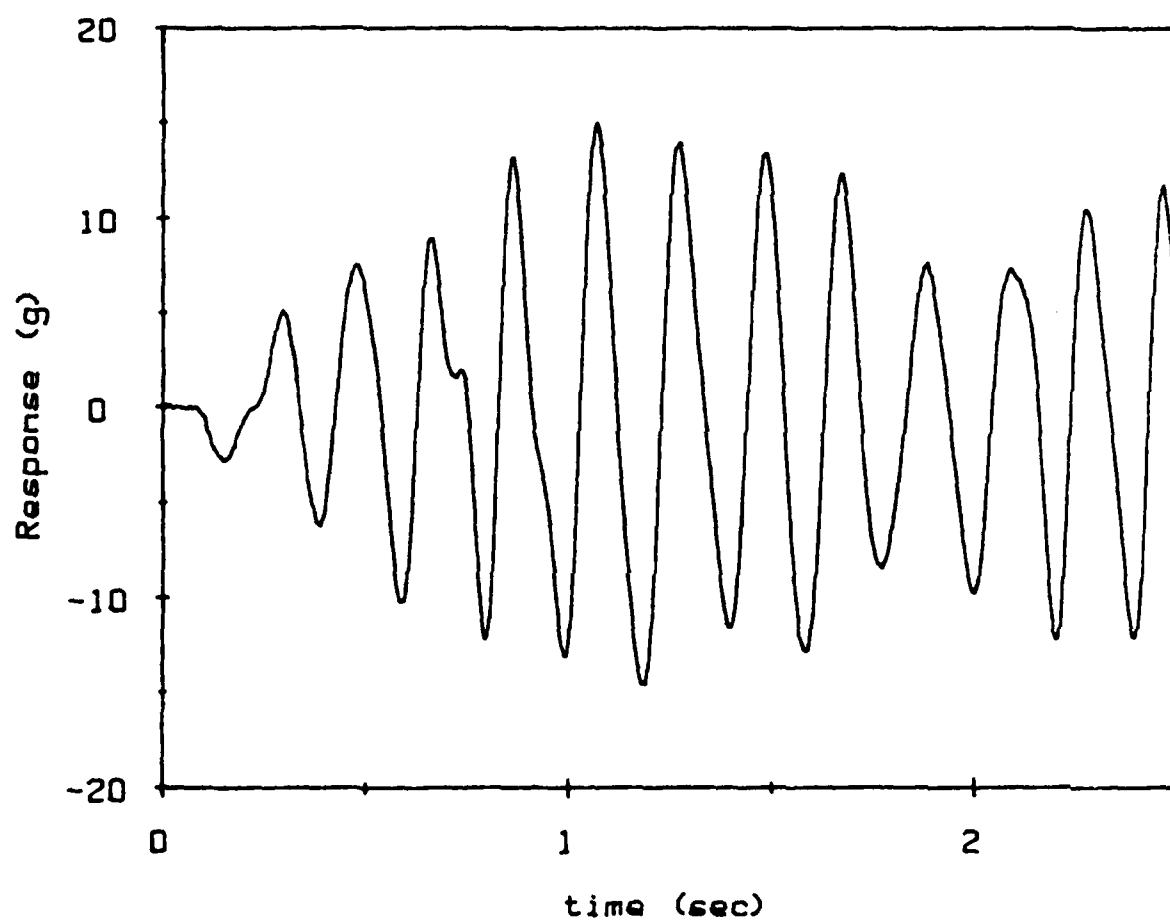


Figure 33: Noisy response to the pseudo-random binary input.

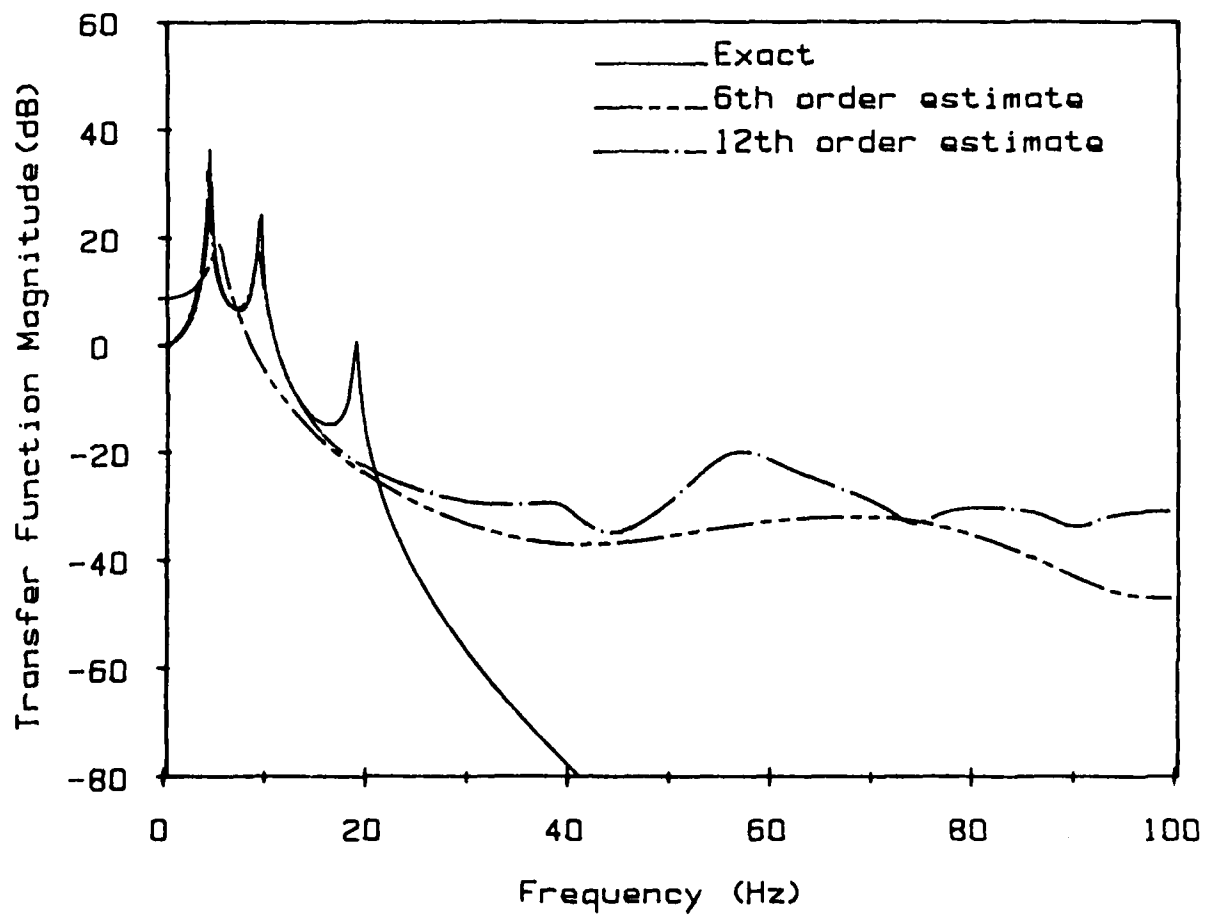


Figure 34: Frequency Response Function magnitude for SLS models (unfiltered data used).

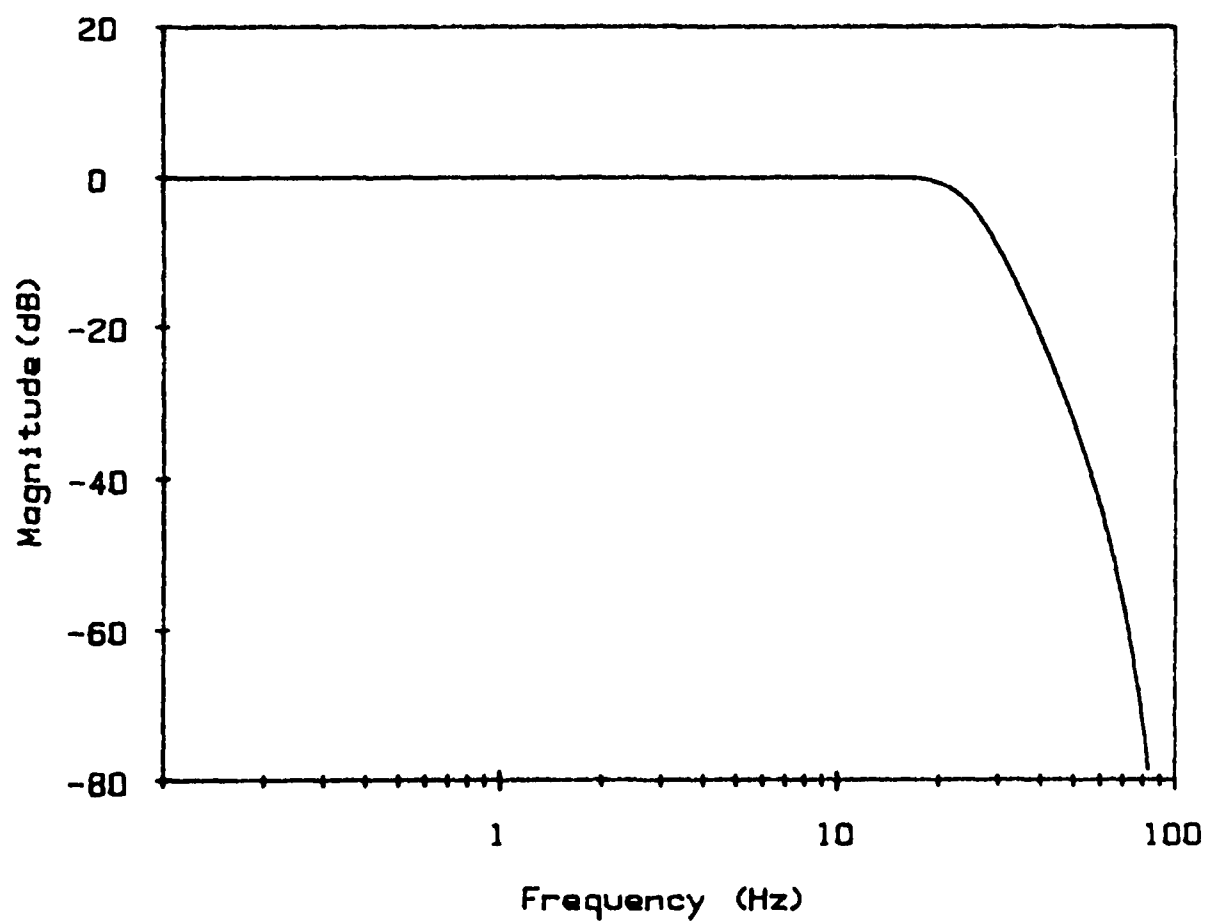


Figure 35: Frequency Response of digital filter.

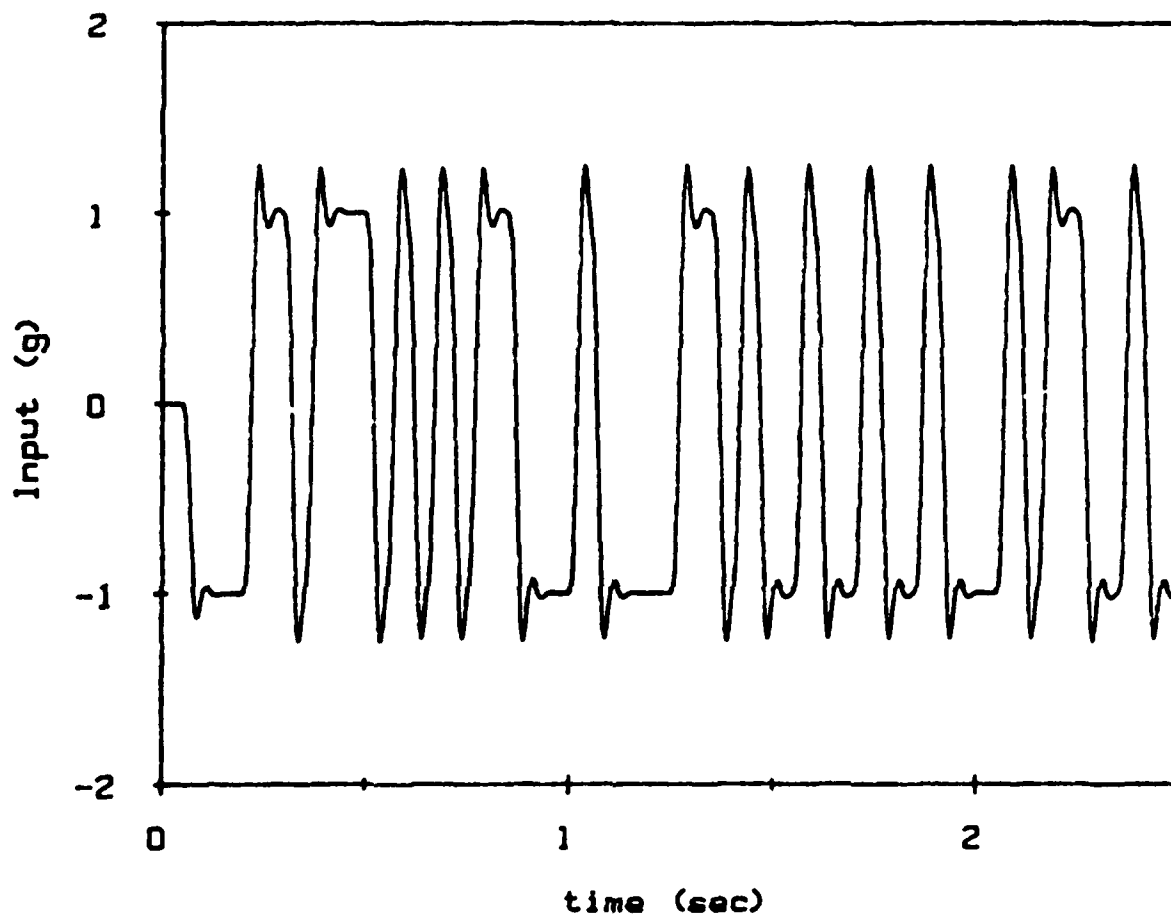


Figure 36: Filtered pseudo-random binary input.

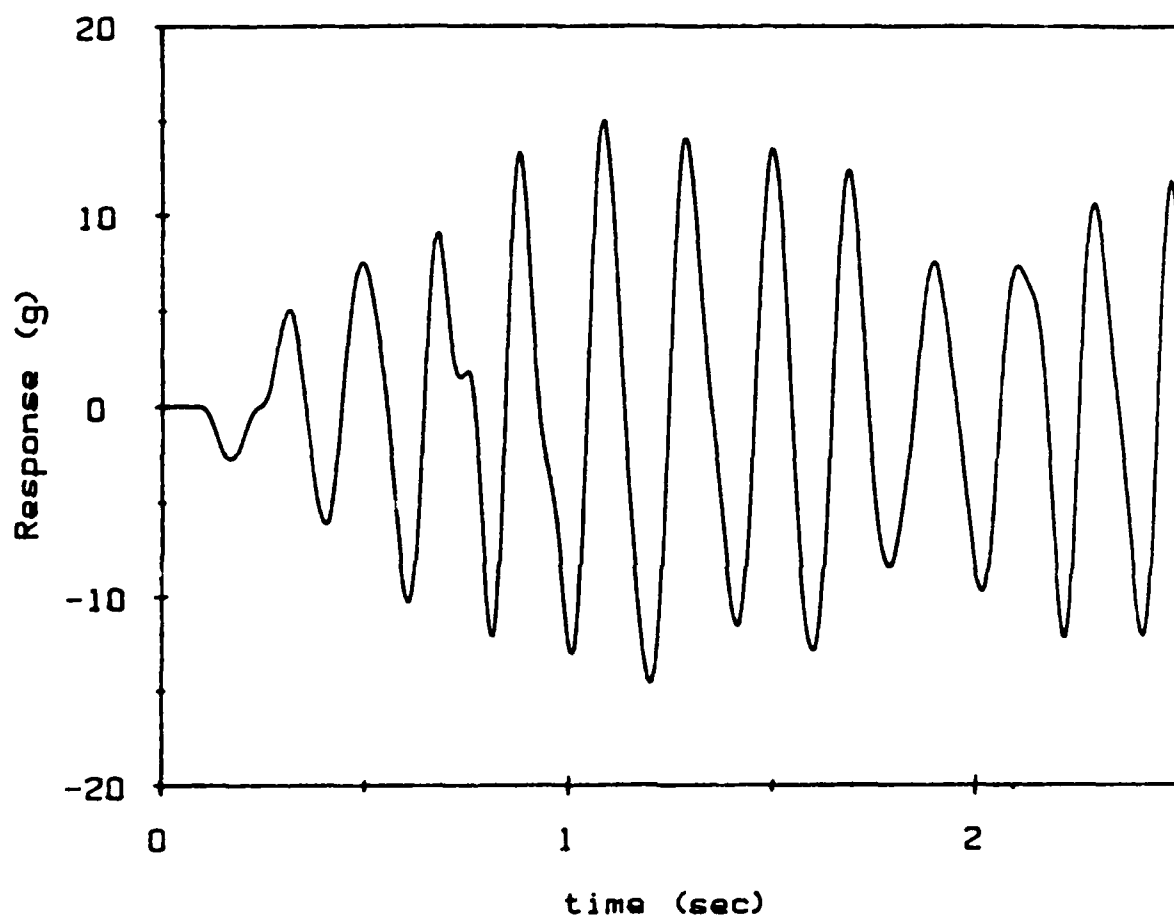


Figure 37: Filtered noisy response to the pseudo-random binary input.

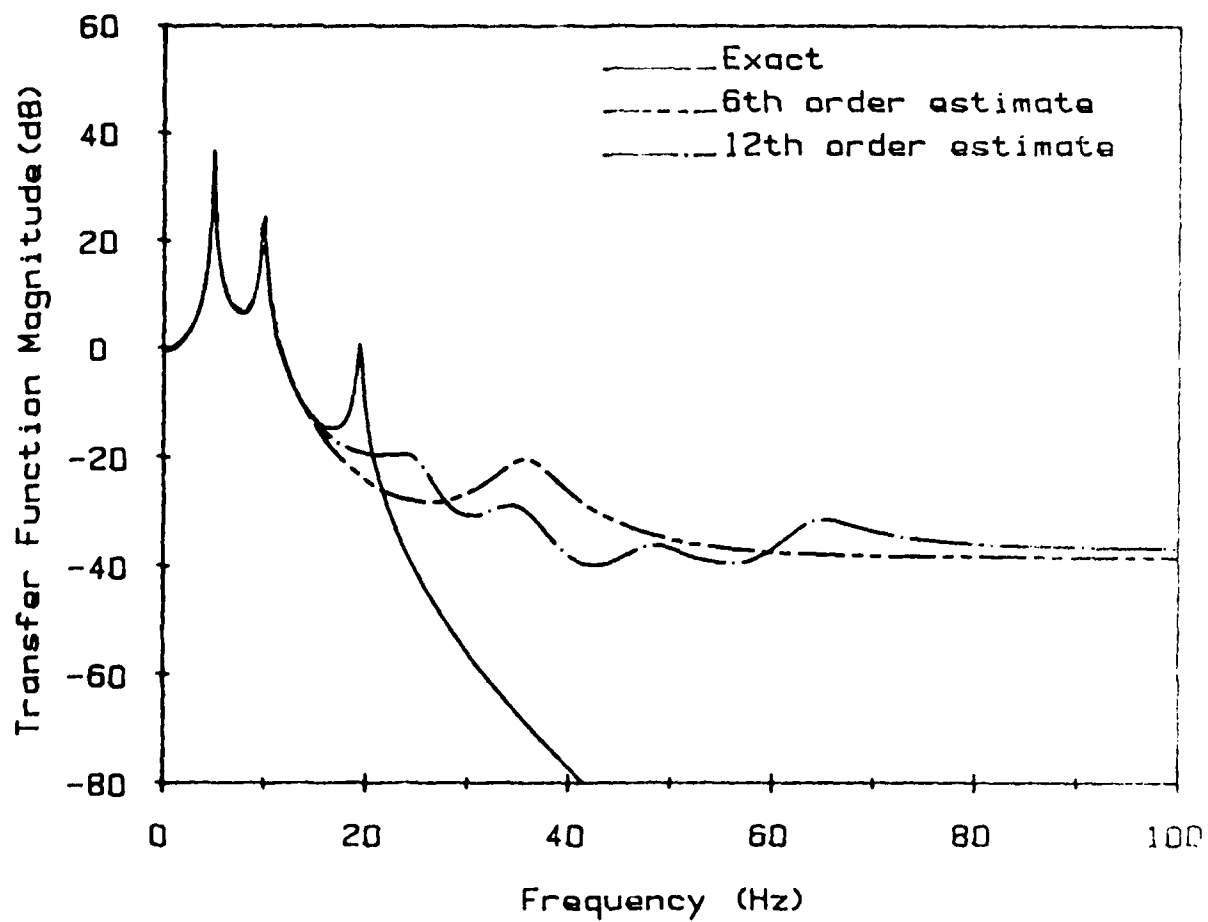


Figure 38: Frequency Response Function magnitude for SLS models (filtered data used).

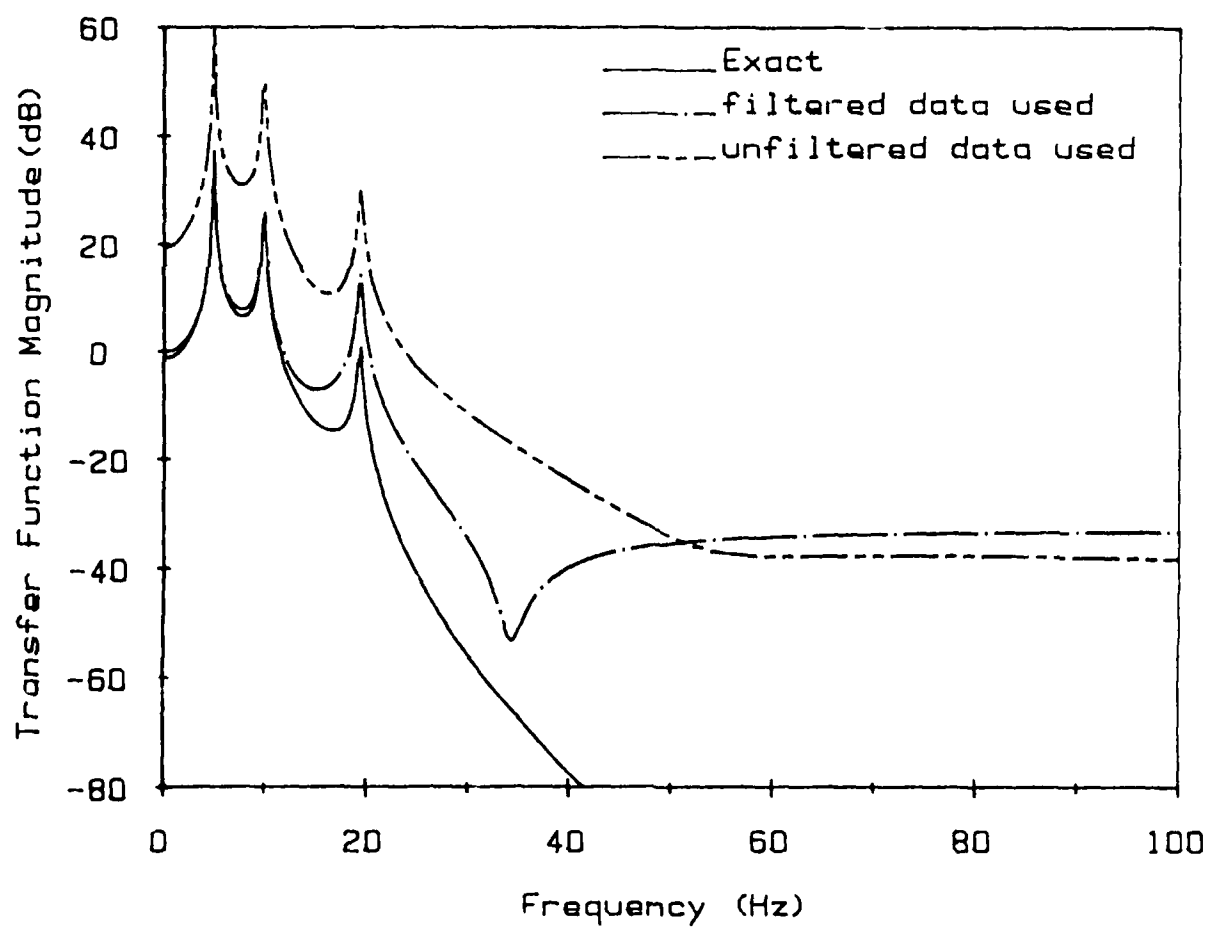


Figure 39: Frequency Response Function magnitude for 2LS models.

If the AR portion of the model can be identified accurately, the 2LS algorithm can produce the lowest possible order model which is as accurate as a much higher order SLS model. The overspecified SLS models will have dynamics past the bandwidth of interest. A high order SLS and a 2LS model can be compared on a FRF magnitude plot to compare accuracy.

2. The SDOF experiment

A mechanical system similar to that depicted in Figure 1 was used to acquire input-output time histories to test the 2LS identification procedure. The system was fabricated using two masses which were constrained to one-dimensional movement by linear bearings and two parallel, cylindrical rods. The masses were connected by springs. The left-hand or base mass could be moved manually to provide input to the system; the response of the free mass was considered the output of the system. The experiment corresponds to a SDOF base motion problem. The system damping was provided by the bearing friction and is nonviscous.

The 2LS procedure requires the free response for AR parameter estimation in the first stage. Experimental data was acquired by constraining the base mass and displacing the free mass from equilibrium. A strain-gage accelerometer was used to measure the low frequency acceleration response. A typical free response is shown in Figure 40. This record contains 500 data points with a sample frequency of 100 Hz, so there is a total of 5 seconds of free response data. The ordinary LS estimates for the damped natural frequency and damping factor are 1.820 Hz and 23% for this data set. The MPEM estimates ($L=10$) are 1.806 Hz and 2.0%. The frequency estimates are similar but the damping factors differ by an order of magnitude. A log decrement procedure was used to estimate the damping factor (between 1.5 and 1.8%), verifying that the MPEM estimate of the damping factor is more reasonable. Other experimental free response records were acquired and repeatability of the MPEM estimates verified. The average damped natural frequency and damping factor from four MPEM estimates were 1.805 Hz and 2.1%. The average estimates were used to produce the AR parameters used in the second stage. Experimental input-output time histories were obtained by manual excitation of the base mass. The input to the system was measured as the acceleration of the base mass by a second strain-gage accelerometer. Figures 41 to 43 show three different inputs (500 pts, $f_s=100$ Hz), Case A, Case B, and Case C, respectively, which were applied to the system. The single-stage LS (SLS) model estimates (without overspecification) obtained from the three input-output time histories were inconsistent, and the resulting ARMA models provided inaccurate

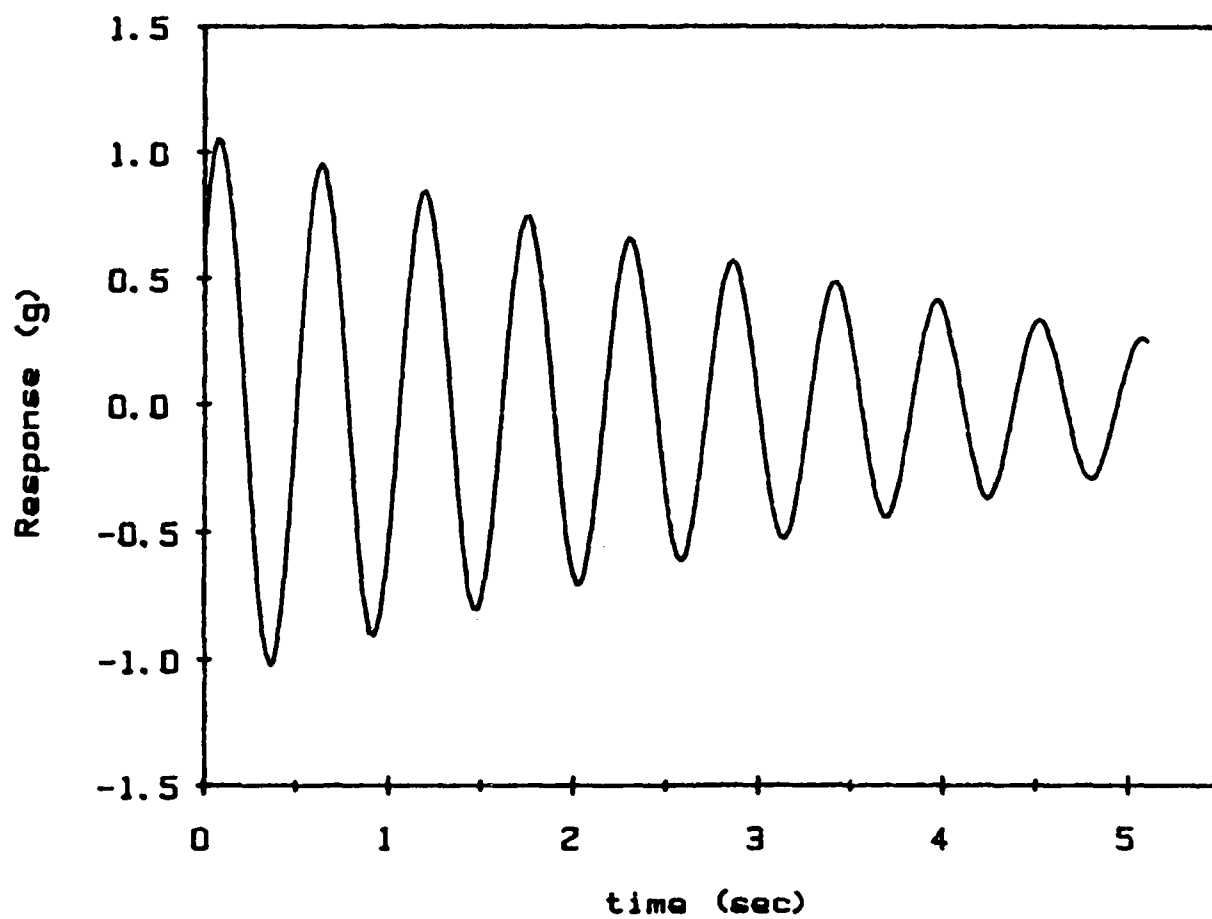


Figure 40: Typical free response of the SDOF system.

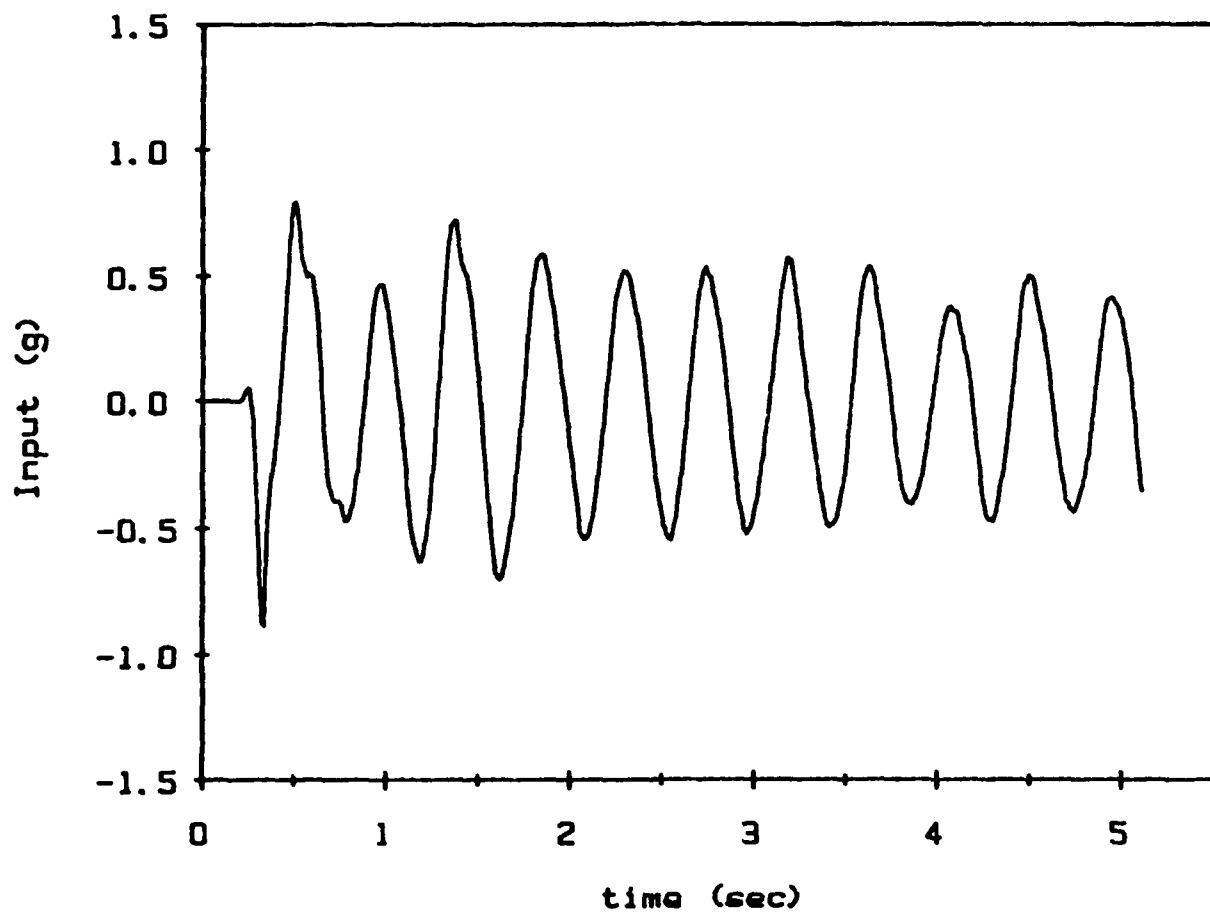


Figure 41: Base acceleration, Case A.

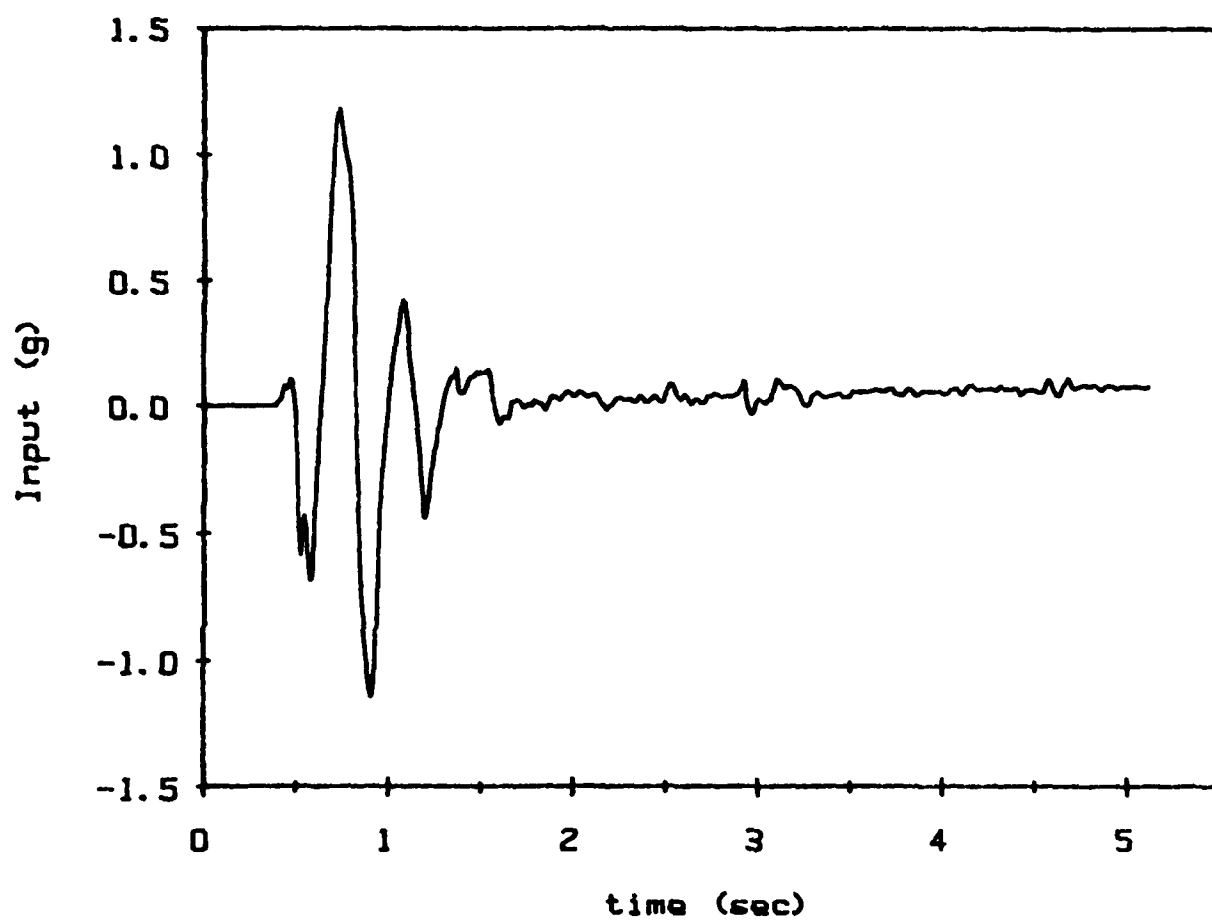


Figure 42: Base acceleration, Case B.

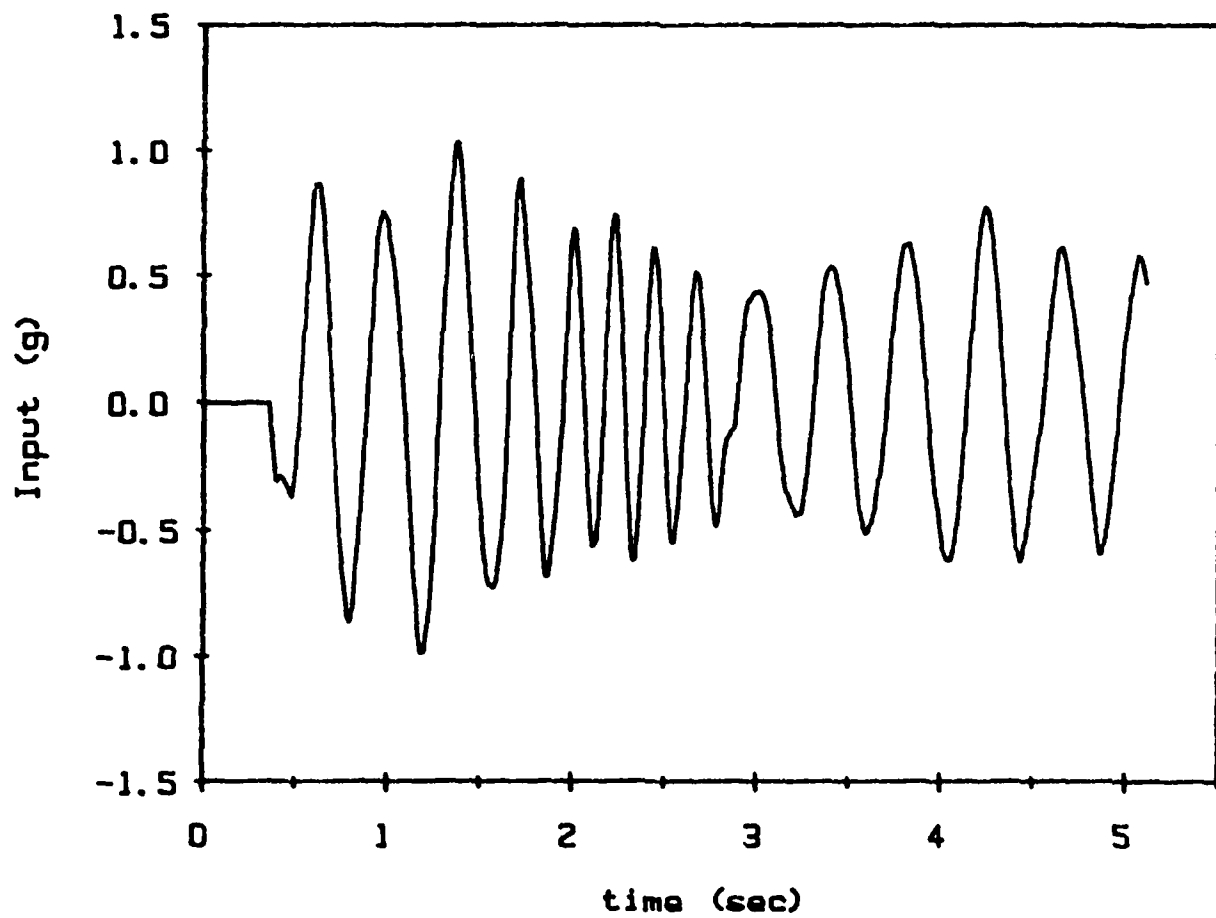


Figure 43: Base acceleration, Case C.

predictions of system response. The predicted responses are obtained through the use of the estimated ARMA models and the input time histories without knowledge of the actual output time histories. Figure 44 shows the predicted response (in comparison to the actual response) to the input Case B using the SLS model obtained from input-output time histories for Case A. The predicted response is typical of the cases considered with models developed using the SLS estimates. Figures 45 to 47 show the predicted responses (in comparison to the actual responses) to input Cases A, B, and C, respectively, from the 2LS model obtained from the input-output time histories for Case A. The 2LS model obtained using the input-output time history corresponding to input Cases B and C provide similar predicted responses. The magnitude frequency response plots for the three 2LS ARMA models are shown in Figure 48 while the frequency response plots for the three SLS ARMA models are shown in Figure 49. The SLS ARMA models have grossly overestimated the damping. The 2LS ARMA models are very similar to each other when compared using the FRF, and appear to be more reasonable than the SLS models.

Overspecification of the model in the SLS procedure improves the damping estimates but introduces extraneous poles and zeroes as shown in Figure 50. The damping and frequency estimates are given in Table 9 as the model order is increased in the SLS procedure. The damped natural frequency is about 4 percent of the nyquist frequency, and one would expect high errors in the damping factor estimates. The response prediction of input Case B using the tenth order SLS ARMA model obtained from input Case A is shown in Figure 51. Note that the damping estimate is still too high and there is some error in frequency.

3. The MDOF Experiment

A cantilevered thin steel beam (length=37.25", width=1.5", thickness= 0.0625") was used as a MDOF experimental system. The beam was cantilevered on a block, the block was fixed, and the beam was initially deformed to provide free vibration. A strain-gage accelerometer was mounted on the tip of the beam to measure free response. The analog data was filtered (with cutoff frequencies of 16, 31.5, and 63 Hz) using an analog four-pole low-pass Butterworth filter and then digitized. The MPEM algorithm was used to identify the natural frequencies and damping factors from the free vibration response. The results appear in Table 10 along with the analytical frequency values computed for a cantilevered beam. Note that the fourth mode was identified in Trial 5 as an extraneous mode. In this case, the noise perturbed the pole locations (corresponding to the fourth

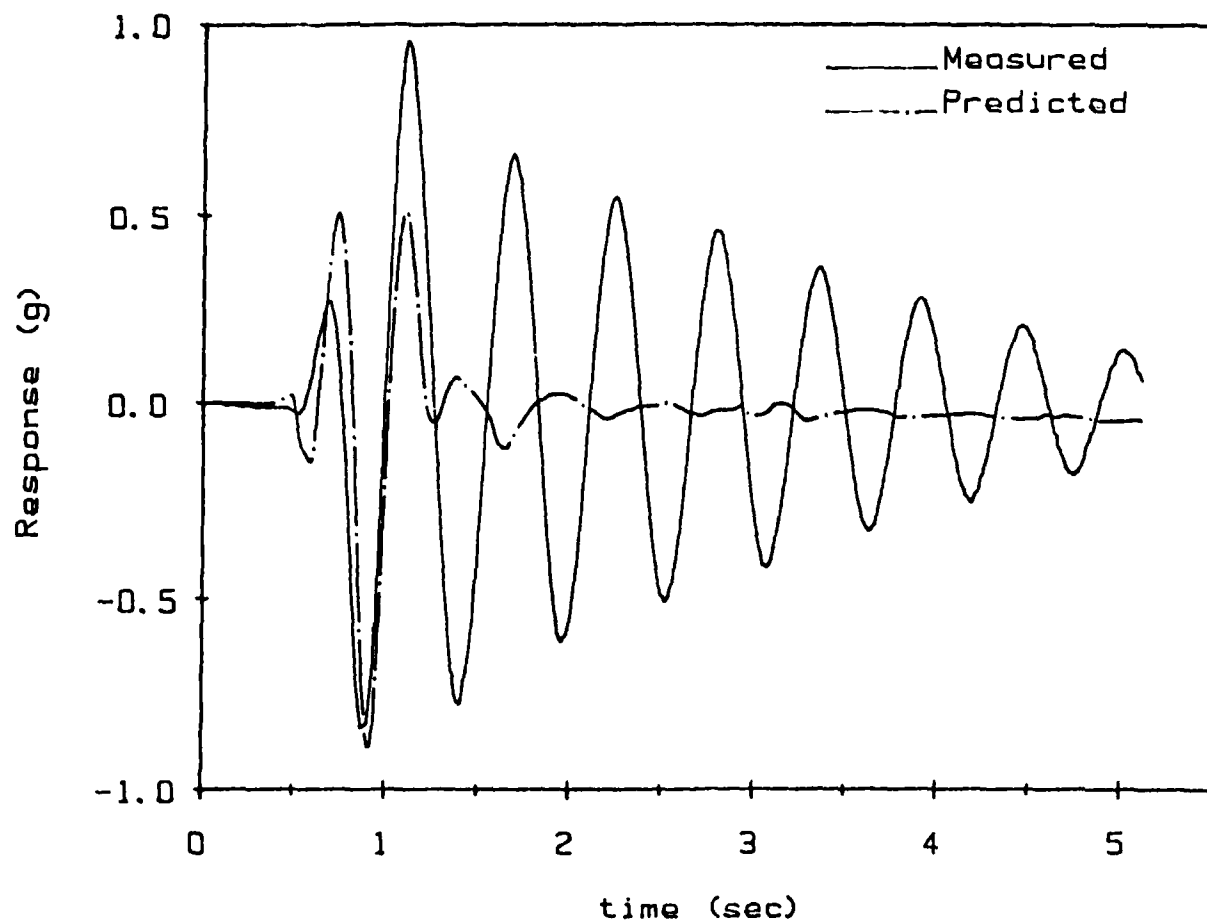


Figure 44: Second order SLS model prediction of SDOF response to input Case B.

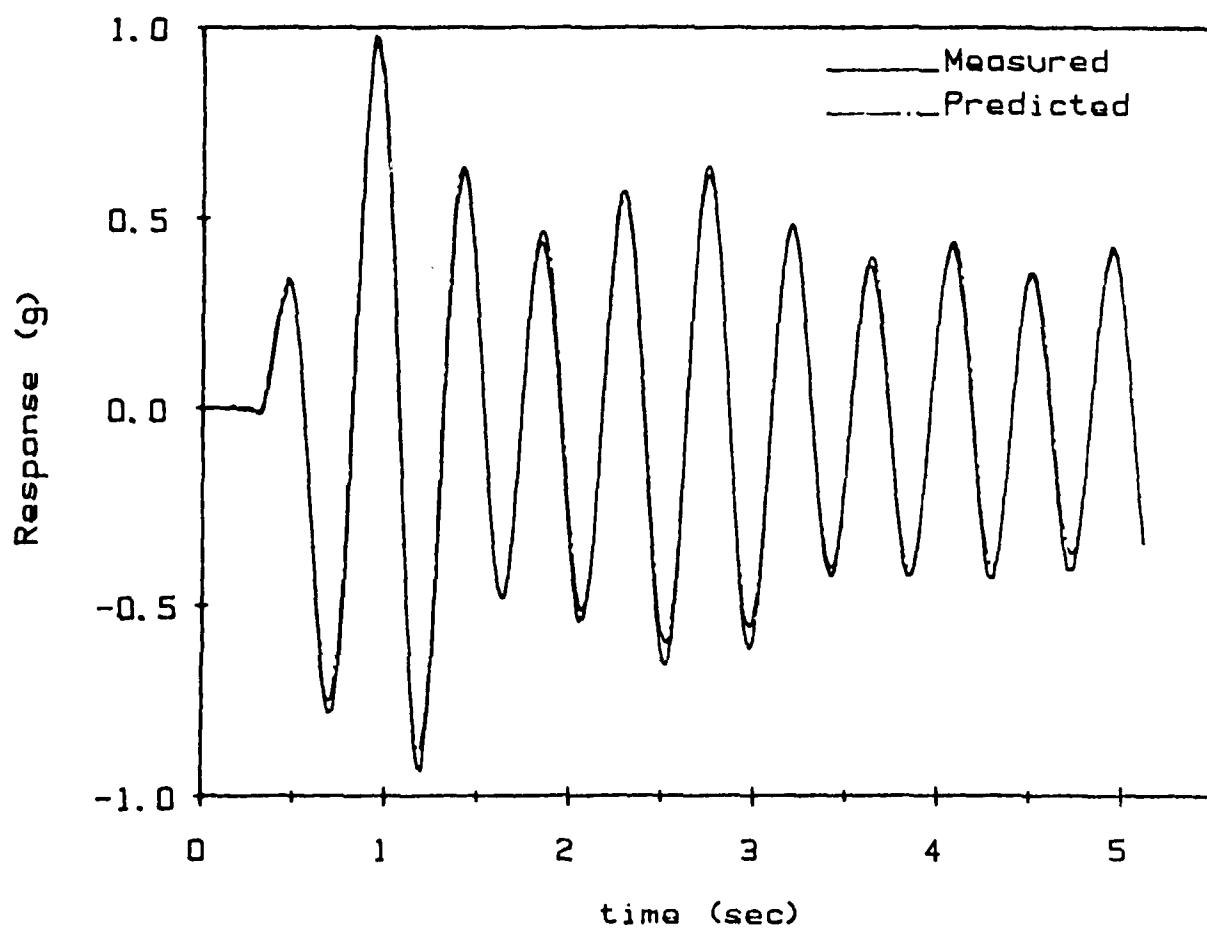


Figure 45: Second order 2LS model prediction of SDOF response to input Case A.

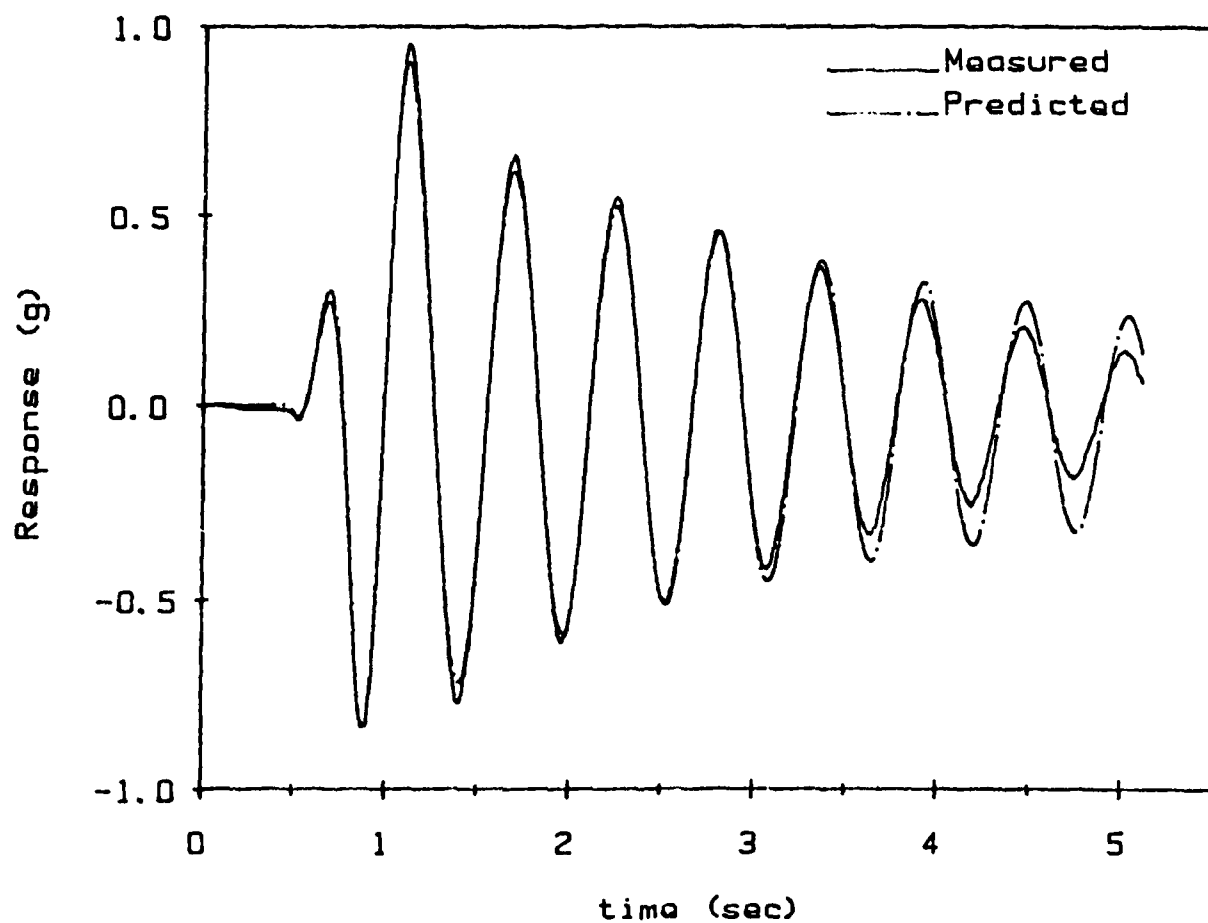


Figure 46: Second order 2LS model prediction of SDOF response to input Case B.

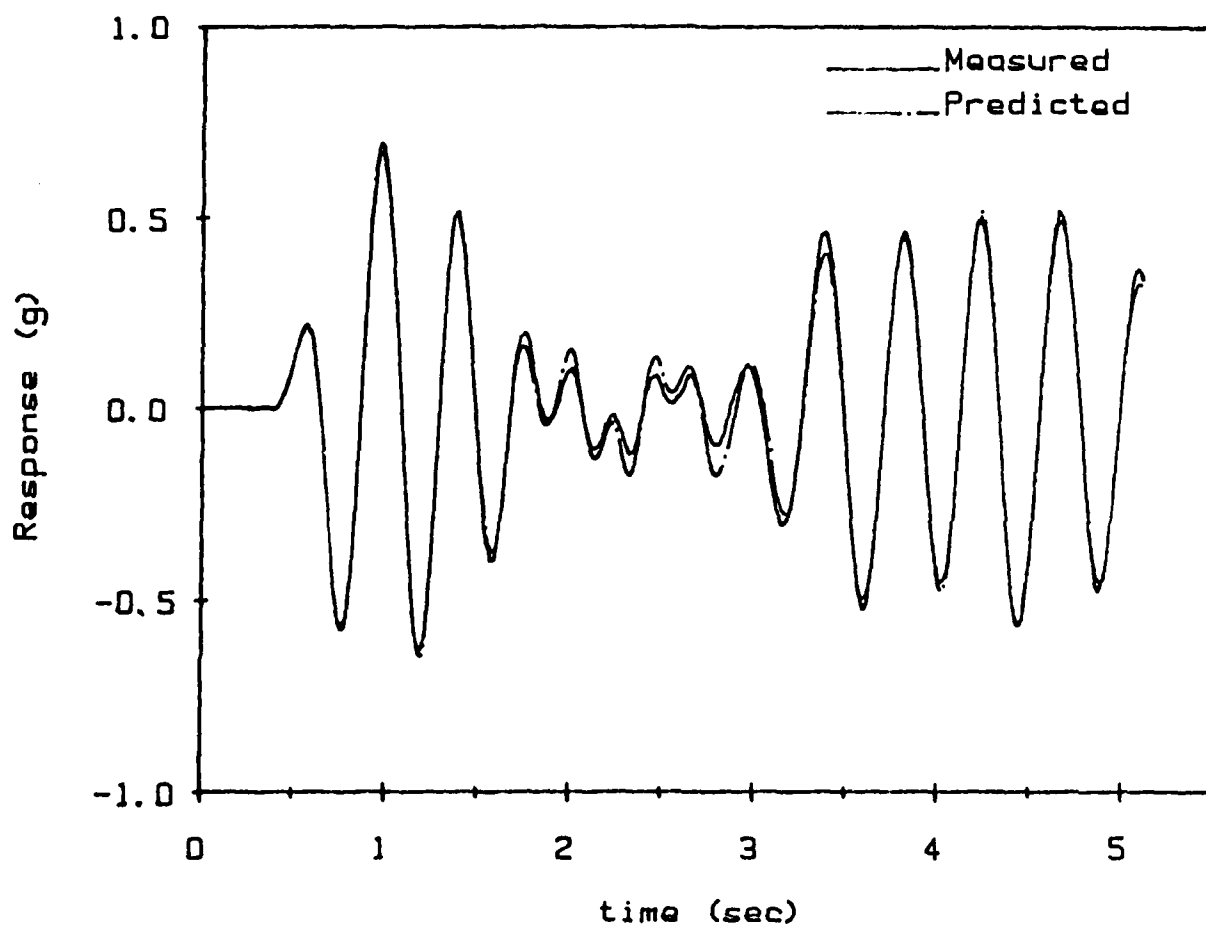


Figure 47: Second order 2LS model prediction of SDOF response to input Case C.

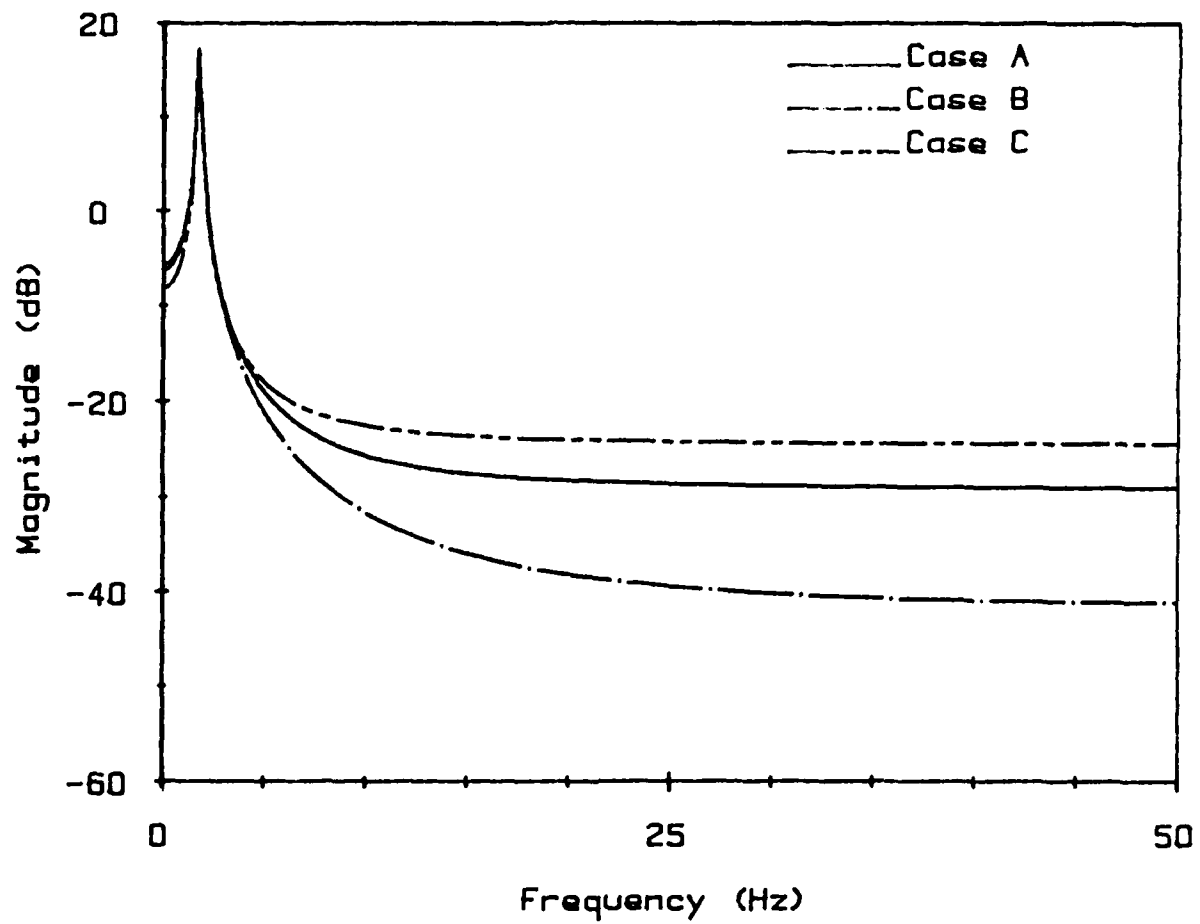


Figure 48: Magnitude frequency response plots of second order 2LS models.

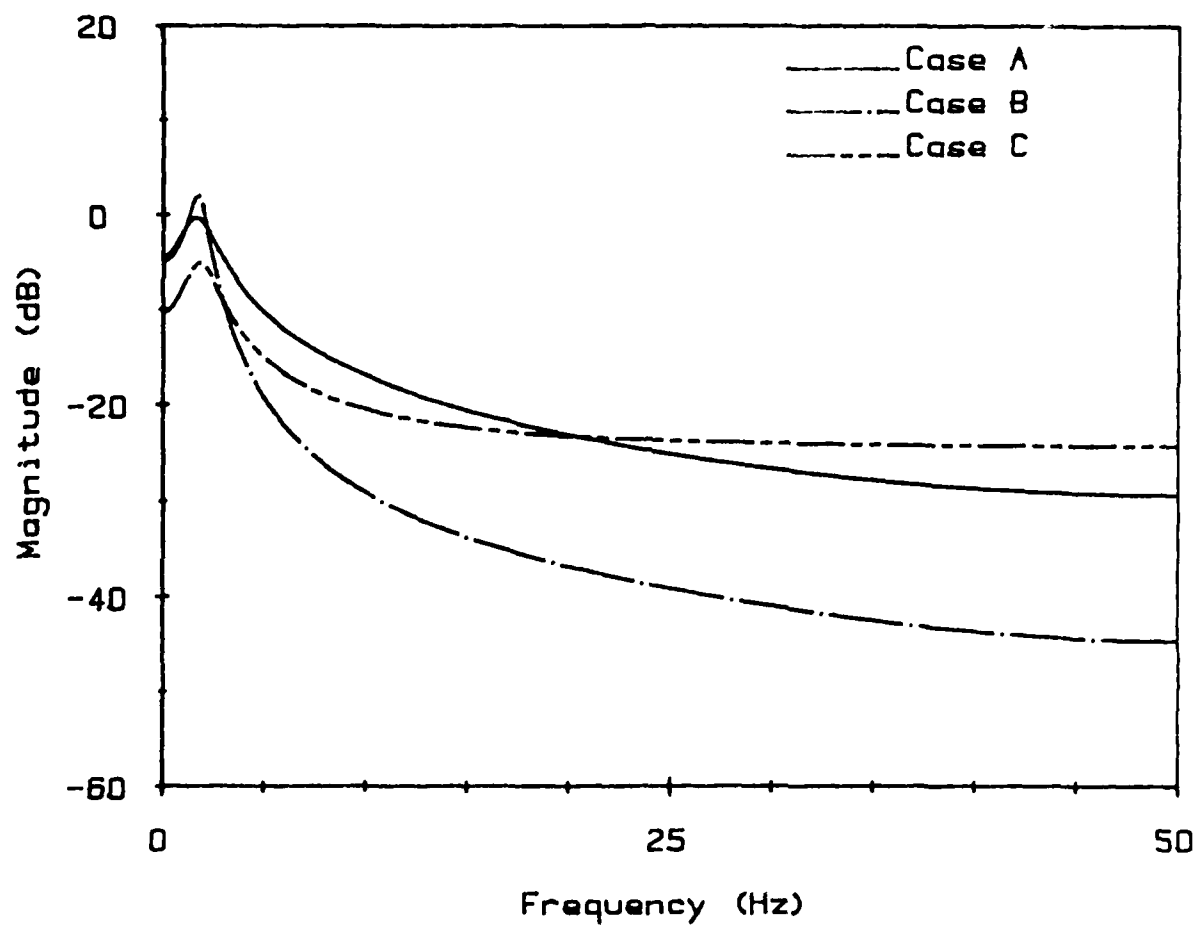


Figure 49: Magnitude frequency response plots of second order SLS models.

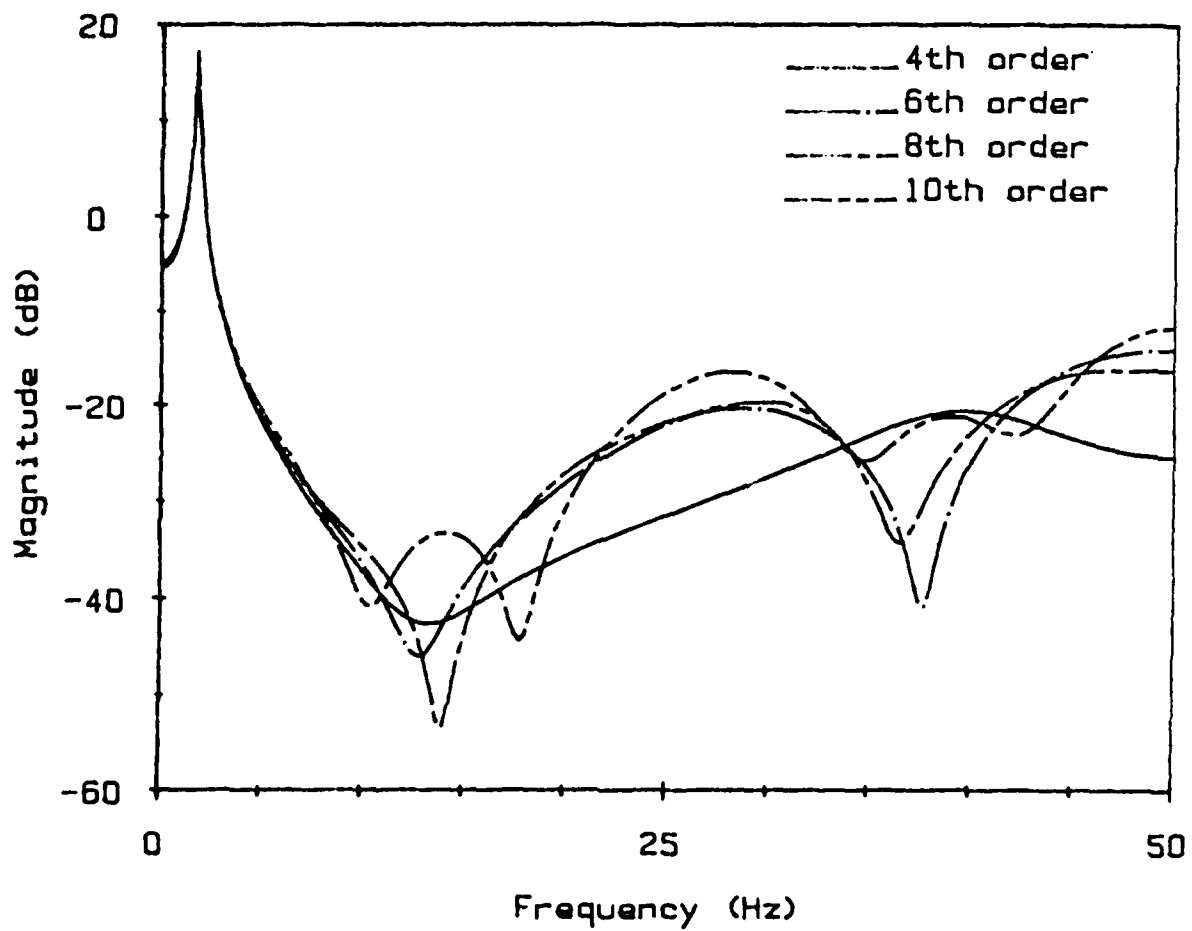


Figure 50: Magnitude frequency response plots of overspecified SLS models (input Case A).

Table 9: Frequency and damping estimates
from single stage LS estimates of Case A

Order	Freq (Hz)	ζ (%)
2	1.600	13.2
4	1.800	5.6
6	1.798	3.9
8	1.798	3.8
10	1.793	3.1
12	1.794	3.1
20	1.788	2.8

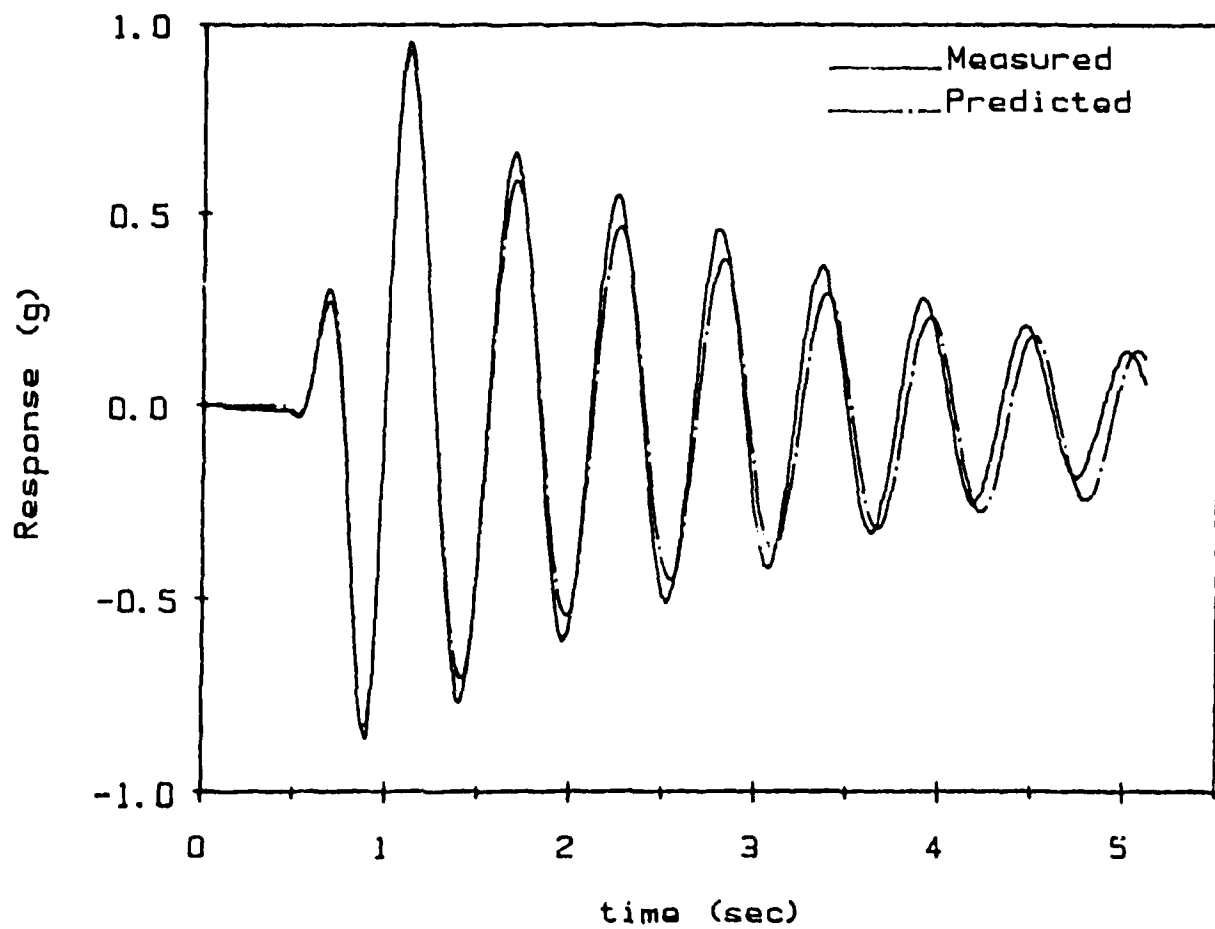


Figure 51: Tenth order 2LS model prediction of SDOF response to input Case B.

Table 10: MPEM estimates for MDOF exp. data

Trial L		mode 1		mode 2		mode 3		mode 4	
		freq	damp	freq	damp	freq	damp	freq	damp
#		Hz	%	Hz	%	Hz	%	Hz	%
1	30	1.516	.500	8.801	.223	(filtered)		(filtered)	
2	30	1.518	.594	8.801	.229	(filtered)		(filtered)	
3	40	1.512	.322	8.804	.205	24.66	.168	(filtered)	
4	40	1.512	.454	8.800	.271	24.64	.181	(filtered)	
5	50	1.517	.686	8.793	.307	24.57	.201	(unidentified)	
6	50	1.518	.463	8.800	.274	24.55	.330	48.29	.034
AVG		1.515	.503	8.800	.251	24.60	.220	48.29	.034
Analytical		1.45		9.10		25.49		49.95	

mode) inside the unit circle, indicating that more trials are necessary. The average of the identified values were then used in the second stage of the 2LS procedure.

The base block that the beam was cantilevered from was attached to a shaker to provide controllable system input. The input was measured as the acceleration response of the base block using a strain gage accelerometer and the system response was measured as the beam tip acceleration. The voltage sent to the shaker was a random binary voltage generated by computer. The voltage was randomly either +1V or -1V for a discrete time. Two sets of filtered input accelerations to this system are shown in Figures 52 and 53 (Case D and Case E, 500pts, $f_s=250$ Hz). Most of the input energy was contained between the frequencies of approximately 5 and 35 Hz. The shaker was unable to provide input at frequencies as low as the first mode, and therefore the first mode was not excited. The MA parameters for this system were estimated from the data assuming either two or three significant modes.

The frequency response plots of SLS ARMA models of order 4, 6, 8, and 10 obtained using data from input Case D are shown in Figure 54. As the overspecification is increased, the peaks are better defined. 2LS models of order four and six were also obtained from input Case D using the frequency and damping estimates of just the second and third mode for the fourth order model and the estimates of the second, third and fourth modes for the sixth order model to determine the AR parameters. The frequency response plots for these two cases are shown in Figure 55. The frequency response plot shows that the sixth order model is approximately equivalent to the fourth order model in the frequency range of interest. The response predictions from input Case E using the sixth and tenth order SLS models are shown in Figures 56 and 57 in comparison with the actual system response. The sixth order model does not predict response as well as the overspecified model. The fourth order 2LS model predicts the response as well as the overspecified SLS model as shown in Figure 58, and the prediction can be developed in approximately 40% of the time required for the tenth order overspecified model.

Overview

The comparison of results from the numerical simulations show the improved transient response predictions from using models developed with the 2LS method. The results from experimental systems are quite good even though the experimental system is nonviscously damped, and the ARMA model is better suited for a viscously damped system. The MPEM was successful in identifying the frequency and damping factors of the first four modes for the cantilever beam. The MPEM did fail to provide estimates of the fourth mode of the experimental MDOF system in Trial 5. In this case, the measured free

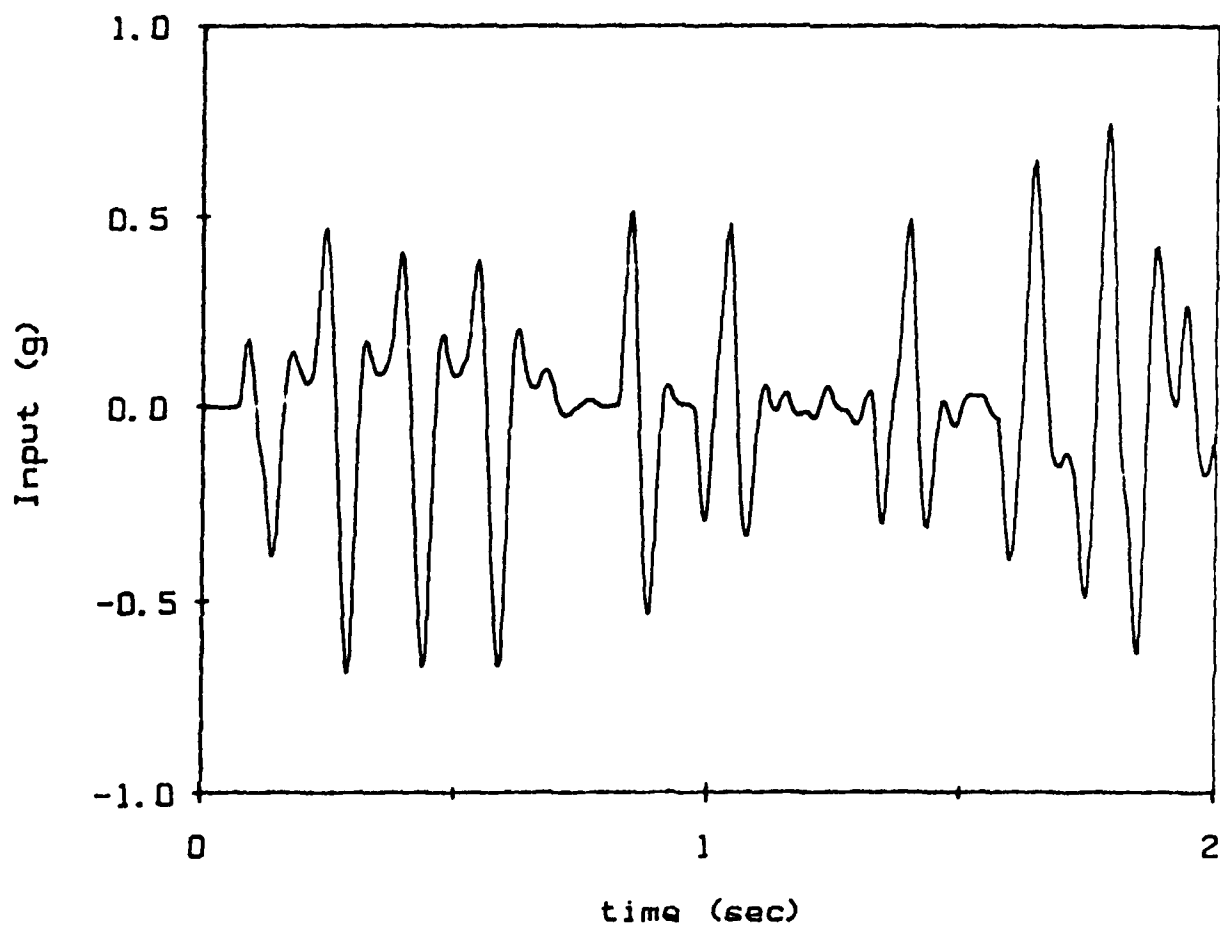


Figure 52: Acceleration input to the MDOF system, input Case D.

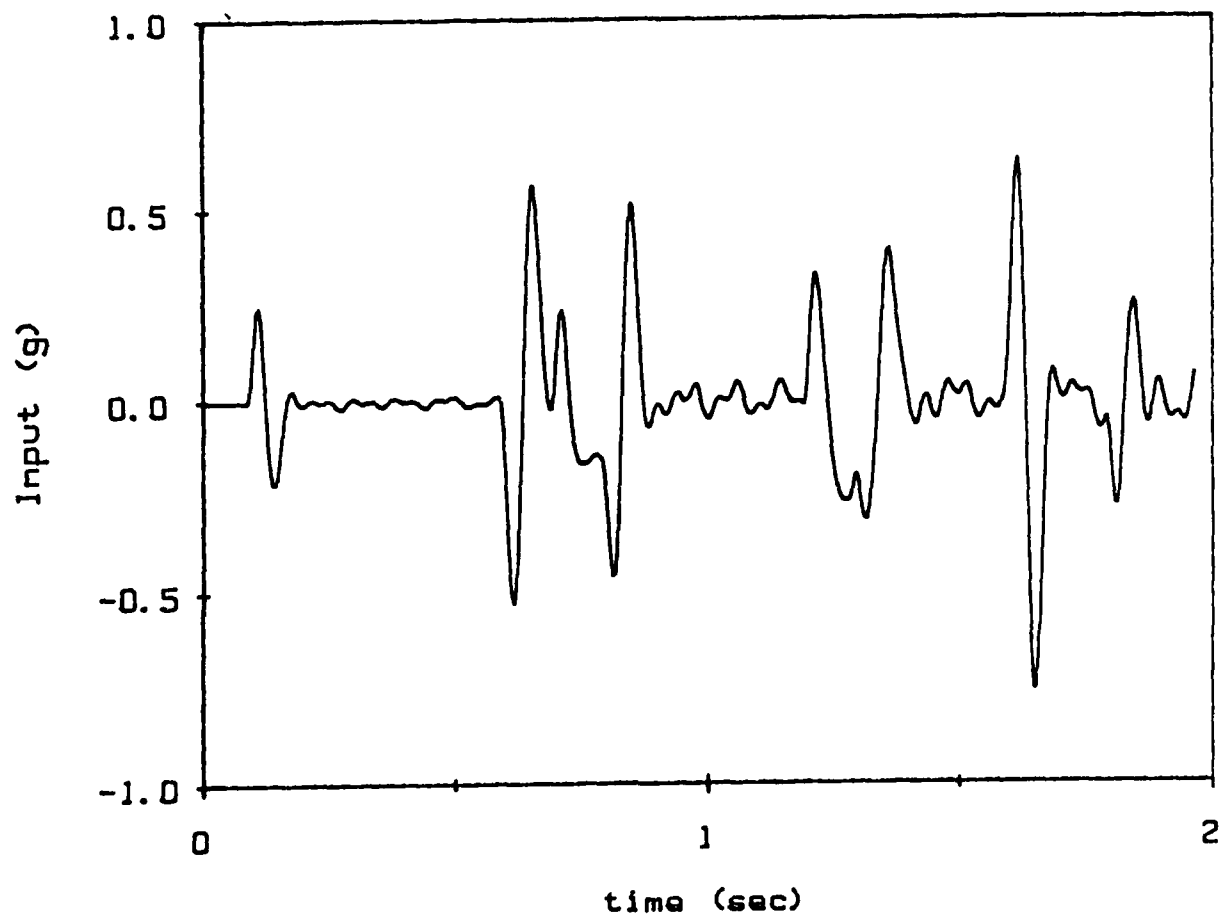


Figure 53: Acceleration input to the MDOF system, input Case E.

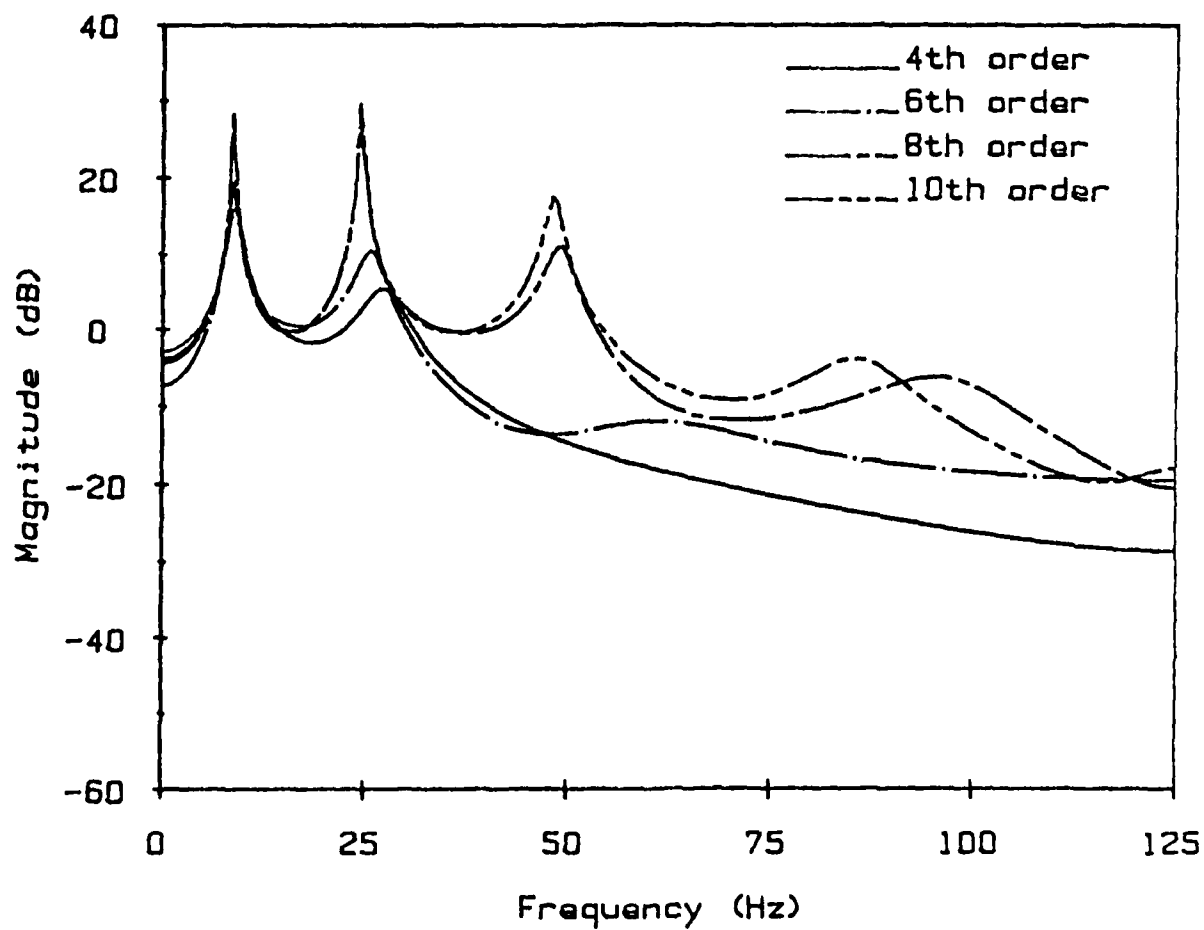


Figure 54: Magnitude frequency response plots of SLS models (input Case D).

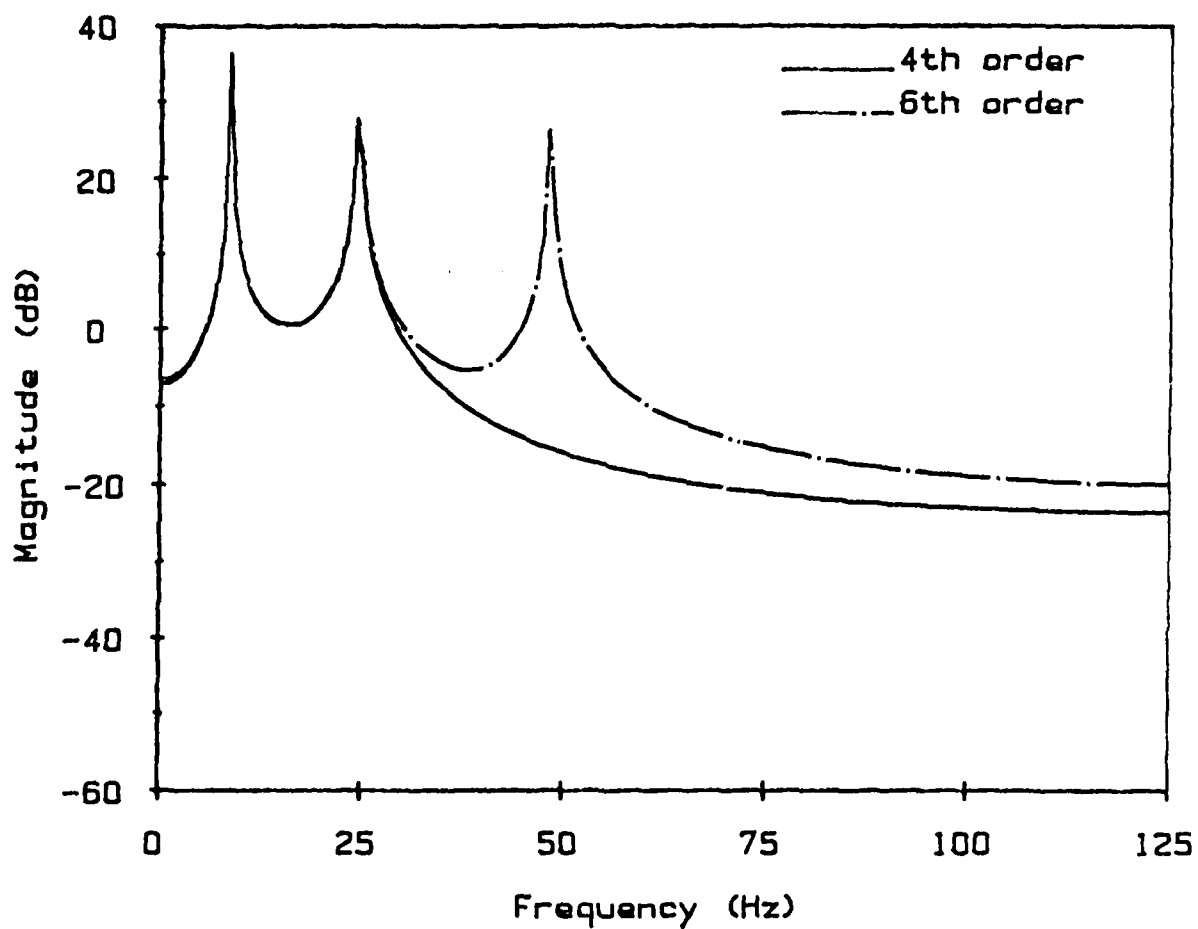


Figure 55: Magnitude frequency response plots of 2LS models (input Case D).

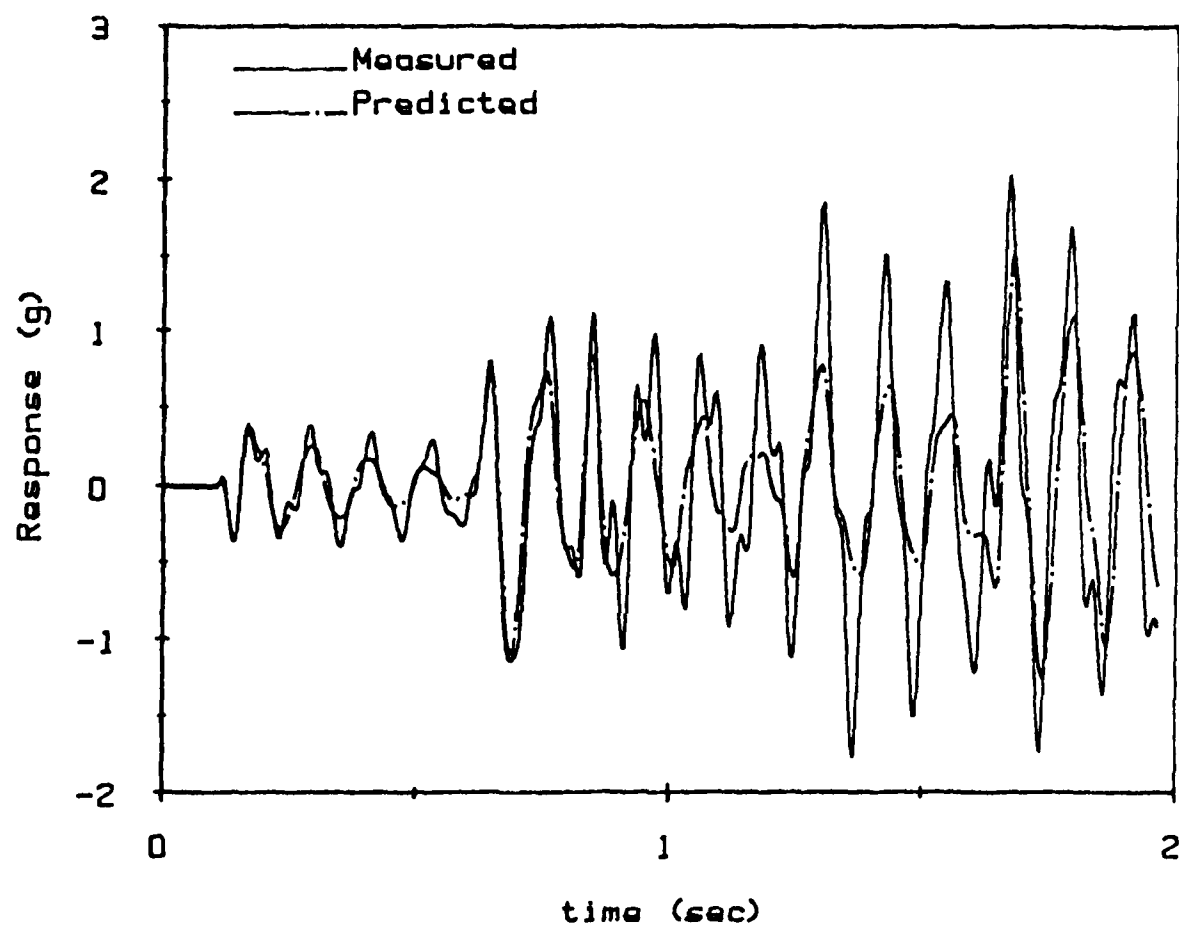


Figure 56: Sixth order SLS model used to predict response of the MDOF system to input Case E.

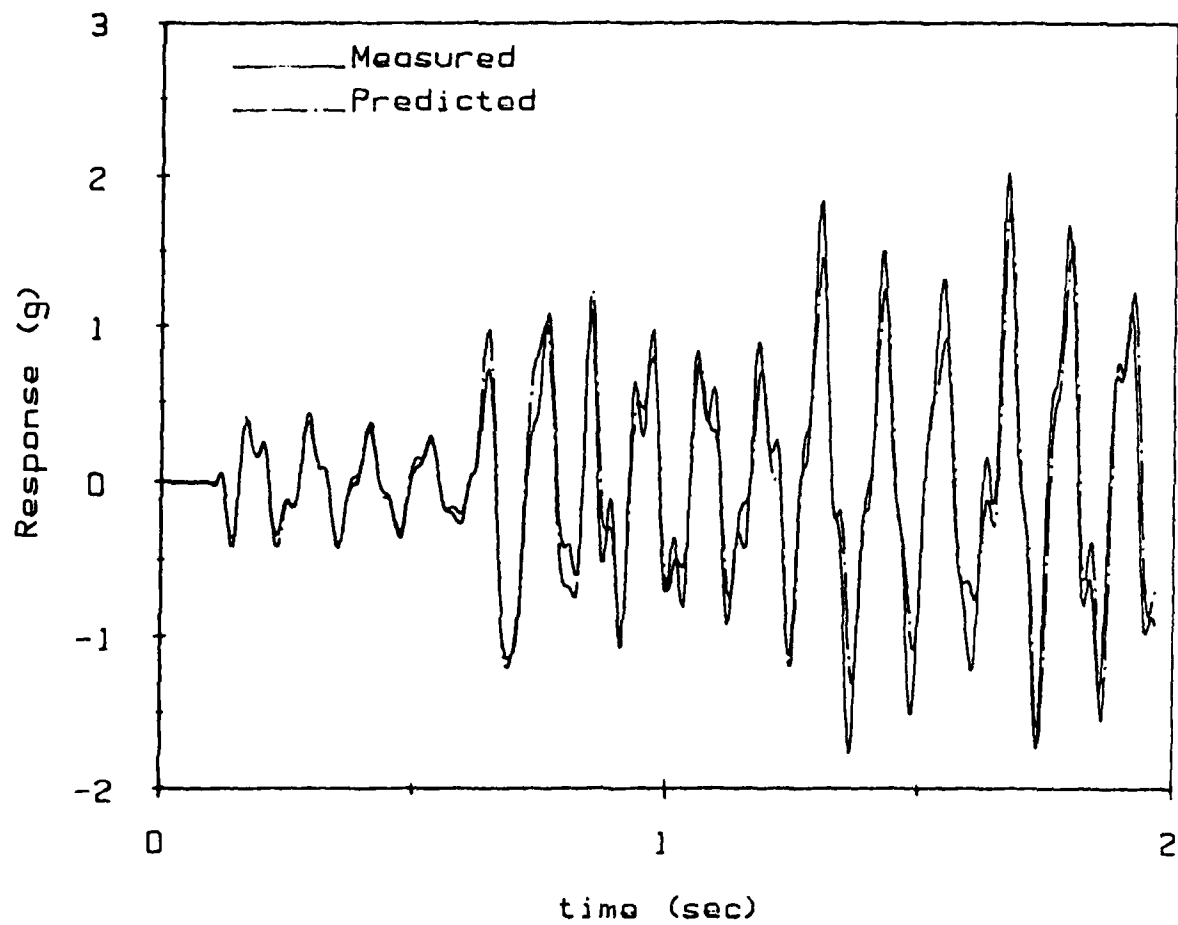


Figure 57: Tenth order SLS model used to predict response of the MDOF system to input Case E.

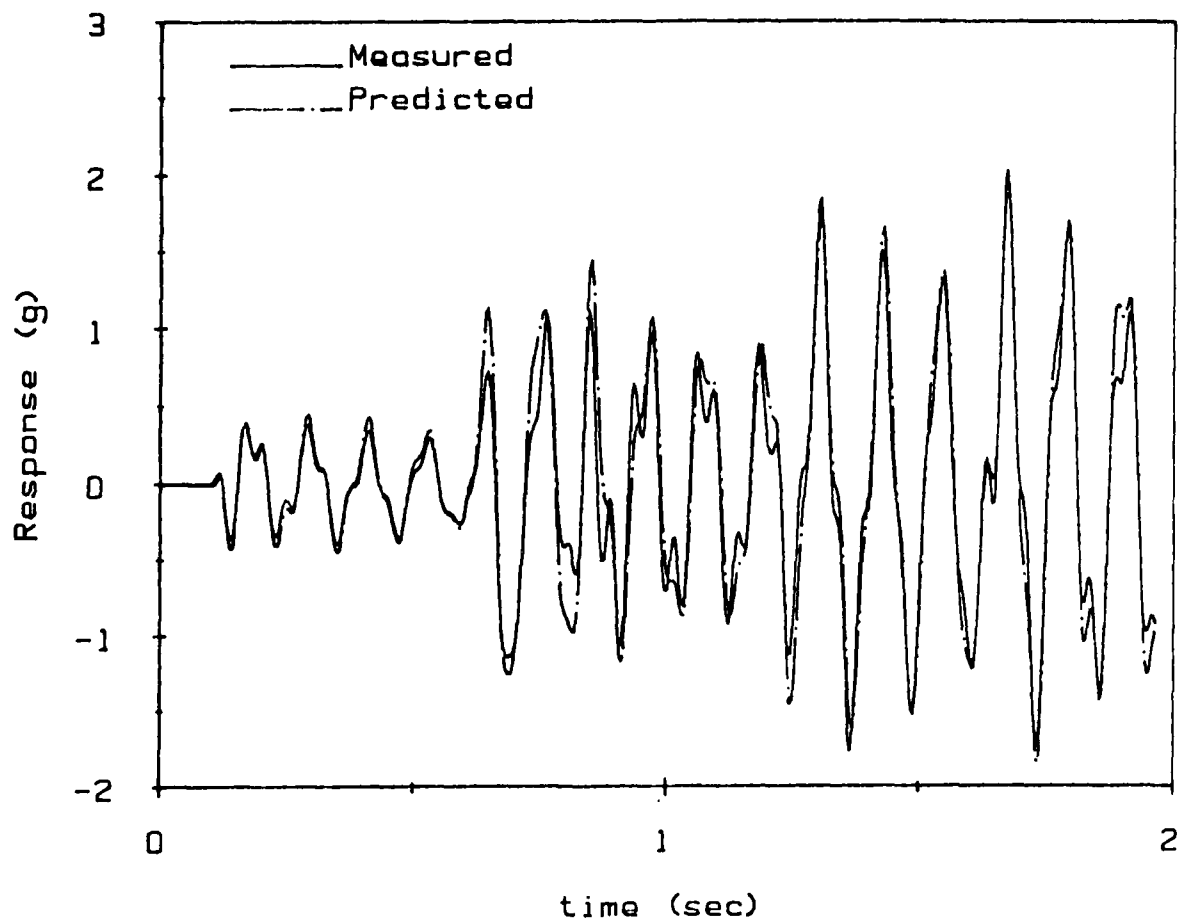


Figure 58: Fourth order 2LS model used to predict response of the MDOF system to Case E.

response contained too much noise. The MPEM sensitivity toward noise can be diminished by further overspecification of the model but that was not attempted in this study. An overspecified ordinary LS estimate of the AR parameters could have been used to identify the frequencies and dampings, but it would have been difficult to distinguish the signal roots from the extraneous roots.

The deficiencies of an ordinary single-stage identification scheme arise from bias problems in the estimation of the AR parameters of the ARMA model. The advantage of the two-stage procedure is in the determination the AR parameters separately from the MA parameters allowing greater accuracy in the estimation. The 2LS method reduces the bias in the AR parameters before the second stage and allows for the identification of a reduced order ARMA model. The disadvantage of the 2LS method is that it requires an additional set of data, a free response record. An alternative is to form the impulse response function using time domain data, but this usually requires an ensemble average of multiple tests. Ideally, the single-stage algorithm can be used with overspecified systems and the extraneous poles and roots can be eliminated providing a small order accurate model. The difficulty is in the automatic sorting of the extraneous poles and roots from the signal pole and roots.

NONLINEAR MODELS

Discrete time series can be used for transient response prediction of linear structures. Free vibration can be modeled by a special form called an Autoregressive (AR) model. When structural nonlinearities are present, it may be possible to modify the form of the AR model to incorporate the nonlinearities. One possibility is to allow the model parameters to become functions of state. This report explores the proper form of the parameter functions for various nonlinear structures. Two numerical case studies and experimental results are used to evaluate the model form. This section presents the results of a preliminary study intended to investigate the suitability of modeling nonlinear structural systems with Discrete Time Series models.

The Nonlinear AR Model

Free vibration for linear structures can be modeled as an Autoregressive process. The Autoregressive (AR) models can be used to extract modal parameters such as damping factors and natural frequencies. The AR models can be parameterized from measured free vibration using the identification algorithm presented in the previous sections. The models can then be used, if initial conditions are known, to predict vibration. The standard AR model for a single output system is

$$x(k) = -a_1 x(k-1) - a_2 x(k-2) - \dots - a_p x(k-p) + \epsilon(k) \quad (83)$$

where $x(k)$ is the system's free response at discrete time k , the a 's are the parameters of the model, $\epsilon(k)$ is the residual or error, and p is the system order. For multiple output systems, x becomes a vector of responses and the parameters become matrices. The AR model can be put into the form

$$[1 + a_1 z^{-1} + a_2 z^{-2} + \dots + a_p z^{-p}] x(k) = \epsilon(k) \quad (84)$$

using the definition of the forward shift operator, z . The AR model used to predict the free response of a linear system can be modified in an attempt to incorporate certain types of system nonlinearities. In this report the constant coefficients of the AR model become functions of state in order to form the nonlinear Autoregressive (NLAR) models. The general NLAR model is

$$[1 + a_1(x) z^{-1} + \dots + a_p(x) z^{-p}] x(k) = \epsilon(k) \quad (85)$$

where the x vector represents the state

$$x = [x(k-1), x(k-2), \dots, x(k-p)] \quad (86)$$

The NLAR model is an approximation. The accuracy of the NLAR model depends upon the magnitude of nonlinearity, the form of individual AR functionals, the accuracy in the parameterization of the functionals, and the initial conditions. The form of the NLAR model has to be determined before the predictive model is parameterized. Single-degree-of-freedom (SDOF) nonlinear oscillators were studied to gain insight into model forms. The general NLAR model for a nonlinear SDOF oscillator is

$$[1 + a_1(x) z^{-1} + a_2(x) z^{-2}] x(k) = \varepsilon(k) \quad (87)$$

The studies focused upon the form of the functionals a_1 and a_2 .

Examples

Two case different systems were studied using simulated time series data. These systems were a Duffing Oscillator and a viscous-coulomb damped oscillator. Noiseless position time history data were generated numerically by integrating the equations of motions via the fourth order Runge-Kutta algorithm.

System response data for a complex nonlinear mechanical system was also acquired experimentally. A Piper Apache oleo-pneumatic landing gear strut was used. Experimental position data were acquired using the oleo-pneumatic strut test facility shown in Figure 59. Regardless of its source, the position data were used to estimate the parameters of the proposed models in a least squares (LS) fashion. The first two points from the position data were then used along with the models to generated predicted response. The position data and the predicted response were compared to qualitatively compare the models. The investigations were focused upon the evaluation of the model form and not necessarily upon the identification algorithms or the influence of noise. For these reasons the simulation data were not corrupted with noise, but noise in the experimental data was unavoidable.

1. The Duffing Oscillator

The Duffing Oscillator represents an SDOF system where the stiffness is nonlinear and the damping is viscous. The equation of motion for a Duffing Oscillator is

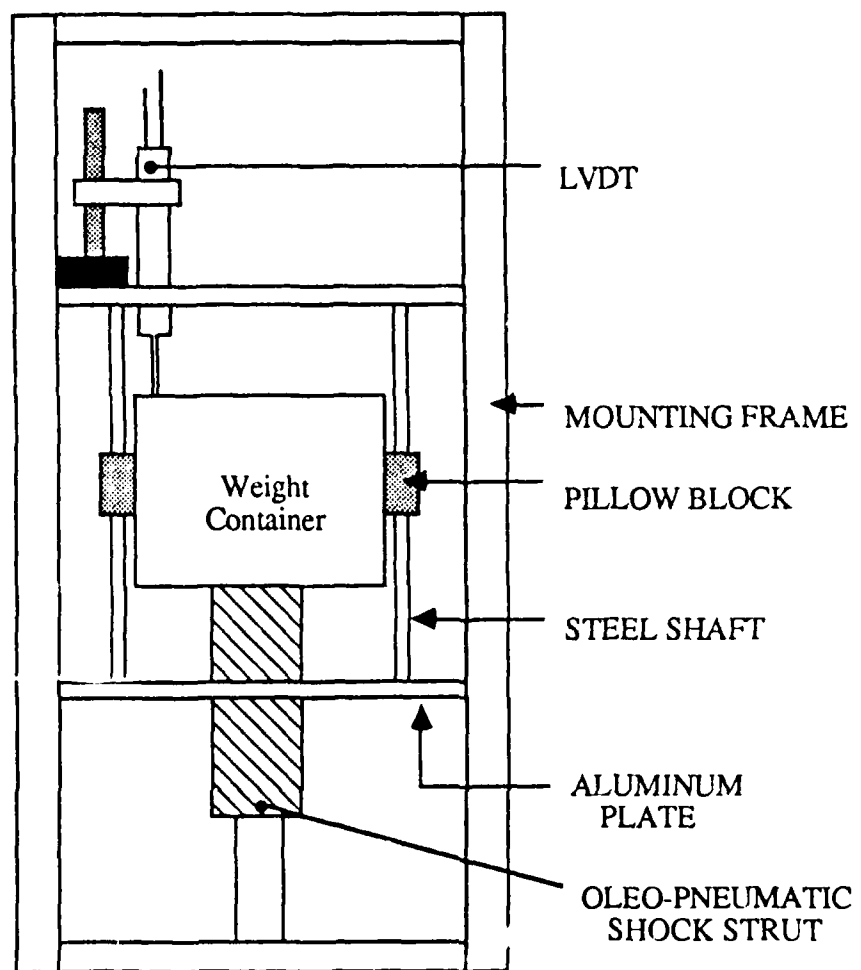


Figure 59: Oleo-pneumatic shock strut experimental apparatus.

$$\ddot{x} + c \dot{x} + \alpha x + \beta x^3 = 0 \quad (88)$$

If β is positive, the oscillator becomes more stiff as the displacement, x , increases and the oscillator is said to have a hard spring. If β is negative, the oscillator becomes less stiff as the displacement increases, and the oscillator is said to have a soft spring. Only the results using hard springs will be presented in this report. NLAR models for the Duffing oscillator have been cited in the literature in the past, Reference 24 suggests that the NLAR model

$$x(k) + (b_1 + c_1 \exp(-x^2(k-1))) x(k-1) + a_2 x(k-2) = \epsilon(k) \quad (89)$$

could be used to approximate the Duffing Oscillator. This model will be referred to as the exponential model, since reference 24 has incorporated the stiffness nonlinearity of the Duffing oscillator into an exponential functional for a_1 . Usually differential equations can be approximated through finite differencing procedures. Here, central differencing of Eqn 88 is used to suggest an alternate and somewhat simpler nonlinear form,

$$x(k) + (b_1 + c_1 x^2(k-1)) x(k-1) + a_2 x(k-2) = \epsilon(k) \quad (90)$$

This NLAR model will be referred to as the parabolic model, since a_1 has a parabolic functional form. Also, the linear AR model, where the parameter are constants, can also be used to approximate the Duffing Oscillator and the influence of the nonlinearity investigated.

The numerical simulations used the following form of the hard spring Duffing Oscillator

$$\ddot{x} + 0.25 \dot{x} + 14.8 x + 34.02 x^3 = 0 \quad (91)$$

which is also the oscillator used by reference 24. The initial conditions and time increment used in the numerical integration were

$$x(0) = 1. \quad \dot{x}(0) = 0. \quad \Delta t = 0.01 \text{ sec} \quad (92)$$

The three models, the exponential NLAR model, the parabolic NLAR model, and the AR model, were estimated from 500 points of data. The linear model, identified by the Modified Principal Eigenvectors Method, the exponential model, identified by a LS algorithm, and the parabolic model, identified by a LS algorithm, are all given in Table 11.

Table 11: Models used for Duffing Oscillator

Trial	AR Model		Exponential Model			Parabolic Model		
	a ₁	a ₂	a ₁	b ₁	a ₂	a ₁	b ₁	a ₂
1	-1.9946	0.9978	-1.9910	-0.00545	0.9975	-1.9960	0.00339	0.9975
2	*	*	-1.9862	-0.0153	0.9975	-1.9960	0.00338	0.9975

* not considered

Figure 60 shows the predictions of the three models (using the first two simulated data points as initial conditions) in comparison to the simulated data. Both NLAR models perform better than the linear model. The differences between the models and the analytical Duffing Oscillator can be examined by plotting the damped natural frequency versus displacement x , as shown in Figure 61. The percent of critical damping as a function of displacement can also be examined, but is not included in this report. The natural frequency of the Duffing Oscillator is $(\alpha + \beta x^2)^{1/2}$. The natural frequency of the NLAR models are determined by linearizing the models with $x(k-1)$ equal to x . Figure 61 shows that the exponential model is a good approximation for $.2 < |x| < 1$, while the parabolic model is good for much higher amplitudes.

Simulated data were used to test if the performance of the NLAR models degrade as the amplitude is increased (essentially, increasing the nonlinearity). The equation of motion was integrated again with the initial position value doubled. The models were then used with the new initial conditions to predict the response. Figure 62 shows the response predictions of the NLAR models in comparison to simulated data. The exponential model fails to predict the nonlinear response. The parabolic model's response prediction is good within the resolution of the plot. The results suggest that the exponential model does not approximate the amplitude dependence of the Duffing Oscillator as well as the parabolic model. This can be confirmed by estimating the parameters of the models using the new simulated Duffing Oscillator data. The form of an NLAR model should remove the amplitude dependence of the parameters. The NLAR models estimated from the new data are also given in Table 11. The exponential model's parameters change while the parabolic model is invariant to the change in initial conditions.

2. Viscous-Coulomb Damped Oscillator

The numerical studies also included a viscous-coulomb damped oscillator. The equation of motion for the viscous-coulomb damped oscillator is

$$\ddot{x} + 2\zeta\omega \dot{x} + \omega^2 x + c_d \text{sign}(\dot{x}) = 0 \quad (93)$$

where c_d is the coulomb damping coefficient. No NLAR model for this system was found in the literature. Finite differencing of Eqn 93 suggests an NLAR model of the form

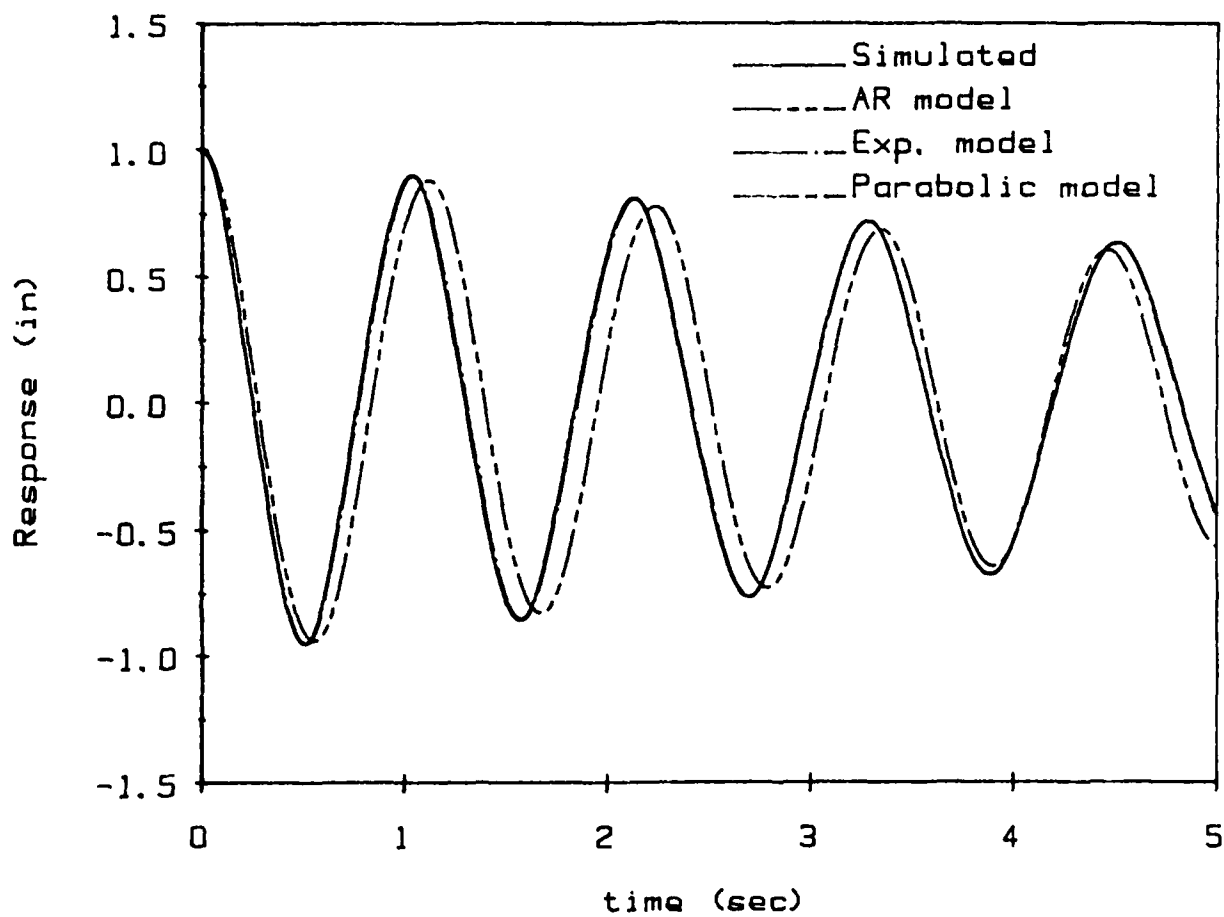


Figure 60: Duffing oscillator response and predictions from NLAR and AR models.

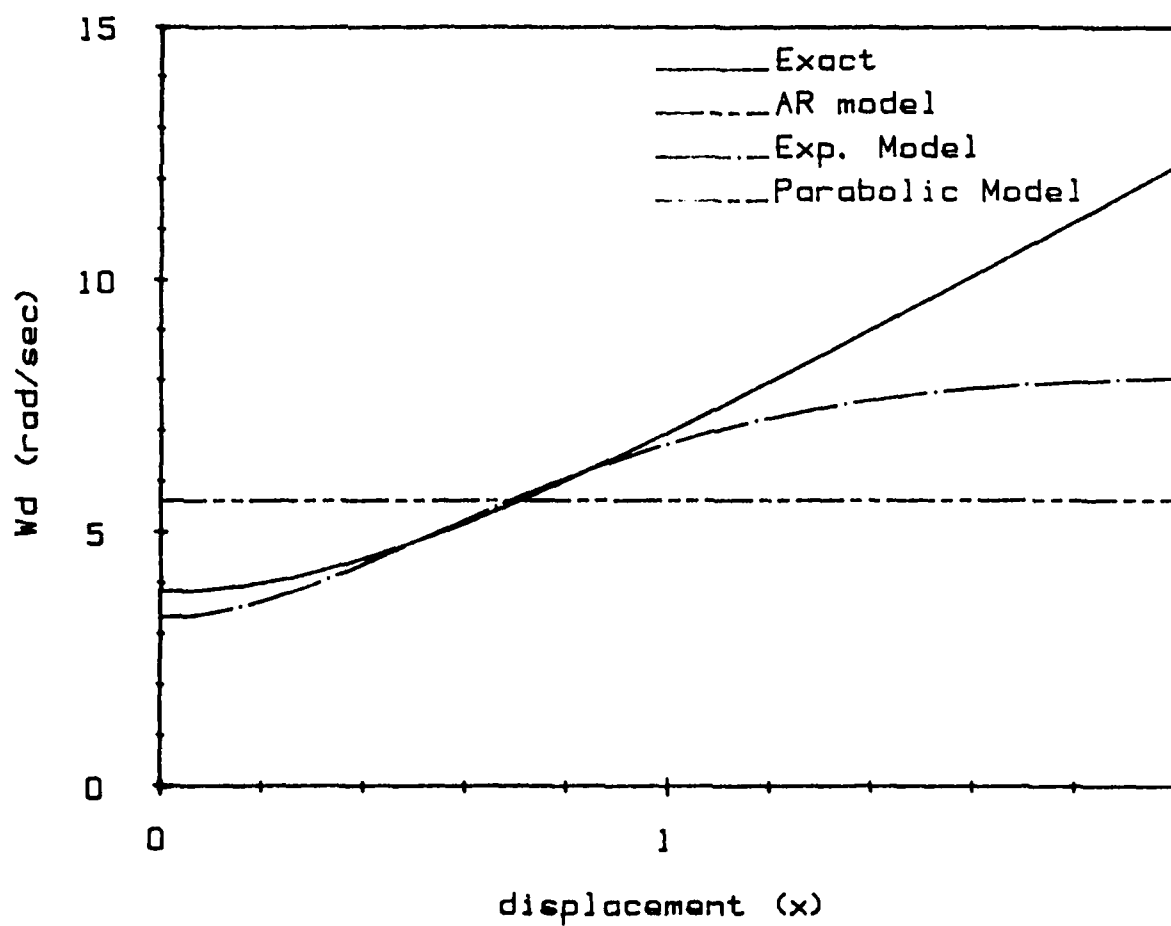


Figure 61: Frequency of the Duffing oscillator and the models as a function of displacement.

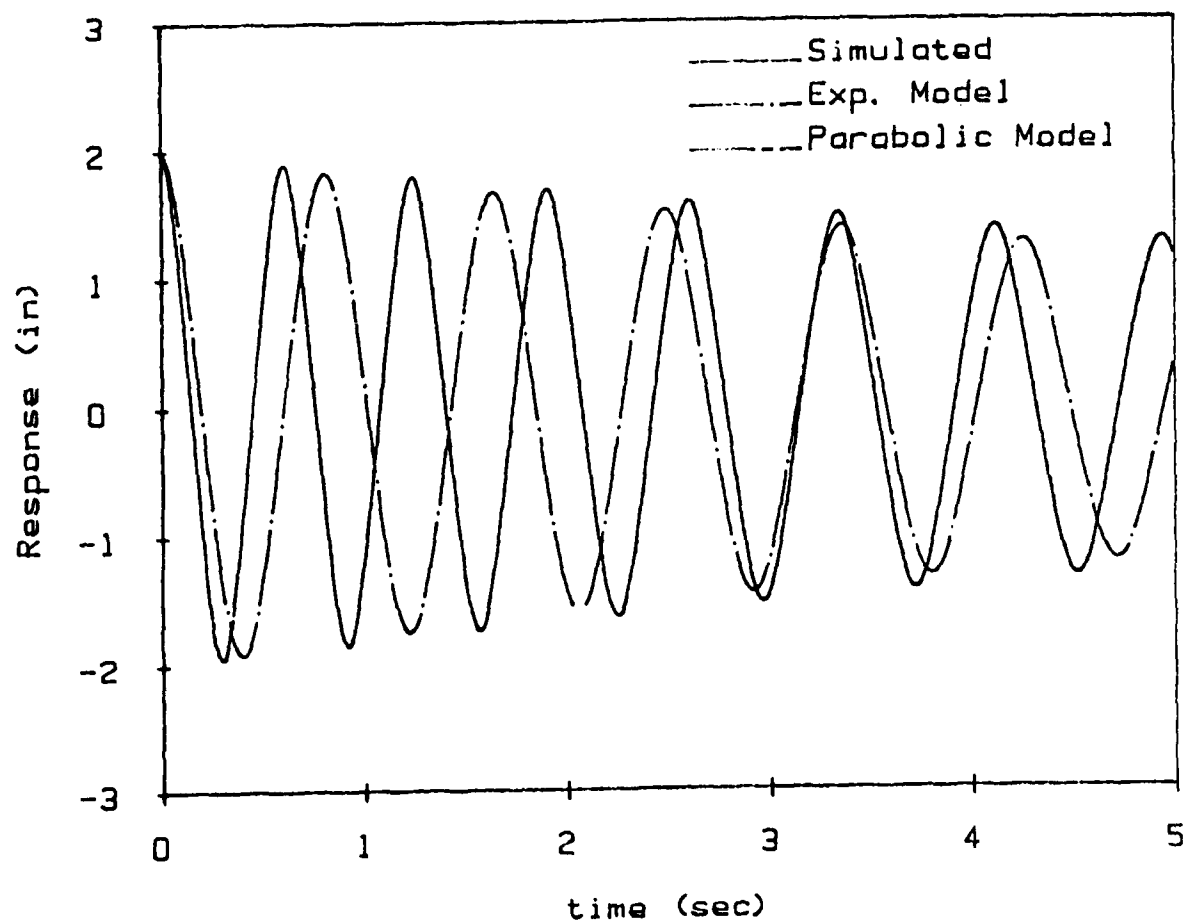


Figure 62: Duffing oscillator response and response predictions from NLAR models (larger initial amplitude).

$$x(k) + a_1 x(k-1) + a_2 x(k-2) + b_1 \text{sign} [x(k-1) - x(k-2)] = \epsilon(k) \quad (94)$$

The linear AR model may also be used if the coulomb damping term is insignificant. The viscous-coulomb damped oscillator used in the simulation was

$$\ddot{x} + 0.5 \dot{x} + 25 x + 0.5 \text{sign}(\dot{x}) = 0 \quad (95)$$

The initial conditions and time increment used in the numerical integration were the same as Eqn 92. The linear model, identified by the MPEM, and the NLAR model identified by a LS algorithm are given in Table 12. Figure 63 shows the predictions of the two models in comparison to the simulated data. Both predictions are very good with the NLAR model prediction following the simulated data more closely. The effectiveness of the linear model in the vibration prediction shows the nonlinearity of Eqn 93 may not be great enough to warrant an NLAR model for this particular set of parameters.

3.A Landing Gear

Nonlinear data from a Piper Apache landing gear strut (see reference 25) was used to evaluate the NLAR models. The experimental data (500 pts, $f_s=200$ Hz) appear in Figure 64. Notice the constant value of the data past about 1.5 second. The landing gear sticks at a new equilibrium after every oscillation due to the strong effect of the bearing friction in the gear. This bearing friction can be modeled as coulomb damping. The NLAR used to model the vibration was of the form

$$x(k) + a_1 x(k-1) + a_2 x(k-2) + b_1 \text{sign} [x(k-1) - x(k-2)] + b_2 = \epsilon(k) \quad (96)$$

which is the same as the viscous-coulomb damped NLAR model plus a constant term to represent the nonzero equilibrium position. An AR model has no mechanism to simulate coulomb sticking, so only the NLAR model was identified by a LS algorithm. The NLAR model identified at the 200 Hz sample rate is not accurate, possibly due to noise bias. However, when the data is decimated by using only every fifth data point (reducing the sample rate to 40 Hz), the effect of the noise bias is not as great. The resulting NLAR model is given in Table 12, and the response prediction of the NLAR model is shown in Figure 64. The NLAR prediction is more accurate than the predictions of the oscillation given by reference 25 and exhibits the sticking phenomenon associated with coulomb damping.

Table 12: Models used for Viscous-Coulomb Damped Oscillator

	a_1	a_2	b_1	b_2
<u>Simulation</u>				
AR model	-1.9904	0.9929		
NLAR model	-1.9924	0.9949	4.77E-5	
<u>Experimental</u>				
Strut	-1.9156	0.9512	0.00175	-0.08677

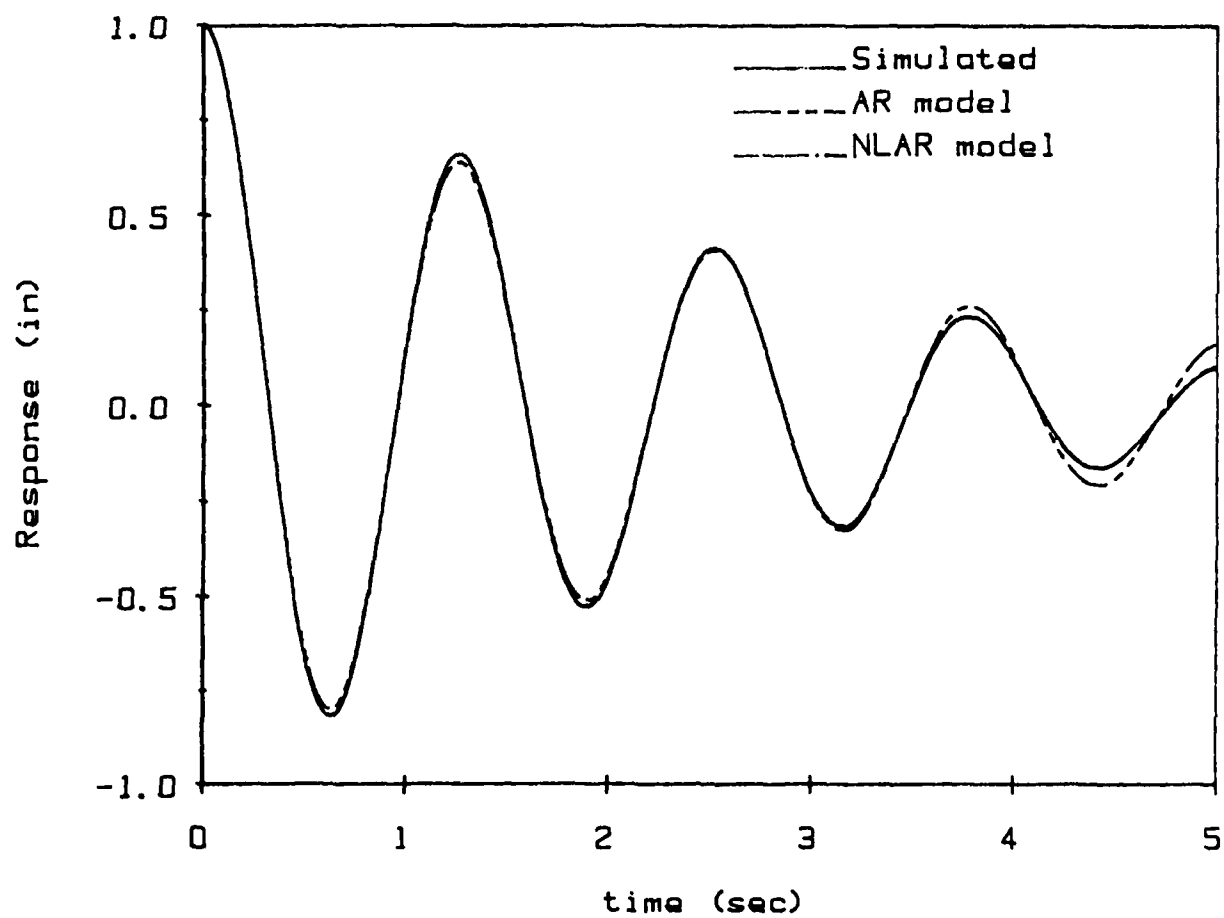


Figure 63: Viscous-coulomb damped oscillator response and predictions from NLAR and AR models.

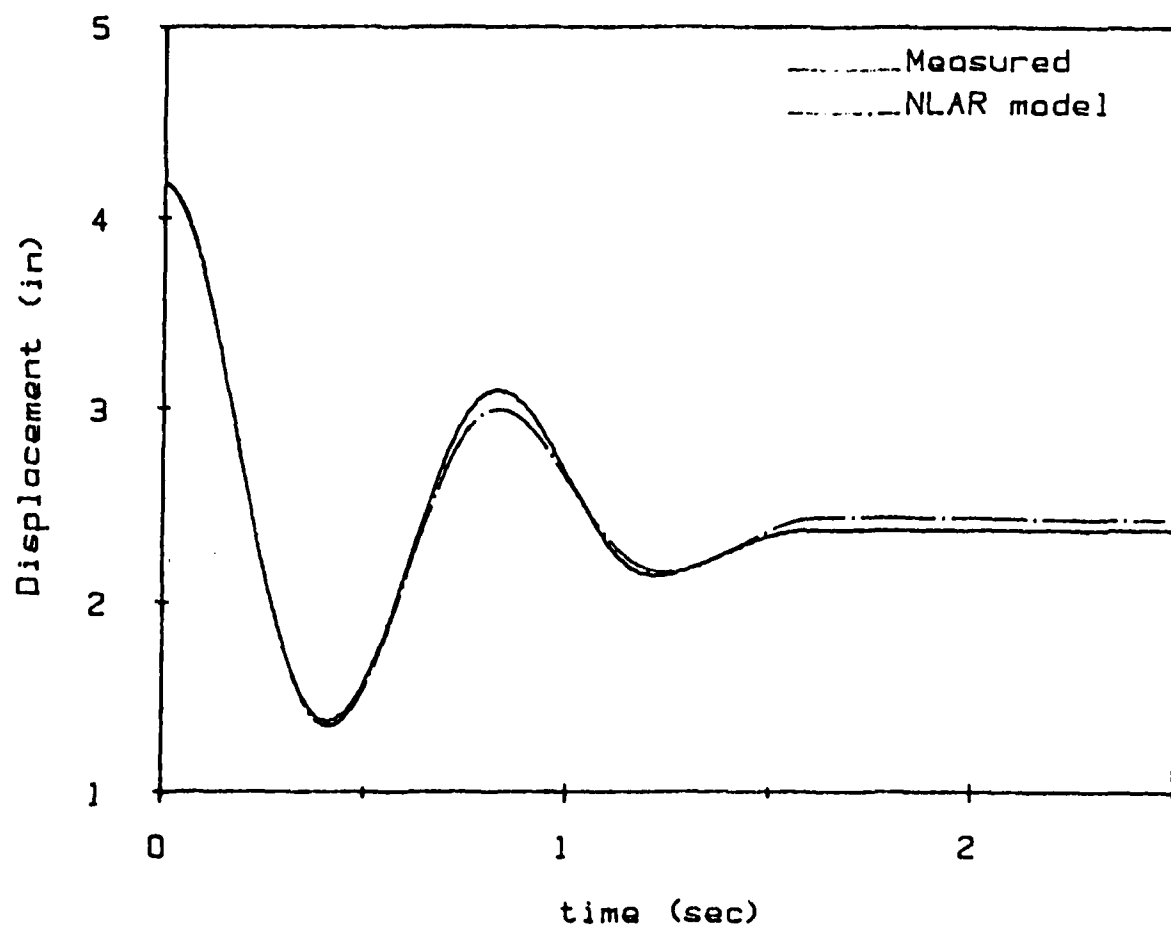


Figure 64: Experimental data and NLAR and AR model response predictions.

Overview

Finite differencing techniques were used to suggest forms for nonlinear autoregressive models. The NLAR models when parameterized by LS techniques using noiseless simulated data provided excellent prediction. Linear AR models provided response predictions nearly as good as the NLAR models when the degree of the nonlinearity was not great. The exponential NLAR model is accurate when the degree of nonlinearity of the Duffing Oscillator is small. But, the parabolic model is a better model for the Duffing Oscillator particularly for large amplitude response. Experimental data from an oleo-pneumatic strut was also used to evaluate NLAR models. The prediction of the experimental response by the NLAR was very reasonable and is better than the predictions by the nonlinear differential equations parameterized by reference 25.

The use of time domain discrete models in the form of Autoregressive Moving Average (ARMA) models has been shown to be advantageous in the response prediction of forced linear vibration. When the structure is nonlinear, the ARMA models may have to be extended to model the nonlinearities just as the AR models are extended to NLAR models. The new nonlinear ARMA model's parameters will be functions of state. This is a topic requiring further research.

CONCLUSIONS AND RECOMMENDATIONS

Discrete time series models for both linear and nonlinear systems have been shown to be an effective and accurate means of representation and prediction. Linear models are effective when the order is large enough and the sample rate is at least an order of magnitude higher than the upper bandwidth limit. The time series models become more accurate as the sample rate increases, but the effect of noise perturbations on the parameters also become greater as the sample rate increases. Some trade-off must be made when selecting a sample rate for acquiring data to be used in parameter identification. The sample rate must be high enough to insure accurate predictions once the model is parameterized. But the sample rate must be low enough, so that the model can be parameterized in the presence of noise.

There are various techniques to reduce the effect of noise bias ranging from iterative techniques to overspecification techniques. The iterative techniques often experience convergence problems when an interim model is identified as unstable. The overspecification techniques are easier to implement but result in excessively large model order. The model must be reduced to the proper order by some technique if it is to be effective in response prediction or control. Time domain modal methods compare mode shapes using modal confidence factors and are able to eliminate the noise model from the system model in the identified model. The difficulties with modal methods are they require multiple measurement locations, are time consuming, and are not well suited for automated data processing. Ideally, one would like to measure a limited number of inputs and outputs to parameterize the model. When a SISO ARMA model is desired, only the single input and the single output time histories should be needed to characterize the model. The traditional signal processing techniques utilize single input and single output time histories but provide no means of separating noise from signal modes in the identified model. One has to use the entire model, with noise and signal fractions, to predict vibration as was done with the overspecified SLS models. The 2LS algorithm allows the AR part of the model to be reduced to its proper size through the use of the MPEM. A non-overspecified LS estimation of the MA parameters completes the algorithm. The MPEM was shown to be a highly accurate and automatic method for determining system order. The MPEM identifies natural frequencies and eliminates noise bias from free response records even in the case of closely spaced modes. The main drawback of the 2LS algorithm is that it requires the additional free response record. The frequency and damping error envelopes demonstrate the high accuracy required when identifying the autoregressive part of the model.

Experimental data from a SDOF and a MDOF was obtained, and ARMA models were successfully identified using the SLS and the 2LS algorithms. The 2LS models, with orders of the proper size, successfully predicted forced dynamic response. The SLS models had to be much larger, greatly overspecified, to be as accurate as the 2LS models. The FRF plots graphically show how the SLS models begin to follow the first few modes of vibration and how all modes are accurately represented when the order is overspecified to large values. The FRFs also show the dynamics of the noise modes beyond the bandwidth limit. There are also noise modes in the bandwidth, but their effects cannot be uncovered because their amplitudes are small when compared to the signal modes. There does not seem to be any ill-effects of carrying the noise modes in the model when it is used for vibration prediction, other than the additional computational time required. But, it is conceivable that there are some contributions in the predicted response from these noise modes. The 2LS models have no noise modes and may be used effectively for response prediction purposes, and also for control algorithm purposes where pole and zero cancellations are required.

The optimum algorithm would require only the single input single output time histories and would overspecify the model and eliminate the extraneous noise modes. A two-stage algorithm would first have to identify the AR model from an overspecified ARMA model and then identify the MA parameters in a LS fashion without requiring the addition set of free response data. The other drawback of the 2LS method, as it is proposed, is that the MA part of the model is not overspecified. There is some noise in the input and overspecification would allow the MA parameters to be better identified. But, there is no way of identifying which part of the MA model is extraneous without the use of the AR parameters. The best method would identify an overspecified ARMA model and split it into a modal form using partial fraction expansion, and identify the true modes of the system using some criteria. The problem is what type of criteria to use.

Real nonlinear free response was used to evaluate the NLAR models. The NLAR model predicts the free vibration of an oleo-pneumatic strut fairly well. However, an accurate model requires the careful selection of the data sampling rate and the determination of the influence of measurement noise on the parameters. This has not been considered in this investigation. The algorithm that identified the NLAR models was a non-overspecified LS algorithm which produces biased parameter estimates. The bias at the lower sample rate had a smaller effect than the bias at the high sample rate. No algorithms were investigated to reduce the bias. Given further research in the area, the NLAR models could become easier to parameterize and more attractive to use.

REFERENCES

1. Leuridan J.M., Brown D.L., and Allemang R.J., "Time Domain Parameter Identification Methods for Linear Modal Analysis: A Unifying Approach," *Journal of Vibration, Acoustics, Stress, and Reliability in Design*, Vol. 108, pp.1-8, Jan. 1986.
2. Pappa R.S. and Ibrahim S.R., "A Parametric Study of the Ibrahim Time Domain Modal Identification Algorithm," *The Shock and Vibration Bulletin*, Vol. 51, No. 3, 1981, pp.43-51.
3. Franklin G.F., and Powell J.D., Digital Control of Dynamic Systems, Addison-Wesley Publishing Co., Reading Mass, 1980.
4. Astrom K.J. and Wittenmark B., Computer Controlled Systems, Prentice-Hall, Englewood Cliffs, N.J., 1984.
5. Stanley, W.D., Digital Signal Processing, Reston, Va., Reston Publishing Co., Inc., 1975.
6. Bellanger M., Digital Processing of Signals, John Wiley and Sons, N.Y. 1984.
7. James, P. N., Souter, P., and Dixon, D. C., "A Comparison of Parameter Estimation Algorithms for Discrete Systems," *Chemical Engineering Science*, Vol. 29, pp. 539-547, 1974.
8. Hale A. L., and Bergman L.A., "The Dynamic Synthesis of General Non-Conservative Structures from Separately Identified Substructure Models," *Journal of Sound and Vibration*, Vol 98., pp. 431-446, 1985.
9. Mignolet, M. P., and Spanos, P. D., "ARMA Monte Carlo Simulation in Probabilistic Structural Analysis," AIAA Paper No. 87-0932, Proceedings of the 28th AIAA/ASME/ASCE/AHS Structures, Structural Dynamics and Materials Conference, 1987.
10. Spanos, P. D., and Mignolet, M. P., "Z-Transform Modeling of P-M Wave Spectrum," *Journal of Engineering Mechanics*, Vol. 112, No. 8, August, 1986.
11. Gersch W., and Foutch D.A., "Least Squares Estimates of Structural System Parameters Using Covariance Function Data," *IEEE Trans. on Control*, Vol. AC-19., No. 6.,1974, pp. 898-903.
12. Press W.H., Flannery B. P., Teukolsky S.A., and Vetterling W.T., Numerical Recipes, Cambridge Mass, 1986.
13. Kay S.M., and Marple S.L., "Spectrum Analysis-A Modern Perspective," *IEEE Proceedings*, Vol. 69, No. 11, 1981, pp. 1380-1419.
14. Gray R.M. and Davisson L.D., Random Processes, A Mathematical Approach for Engineers, Prentice Hall, 1986.
15. Shinozuka M., Yun C., and Imai H., "Identification of Linear Structural Dynamic Systems," *Journal of the Engineering Mechanics Division*, ASCE, Vol. 108, EM 6, pp. 1371-1390, 1982.

16. Astrom K.J., and Eykhoff P., "System Identification-A Survey," *Automatica*, Vol. 7, pp. 123-162, 1971.
17. Hsia T.C., "On Least Squares Algorithms for System Parameter Identification," *IEEE Transactions on Automatic Control*, pp. 104-108, Feb. 1976.
18. Finnegan B.M., and Rowe I.H., "Strongly Consistent Parameter Estimation by the Introduction of Strong Instrumental Variables," *IEEE Trans. Automatic Control*, vol AC-19, pp. 825-30, 1974.
19. Astrom K.J. and Bohlin T., "Numerical Identification of Linear Dynamic Systems from Normal Operating Records," Theory of Self-Adaptive Control Systems, (Ed.-Hammond), Plenum Press, 1966.
20. Sinha N.K. and Kuszta B., Modeling and Identification of Dynamic Systems, Van Nostrand Reinhold Co., N.Y., 1983.
21. Cooper J. E., "Comparison of Some Time Domain System Identification Techniques using approximation Data Correlations," *Proceedings of IMAC-IV*, 1986.
22. Kumaresan R., and Tufts D.W., "Estimating the Parameters of Exponentially Damped Sinusoids and Pole-Zero Modeling in Noise," *IEEE Trans. on Acoustics.*, Vol. ASSP 30, No.6, 1982, pp.833-840.
23. Batill S.M, and Hollkamp J.J., "Parameter Identification of Discrete Time Models for Structural Response Prediction," Submitted to the AIAA Journal, 1988.
24. Ozaki T., "Non-Linear Threshold Autoregressive Models for Non-Linear Random Vibrations," *J. of Applied Probability*, Vol. 18, 1981, pp. 443-451.
25. Batill S.M, and Baccaro J. M., "Modeling and Identification of Nonlinear Dynamic Systems with Application to Aircraft Landing Gear," *Proceedings of the 29th AIAA/ASME/ASCE/AHS Structures, Structural Dynamics and Materials Conference*, pp.871-884, 1988.
26. Golub G.H., and Van Loan C.F., Matrix Computations, John Hopkins University Press, Baltimore Md., 1983.
27. Goodwin G.C. and Payne R.L., Dynamic System Identification: Experiment Design and Data Analysis, Academic Press, New York, 1977.
28. Brandon J.A., "On the Robustness of Algorithms for the Computation of the Pseudo Inverse for Modal Analysis," *Proceedings of the 6th IMAC*, 1988.
29. Vold H. and Rocklin G.T., "The Numerical Implementation of a Multi-Modal Estimation Method for Mini-Computers," *Proceedings of the 1st International Modal Analysis Conference*, pp. 542-548, 1982.

BIBLIOGRAPHY

Identification Survey Papers and Books

1. Astrom K.J., and Eykhoff P., "System Identification-A Survey," *Automatica*, Vol. 7, pp. 123-162, 1971.
2. James, P. N., Souter, P., and Dixon, D. C., "A Comparison of Parameter Estimation Algorithms for Discrete Systems," *Chemical Engineering Science*, Vol. 29, pp. 539-547, 1974.
3. Goodwin G.C. and Payne R.L., Dynamic System Identification: Experiment Design and Data Analysis, Academic Press, New York, 1977.
4. Kay S.M., and Marple S.L., "Spectrum Analysis-A Modern Perspective," *IEEE Proceedings*, Vol. 69, No. 11, 1981, pp. 1380-1419.
5. Shinozuka M., Yun C., and Imai H., "Identification of Linear Structural Dynamic Systems," *Journal of the Engineering Mechanics Division*, ASCE, Vol. 108, EM 6, pp. 1371-1390, 1982.
6. Sinha N.K. and Kuszta B., Modeling and Identification of Dynamic Systems, Van Nostrand Reinhold Co., N.Y., 1983.
7. Cooper J.E. and Wright J.R., "Comparison of Some Time Domain Methods for Structural System Identification," Presented at the 2nd International Symposium on Aeroelasticity and Structural Dynamics, Aachen W. Germany, 1985.
8. Cooper J. E., "Comparison of Some Time Domain System Identification Techniques using approximation Data Correlations," *Proceedings of IMAC-IV*, 1986.
9. Mohanty N., Random Signal Estimation and Identification, Van Nostrand Reinhold Co., N.Y., 1986.
10. Braun S. and Ram Y., "Time and Frequency Identification Methods in Over-Determined Systems," *Mechanical Systems and Signal Processing*, Vol. 1, pp.245-257, 1987.

Maximum Likelihood Method

1. Astrom K.J. and Bohlin T., "Numerical Identification of Linear Dynamic Systems from Normal Operating Records," Theory of Self-Adaptive Control Systems, (Ed.-Hammond), Plenum Press, 1966.
2. Astrom K.J., "Maximum Likelihood and Prediction Error Methods," *Automatica*, Vol. 16, pp. 551-574, 1980.

Generalized Least Squares

1. Soderstrom, T., "Convergence Properties of the Generalized Least Squares Identification Method", *Automatica*, Vol. 10, pp. 617-626, Pergamon Press, 1974.
2. Hsia T.C., "On Least Squares Algorithms for System Parameter Identification," *IEEE Transactions on Automatic Control*, pp. 104-108, Feb. 1976.

Instrumental Variables Method

1. Wong, K. Y. and Polak, E., "Identification of Linear Discrete Time Systems Using the Instrumental Variable Method," *IEEE Transactions on Automatic Control*, Vol. AC-12, No. 6, pp. 707-718, December 1967.
2. Young, P. C., "An Instrumental Variable Method for Real-time Identification of a Noisy Process," *Automatica*, Vol. 6, pp. 271-287, Pergamon Press, 1970.
3. Finnegan B.M., and Rowe I.H., "Strongly Consistent Parameter Estimation by the Introduction of Strong Instrumental Variables," *IEEE Trans. Automatic Control*, vol AC-19, pp. 825-30, 1974.

Ibrahim's Time Domain Method

1. Ibrahim S.R. and Mikulcik E.C., "A Time Domain Modal Vibration Test Technique," *The Shock and Vibration Bulletin*, Vol. 43, No. 4, pp. 21-37, 1973.
2. Ibrahim S.R. and Mikulcik E.C., "The Experimental Determination of Vibration Parameters from Time Responses," *The Shock and Vibration Bulletin*, Vol 46, pp.187-196, Aug. 1976.
3. Ibrahim S.R. and Mikulcik E.C., "A Method for the Direct Identification of Vibration Parameters from the Free Response," *The Shock and Vibration Bulletin*, Vol 47., No. 4, pp.183-198, 1977.
4. Ibrahim S.R., "Random Decrement Technique for Modal Identification of Structures," *J.Spacecraft*, Vol. 14, No.11, pp. 696-700. , 1977.
5. Ibrahim S.R., "Modal Confidence Factor in Vibration Testing," *J. Spacecraft*, Vol. 15, No. 5, pp 313-316, 1978.
6. Pappa R.S. and Ibrahim S.R., "A Parametric Study of the Ibrahim Time Domain Modal Identification Algorithm," *The Shock and Vibration Bulletin*, Vol. 51, No. 3, 1981, pp.43-51.
7. Smith W.R., "Least-Squares Time-Domain Method for Simultaneous Identification of Vibration Parameters form Multiple Free-Response Records," AIAA conference paper 81-0530.
8. Andrew L.V., "An Automated Application of Ibrahim's Time Domain Method to response of the Space Shuttle," AIAA conference paper 81-0526.
9. Ibrahim S.R. and Pappa R.S., "Large Modal Survey Testing using the Ibrahim Time Domain Identification Technique," *J. Spacecraft*, Vol. 19, No.5, pp. 459-465, 1982.
10. Ibrahim S.R., "Dynamic Modeling of Structures from Measured Complex Modes," *AIAA Journal*, pp. 446-451, June 1983.
11. Ibrahim S.R., "Computation of Normal Modes from Identified Complex Modes," *AIAA Journal*, Vol. 21, No. 3, pp. 446-451, 1983.

12. Ibrahim S.R., "Time-Domain Quasilinear Identification of Non-linear Dynamic Systems," *AIAA Journal*, Vol. 22, pp. 817-823, June 1984.
13. Brandon J.A., "On the Theoretical Justification of Ibrahim's Method," *AIAA Journal*, Vol. 23, No. 5, pp. 815-816, 1985.
14. Ibrahim S.R., "Double Least Squares Approach of Use in Structural Modal Identification," *AIAA Journal*, Vol 24., March 1986.
15. Ibrahim S.R., "An Approach for Reducing Computational Requirements in Modal Identification," *AIAA Journal*, pp 1725-1727, Oct. 1986.
16. Hollkamp J.J. and Batill S.M., "Noise Bias in Various Formulation of Ibrahim's Time Domain Technique," *AIAA Journal*, To be published

The Complex Exponential Method

1. Keller C., "Determination of complex characteristic values and vectors from sinusoidal excitations at near resonance frequencies," AFWAL-TR-80-3136, U.S. Air Force, June 1981.
2. Mergeay M., "Least Square Complex Exponential Method and Global System Parameter Estimation used by Modal Analysis," *Proceedings of the 8th International Seminar on Modal Analysis*, 1983.

The Eigensystem Realization Algorithm

1. Juang J.N. and Pappa, R.S., "An Eigensystem Realization Algorithm for Modal Parameter Identification and Model Reduction," *J. of Guidance, Control and Dynamics*, Vol. 8, 1985, pp. 620-627.
2. Pappa R.S. and Juang J.N., "Galileo Spacecraft Modal Identification using an Eigensystem Realization Algorithm," *Journal of Astronautical Sciences*, Vol. 33, No. 1, pp. 15-33, 1985.
3. Horta L.G. and Juang J.N., "Identifying Approximate Linear Models for Simple Nonlinear Systems," *Proceedings of the 26th AIAA/ASME/ASCE/AHS Structures, Structural Dynamics and Materials Conference*, pp. 282-289, 1985.
4. Juang J.N. and Pappa R.S., "Effects of Noise on Modal Parameter Identified by the Eigensystem Realization Algorithm," *J. of Guidance, Control and Dynamics*, Vol. 9, 1986, pp. 294-303.

ARMA models

1. Venkatesan, C., and Krishnan, V., "Stochastic Modeling of an Aircraft Traversing a Runway Using Time Series Analysis," AIAA Paper No. 81-4047, *Journal of Aircraft*, Vol. 8, No. 2, pp. 115-120, February 1981.
2. Hale A. L., and Bergman L.A., "The Dynamic Synthesis of General Non-Conservative Structures from Separately Identified Substructure Models," *Journal of Sound and Vibration*, Vol 98., pp. 431-446, 1985.

3. Lee, D. T. L., "System Order Determination of ARMA Models Using Ladder Estimation Algorithms," *The Journal of the Astronautical Sciences*, Vol. 33, No. 1, January-March 1985, pp. 49-61.
4. Green, M. and Moore, J. B., "Persistence of excitation in linear systems," *Systems Control Letters*, Vol. 7, pp. 351-360, 1986.
5. Taylor, I. F. "Identification of finite-order models of distributed systems," *IEE Proceedings*, Vol. 133, pt. D, No. 6, pp. 276-278, November 1986.
6. Batill S.M, and Hollkamp J.J., "Parameter Identification of Discrete Time Models for Structural Response Prediction," Submitted to the AIAA Journal, 1988.
7. Batill S.M, and Hollkamp J.J., "Parameter Identification of Discrete Time Models for Transient Response Prediction," Proceedings of the 29th AIAA/ASME/ASCE/AHS Structures, Structural Dynamics and Materials Conference, pp.158-166, 1988.

AR models

1. Gersch, W. "Estimation of the Autoregressive parameters of a Mixed Autoregressive Moving-Average Time Series," *IEEE Transactions on Automatic Control*, pp.583-588, October 1970.
2. Gersch W., Nielson N.N., and Akaike H., "Maximum Likelihood Estimation of Structural Parameters from Vibration Data," *Journal of Sound and Vibration*, Vol. 31, No. 3.,1973, pp.295-308.
3. Gersch W., and Foutch D.A., "Least Squares Estimates of Structural System Parameters Using Covariance Function Data," *IEEE Trans. on Control*, Vol. AC-19., No. 6.,1974, pp. 898-903.
4. Gersch, W., "On the Achievable Accuracy of Structural System parameter Estimates," *Journal of Sound and Vibration*, 34(1), pp. 63-79, 1974.
5. Wiberg, D. M., "Frequencies of Vibration Estimated by Lattices," *Journal of Astronautical Sciences*, Vol. 33, No. 1, Jan.-March 1985.
6. Stocia P., Friedlander B., and Soderstrom T., "Least-squares, Yule-Walker, and overdetermined Yule-Walker Estimation of AR parameters: A Monte Carlo analysis of Finite-sample Properties," *Int. J. Control*, Vol. 43, No.1, pp. 13-27, 1986.

Nonlinear Vibrations

1. Marquardt, D.W., "An Algorithm for Least Squares Estimation of Nonlinear Parameters," *Jour. Soc. Ind. Appl. Math.*, 11, 431, 1963.
2. Goodman, T.R., "System Identification and Prediction - An Algorithm Using a Newtonian Iteration Procedure," *Quart. of Applied Math.*, Vol. 24, No. 3, Oct. 1966.
3. Ozaki T. and Oda H., "Non-Linear Time Series Model Identification by Akaike's Information Criterion," *Information and Systems: Proceedings of the IFAC workshop*, Pergamon Press, 1977.

4. Haggan V. and Ozaki T., "Amplitude-Dependent Exponential AR model Fitting for Non-Linear Random Vibrations," Time Series, (O.D. Anderson, Ed.), North-Holland Publishing Company, pp. 57-70, 1980.
5. Ozaki, T., "Nonlinear Time Series Models for Nonlinear Random Vibrations," J. Appl. Prob., 17, pp. 84-93, 1980.
6. Tong H., "A View on Non-Linear Time Series Model Building," Time Series, (O.D. Anderson, Ed.), North-Holland Publishing Company, pp. 41-56, 1980.
7. Ozaki T., "Non-Linear Threshold Autoregressive Models for Non-Linear Random Vibrations," *J. of Applied Probability*, Vol. 18, 1981, pp. 443-451.
8. Batill, S.M., "A Study of Analytic Modeling Techniques for Landing Gear Dynamics," AFWAL-TR-82-3027, Air Force Wright Aeronautical Laboratories, May, 1982.
9. Lai H.Y., "Development of Nonlinear Dynamic Data System for Online Machining Vibratory System Characterization," Ph.d. Thesis, University of Wisconsin, 1984.
10. Batill S.M, and Baccaro J. M., "Modeling and Identification of Nonlinear Dynamic Systems with Application to Aircraft Landing Gear," Proceedings of the 29th AIAA/ASME/ASCE/AHS Structures, Structural Dynamics and Materials Conference, pp.871-884, 1988.

The Principal Eigenvectors Method

1. Kumaresan R., and Tufts D.W., "Estimating the Parameters of Exponentially Damped Sinusoids and Pole-Zero Modeling in Noise," *IEEE Trans. on Acoustics.*, Vol. ASSP 30, No.6, 1982, pp.833-840.
2. D.W. Tufts and R. Kumaresan, "Estimation of Frequencies of Multiple Sinusoids: Making Linear Prediction Perform Like Maximum Likelihood," *Proceedings of the IEEE*, Sept 1982.
3. Tufts D.W. and Kumaresan R., "Singular Value Decomposition and Improved Frequency Estimation Using Linear Prediction," *IEEE Transactions on Acoustics.* , Aug. 1982.

Singular Value Decomposition

1. Press W.H., Flannery B. P., Teukolsky S.A., and Vetterling W.T., Numerical Recipes, Cambridge Mass, 1986.
2. Brandon J.A., "On the Robustness of Algorithms for the Computation of the Pseudo Inverse for Modal Analysis," *Proceedings of the 6th IMAC*, 1988.

Modal Analysis

1. Formenti D., "Analytical and Experimental Modal Analysis," Structural Measurement Systems Training Paper, May 1977.

2. Allemang R.J., "Investigation of Some Multiple Input/Output Frequency Response Function Experimental Modal Analysis Techniques," Phd. Dissertation, University of Cincinnati, Cincinnati Ohio, 1980.
3. Vold H. and Rocklin G.T., "The Numerical Implementation of a Multi-Modal Estimation Method for Mini-Computers," *Proceedings of the 1st International Modal Analysis Conference*, pp. 542-548, 1982.
4. Ewins D.J., Modal Testing: Theory and Practice, John Wiley, 1984.
5. Craig, Jr., R. R., and Blair, M. A., "A Generalized Multiple-Input, Multiple-Output Modal Parameter Estimation Algorithm," *AIAA Journal*, Vol. 23, No. 6, pp. 931-937, June 1985.
6. Leuridan J.M., Brown D.L., and Allemang R.J., "Time Domain Parameter Identification Methods for Linear Modal Analysis: A Unifying Approach," *Journal of Vibration, Acoustics, Stress, and Reliability in Design*, Vol. 108, pp.1-8, Jan. 1986.
7. Liang Z., "On Modal Testing in the Time Domain," Dissertation at State University of New York, 1987.

Digital Control and Data Processing

1. Brigham, E.O., The Fast Fourier Transform, Englewood Cliffs, N.J., Prentice-Hall, 1974.
2. Stanley, W.D., Digital Signal Processing, Reston, Va., Reston Publishing Co., Inc., 1975.
3. Raven F.H., Automatic Control Engineering, McGraw-Hill, New York, 1978.
4. Franklin G.F., and Powell J.D., Digital Control of Dynamic Systems, Addison-Wesley Publishing Co., Reading Mass, 1980.
5. Astrom K.J. and Wittenmark B., Computer Controlled Systems, Prentice-Hall, Englewood Cliffs, N.J., 1984.
6. Bellanger M., Digital Processing of Signals, John Wiley and Sons, N.Y. 1984.

Spectral Estimation

1. Gersch, W., and Sharpe, D., "Estimation of Power Spectra with Finite-Order Autoregressive Models," *IEEE Transactions on Automatic Control*, pp. 367-369, August 1973.
2. Spanos, P. D., and Mignolet, M. P., "Z-Transform Modeling of P-M Wave Spectrum," *Journal of Engineering Mechanics*, Vol. 112, No. 8, August, 1986.
3. Mignolet, M. P., and Spanos, P. D., "Recursive Simulation of Stationary Multivariate Random Processes - Part I," *Transactions of the ASME*, Vol. 54, pp. 674-680, September 1987.
4. Mignolet, M. P., and Spanos, P. D., "ARMA Monte Carlo Simulation in Probabilistic Structural Analysis," AIAA Paper No. 87-0932, Proceedings of the

28th AIAA/ASME/ASCE/AHS Structures, Structural Dynamics and Materials Conference, 1987.

5. Spanos, P. D. and Mignolet, M. P., "Recursive Simulation of Stationary Multivariate Random Processes - Part II," *Journal of Applied Mechanics*, Vol. 54, pp.681-687, September 1987.
6. Spanos, P. D., Mushung, L. J, Nelson, Jr., D. A. R., and Hamilton, D. A., "Digital Spectral Estimation and Modeling of Space Shuttle Flight Data," AIAA Paper No. 88-2408, Proceedings of the 29th AIAA/ASME/ASCE/AHS Structures, Structural Dynamics and Materials Conference, 1988.

APPENDIX A - Alternative Formulation

The governing differential equation of any linear system can be put into first order state space form

$$\dot{\mathbf{x}}(t) = \mathbf{A} \mathbf{x}(t) + \mathbf{B} \mathbf{u}(t) \quad (\text{A1})$$

$$\mathbf{y}(t) = \mathbf{C} \mathbf{x}(t) \quad (\text{A2})$$

The differential equation, Eqn A1 can be rearranged for solution after multiplying by $\exp(-\mathbf{A}t)$ to

$$\frac{d}{dt} [e^{-\mathbf{A}t} \mathbf{x}(t)] = e^{-\mathbf{A}t} \mathbf{B} \mathbf{u}(t) \quad (\text{A3})$$

The solution of Eqn A3 is made by simply integrating between t_k and t

$$e^{-\mathbf{A}t} \mathbf{x}(t) - e^{-\mathbf{A}t_k} \mathbf{x}(t_k) = \int_{t_k}^t e^{-\mathbf{A}\tau} \mathbf{B} \mathbf{u}(\tau) d\tau \quad (\text{A4})$$

After rearranging and multiplying by $\exp(\mathbf{A}t)$, the solution is

$$\mathbf{x}(t) = e^{\mathbf{A}(t-t_k)} \mathbf{x}(t_k) + \int_{t_k}^t e^{\mathbf{A}(t-\tau)} \mathbf{B} \mathbf{u}(\tau) d\tau \quad (\text{A5})$$

Since the selection of t and t_k is arbitrary, let t_k be kh and t be $(k+1)h$. Notice that the input can vary between the sample times t and t_k and that Eqn A5 is the **exact** solution but the integral depends upon the input time function. However, if one does not know the input over the entire time domain, but only at discrete time instance, Eqn A5 can be approximated. If we assume the input is constant over the interval between t and t_k and is equal to $\mathbf{u}(t_k)$, then Eqn A5 can be reduced to

$$\mathbf{x}([k+1]h) = e^{\mathbf{A}h} \mathbf{x}(kh) + \left[\int_0^h e^{\mathbf{A}\tau} d\tau \right] \mathbf{B} \mathbf{u}(kh) \quad (\text{A6})$$

or

$$\mathbf{x}([k+1] h) = \Phi \mathbf{x}(kh) + \Gamma \mathbf{u}(kh) \quad (\text{A7})$$

Equation A7 allows one to find an approximate solution of Eqn A1 at discrete time instances by performing a recursive matrix operation. The matrix operation can be put into a more compact form through the use of the forward shift operator as

$$(z \mathbf{I} - \Phi) \mathbf{x}(kh) = \Gamma \mathbf{u}(kh) \quad (\text{A8})$$

Finally the solution is found through inversion and the use of Eqn A2 as

$$\mathbf{y}(kh) = \mathbf{C} (z\mathbf{I}-\Phi)^{-1} \Gamma \mathbf{u}(kh) \quad (\text{A9})$$

here, the discrete time transfer function matrix is

$$\mathbf{G}(z) = \mathbf{C} (z\mathbf{I} - \Phi)^{-1} \Gamma \quad (\text{A10})$$

APPENDIX B: The AR model

Complex Exponentials

Consider a summation of exponentials

$$x(t) = \sum_{k=1}^m b_k \exp(\lambda_k t) \quad (B1)$$

where λ_k and b_k can be complex or real. If $x(t)$ represents the response of a structure, λ_k should appear as complex conjugates pairs and the corresponding b_k has to appear as complex conjugates. If the sample interval is h , then the response at j sample instances later is

$$x(t+jh) = \sum_{k=1}^m b_k \exp(\lambda_k (t+jh)) \quad (B2)$$

which can be written as

$$x(t+jh) = z^j x(t) = \sum_{k=1}^m z_k^j b_k \exp(\lambda_k t) \quad (B3)$$

where z is forward shift operator and

$$z_k = \exp(\lambda_k h) \quad (B4)$$

Writing Eqn B3 for $j=0,1,2,\dots, m$ in matrix form

$$\begin{bmatrix} x(t) & -1 & -1 & \dots & -1 \\ zx(t) & -z_1 & -z_2 & \dots & -z_m \\ \vdots & \vdots & \vdots & \dots & \vdots \\ z^m x(t) & -z_1^m & -z_2^m & \dots & -z_m^m \end{bmatrix} \begin{pmatrix} 1 \\ b_1 \exp(\lambda_1 t) \\ \vdots \\ b_m \exp(\lambda_m t) \end{pmatrix} = 0 \quad (B5)$$

or

$$\Psi \beta = 0. \quad (B6)$$

For non-trivial b_k , the determinant of Ψ is zero. The determinant in terms of the first column of Ψ is

$$z^m x(t) C_m + z^{m-1} x(t) C_{m-1} + \dots + z x(t) C_1 + x(t) C_0 = 0 \quad (B7)$$

where C_i is co-factor of the $i+1$ element in column 1 of Ψ . Dividing through by C_m and by z^m , one can write

$$\{ 1 + a_1 z^{-1} + a_2 z^{-2} + \dots + a_m z^{-m} \} x(t) = 0 \quad (B8)$$

Equation B8 is the equation for an Autoregressive process, the polynomial in z is the characteristic equation in the time domain. It is apparent from Eqn B8 that a summation of exponentials (real or complex) is an Autoregressive process. Also, for Eqn B8 to hold, Ψ must be singular. If $\lambda_i \neq \lambda_j$ (that is $z_i \neq z_j$), Ψ becomes singular when the first column is a multiple of any other column; this occurs when $z \in \{ z_1, z_2, \dots, z_m \}$. The roots of the characteristic equation in the time domain are given by Eqn B4 which can be mapped to the roots of the characteristic equation in the Laplace domain and eventually to the modal frequencies and damping factors.

Alternative Formulation

The equations of motion for any linear homogeneous equation can be put into state space form as

$$\dot{\mathbf{x}}(t) = \mathbf{A} \mathbf{x}(t) \quad (B9)$$

$$\mathbf{y}(t) = \mathbf{C} \mathbf{x}(t) \quad (B10)$$

where $\mathbf{x}(t)$ is the vector of states. The exact solution of Eqn B8 is given by Eqn A8 when Γ is zero

$$(\mathbf{zI} - \Phi) \mathbf{x}(kh) = \mathbf{0} \quad (B11)$$

for non-trivial \mathbf{x} , the determinant of $(\mathbf{zI} - \Phi)$ must be zero. The determinant results in the characteristic equation in the Time Domain. Thus, every state must follow an Autoregressive process and since $\mathbf{y}(t)$ is a linear combination of the states at a given time, $\mathbf{y}(t)$ is also an Autoregressive process.

APPENDIX C: Singular Value Decomposition

Any matrix, A , belonging to $C^{m \times n}$ can be decomposed into a product of three matrices,

$$A = U \Sigma V^T \quad (C1)$$

where

$$\begin{aligned} U &\in C^{m \times n} \\ V &\in C^{n \times n} \\ \Sigma &= \text{diag}(\sigma_1, \sigma_2, \dots, \sigma_n) \end{aligned} \quad (C2)$$

and where the σ_i are termed the singular values of A . The singular values are ordered from the largest to the smallest. The columns of U are denoted by u_i and the columns of V are denoted by v_i . The matrices U and V are orthogonal to themselves, that is

$$\begin{aligned} U^T U &= U U^T = I \\ V^T V &= I \\ V V^T &= I \end{aligned} \quad (C3)$$

If A is of rank r , then

$$\sigma_1 > \sigma_2 > \dots > \sigma_r > \sigma_{r+1} = \dots = \sigma_n = 0 \quad (C4)$$

the nullspace of A is

$$N(A) = \text{span} [v_{r+1}, v_{r+2}, \dots, v_n] \quad (C5)$$

and the range of A is

$$R(A) = \text{span} [u_1, u_2, \dots, u_r] \quad (C6)$$

The pseudo-inverse of A is

$$A^\# = (A^T A)^{-1} A^T = V \Sigma^{-1} U^T \quad (C7)$$

A symmetric matrix B , can be represented by

$$B = A^T A = U \Sigma V^T (V \Sigma U^T) = U \Sigma^2 U^T \quad (C8)$$

note that Σ^2 is also a diagonal matrix. The condition number of A is the ratio of the maximum singular value and the minimum singular value. If the singular values past the r th singular value are nearly zero, then the minimum norm approximation of A is

$$\mathbf{A} = \sum_{i=1}^I \sigma_i \mathbf{u}_i \mathbf{v}_i^T \quad (\text{C9})$$

References 12 and 26 provide complete discussions of Singular Value Decomposition (SVD).

APPENDIX D-Singular Value Decomposition Solution of Normal Equations

The ill-conditioning problems associated with the solution of an overdetermined set of equations has been well documented. The LS algorithm requires the solution of an overdetermined set of equations by forming the Normal Equations. Reference 27 states, "the Normal Equations are ill-conditioned especially when the number of parameters is large," and suggests the solution of the overdetermined set of equations by repeated Householder transformations until the equations are in triangular form. Reference 28 recognizes the ill-conditioning problem and proposes solution through singular value decomposition (SVD) or QR decomposition. Reference 29 states, "utilization of the normal equations was numerically unstable, due to the squaring of the condition number of the coefficient matrix," and recommends the use of the QR decomposition in the solution of the overdetermined set of equations. The solution of the overdetermined set of equations via SVD is shown to be equivalent to solution of the normal equations by reference 12.

Solution by SVD has been shown to have many useful properties including rank determination and determination of the conditioning number of a matrix. However, the SVD solution of the overdetermined set of equations will be shown to have another useful property, a well conditioned solution. Given the overdetermined set of equations

$$A\theta = b \quad (D1)$$

where A is $N \times p$. The LS solution involves the normal equations

$$\theta = (A^T A)^{-1} A^T b \quad (D2)$$

A can be decomposed to

$$A = U \Sigma V^T \quad (D3)$$

where U is an $N \times p$ unitary matrix, S is a diagonal matrix, and V is a $p \times p$ orthogonal matrix. Substitution of the decomposition of A into Eqn D2 yields

$$\theta = (V \Sigma U^T U \Sigma V^T)^{-1} V \Sigma U^T b \quad (D4)$$

since U is unitary

$$\theta = (V \Sigma^2 V^T)^{-1} V \Sigma U^T b \quad (D5)$$

Note that $V \Sigma^2 V^T$ is the SVD of $A^T A$ and has the condition number of

$$\kappa(A^T A) = \frac{\sigma_{\max}^2}{\sigma_{\min}^2} \quad (D6)$$

in terms of the singular values of A . The conditioning of the normal equations is the square of the conditioning of the overdetermined equations. The inverse in Eqn D5 is easily computed to be $V \Sigma^{-2} V^T$ reducing Eqn D5 to

$$\theta = V \Sigma^{-1} U^T b \quad (D7)$$

Equation D7 is the solution to the overdetermined set of equation via the pseudo-inverse calculated through the use of the SVD of A . Equation D7 is the solution to the Least Squares problem without the formation of $A^T A$. The condition number of the pseudo-inverse is the square root of Eqn D6. If $1/\kappa(A^T A)$ approaches the precision of the computer, the solution via Eqn D2 will be ill-conditioned while solution via Eqn D7 may not. If $1/\kappa(A^T A)$ does not approach the precision of the computer, Eqn D2 and Eqn D7 will produce the same results. For example, if a minicomputer has 15 and 1/2 digits of resolution in double precision and $\kappa(A^T A)$ approaches 10^{16} the solution of Eqn D2 will be ill-conditioned. The LS solution of normal equations can sometimes be very ill-conditioned. Solution of the overdetermined equation through the use of the SVD can alleviate the problem. But solution via SVD is costly in CPU time and memory storage. In many cases when the normal equation are solved by Eqn D2, $A^T A$ ($m \times m$) and $A^T b$ ($m \times 1$) can be formed directly from data without first forming A ($n \times m$) or b ($n \times 1$) where n is the number of overdetermined equations and m is the number of parameters. If the normal equations are solved by SVD the matrix A has to be formed. Solution by (D2) requires inversion of a $m \times m$ matrix. Solution by SVD requires the decomposition of a $n \times m$ matrix. If n is many times greater than m , then the SVD solution will be considerably slower than the solution via inversion of the normal equations.

APPENDIX E: The frequency error envelopes

Once the roots of the time domain characteristic equation are found, the frequency and damping factors can be extracted from Eqn 16

$$s = \zeta\omega + j\omega_d = \frac{1}{h} [\ln |z| + \arg(z)] \quad (E1)$$

The error in the estimated damped natural frequency is

$$\delta\omega_d = \frac{1}{h} \arg(z_{est} - z) \quad (E2)$$

where z_{est} is the estimated pole location and z is the real location. The maximum error is

$$\delta\omega_d = \frac{1}{h} \arctan \frac{\epsilon}{|z|} = \frac{1}{h} \arctan \frac{\epsilon}{\exp(-\zeta\omega h)} \quad (E3)$$

where ϵ is the radius of uncertainty. The percentage error is found by dividing by ω_d and can be put into non-dimensional form by noting

$$h = \frac{\pi}{\omega_d} \quad (E4)$$

The damped natural frequency percentage error function is

$$\% \text{ error} = \frac{1}{\pi(\omega_d/\omega_{nyq})} \arctan \left(\frac{\epsilon / \exp\left(\frac{-\pi\zeta}{\sqrt{1-\zeta^2}} \frac{\omega_{nyq}}{\omega_d}\right)}{\omega_d/\omega_{nyq}} \right) \quad (E5)$$

which for small ϵ is linear in ϵ .